REFERENCE ONLY

UNIVERSITY OF LONDON THESIS

Degree *PHD* Year *2008* Name of Author *REGAN, JENNIFER, CLAIRE*

COPYRIGHT

This is a thesis accepted for a Higher Degree of the University of London. It is an unpublished typescript and the copyright is held by the author. All persons consulting this thesis must read and abide by the Copyright Declaration below.

COPYRIGHT DECLARATION

I recognise that the copyright of the above-described thesis rests with the author and that no quotation from it or information derived from it may be published without the prior written consent of the author.

LOANS

Theses may not be lent to individuals, but the Senate House Library may lend a copy to approved libraries within the United Kingdom, for consultation solely on the premises of those libraries. Application should be made to: Inter-Library Loans, Senate House Library, Senate House, Malet Street, London WC1E 7HU.

REPRODUCTION

University of London theses may not be reproduced without explicit written permission from the Senate House Library. Enquiries should be addressed to the Theses Section of the Library. Regulations concerning reproduction vary according to the date of acceptance of the thesis and are listed below as guidelines.

A.   Before 1962.   Permission granted only upon the prior written consent of the author. (The Senate House Library will provide addresses where possible).

B.   1962-1974.   In many cases the author has agreed to permit copying upon completion of a Copyright Declaration.

C.   1975-1988.   Most theses may be copied upon completion of a Copyright Declaration.

D.   1989 onwards. Most theses may be copied.

This thesis comes within category D.

☐   This copy has been deposited in the Library of _____ *UCL* _____

☐   This copy has been deposited in the Senate House Library, Senate House, Malet Street, London WC1E 7HU.

Fgf-Signalling and the Development of CNS Asymmetry in Zebrafish

Jennifer C. Regan

Submitted in partial fulfilment of the requirements for
the Degree of Doctor of Philosophy

April 2008

Department of Anatomy and Developmental Biology

University College London

University of London

UMI Number: U593385

UMI®

Dissertation Publishing

ProQuest®

Declaration

I, Jennifer Claire Regan, confirm that the work presented in this thesis is my own. Where information has been derived from other sources, I confirm that this has been indicated in the thesis.

For my family

and

for David

Acknowledgements

Abstract

Neuroanatomical and functional asymmetries are a widespread, probably universal, feature of the vertebrate nervous system. Although brain asymmetry is a fundamental characteristic of the CNS, how it is established is not known.

The epithalamus is a subdivision of the diencephalic region of the forebrain and structural asymmetries in this region are widespread among vertebrates. The epithalamus of the zebrafish shows differences between the left and right sides in terms of neuronal organization, connectivity and gene expression and has become a focus for the study of establishment and elaboration of brain asymmetry.

Unilateral Nodal expression in the dorsal diencephalon of zebrafish embryos is required for correct lateralisation of the epithalamus. However, in embryos lacking Nodal signalling asymmetries still develop, but their sidedness is randomised among siblings. This suggests that Nodal is not required for asymmetric development *per se* and that other signals are responsible for generating asymmetry. In order to uncover signalling pathways required to break symmetry in the brain, we aimed to identify mutant lines that do not show elaboration of CNS asymmetries.

In this thesis I describe the phenotype of the *fgf8* mutant, *acerebellar (ace)*, which develops a symmetric epithalamus. The parapineal does not migrate and remains at the midline and later epithalamic asymmetries do not develop. However, unilateral Nodal signalling in the brain and body axis are largely unaffected in *ace* mutants. Fgf8 is expressed bilaterally in the epithalamus in wild type embryos, as are some Fgf-responsive genes. Additionally, several Fgf-pathway genes are expressed specifically in the migrating parapineal. Using a modified Fgf8 micro-bead implantation technique, I am able to rescue the lateralised migration of the parapineal in *ace* mutants. In situations of unbiased Nodal signalling, exogenous Fgf8 can impose laterality on the epithalamus. In summary, these studies demonstrate that Fgf8 can break neuroanatomical symmetry in the epithalamus through the regulation of the bi-stable left- or right-sided migration of the parapineal. I present a mechanism whereby the combined action of Nodal and Fgf signals ensures the establishment of neuroanatomical asymmetries with consistent laterality.

Contents

8

List of Figures, Graphs and Tables

Chapter Three

Discussion

Introduction

1. Asymmetry in the embryo

1.1 Left/Right asymmetry in the body plan of vertebrates

An outwardly symmetrical body plan can be observed in diverse phyla, from the radial symmetry of the sea anemone to the chiral symmetry of snails and ciliates (Finnerty, 2003). A bilaterally symmetric body plan is a striking feature of all vertebrates; however, it is a pseudo-bilaterality: hidden beneath the symmetric exterior is a left/right (L/R) asymmetric arrangement of viscera, vasculature and nervous system. Asymmetries are found in unpaired organs, such as the heart and gut, which may be placed to one side of the midline or looped in a particular direction, and in paired organs such as the lungs, which differ from each other in their structure. More elusive L/R asymmetries lie within the CNS, some of which are outwardly manifested through lateralised behaviours such as hand preference. Disruptions in L/R patterning can have severe consequences for the developing organism, suggesting that the correct placement of organs or neural processing regions is essential for their proper function.

The anterior/posterior (A/P) and dorsal/ventral (D/V) axes appear first in the embryo and automatically define the L/R axis. However, there are no extra-embryonic cues for left and right (as these are referential to the organism), therefore 'left' and 'right' have to initiate autonomously within the embryo, with respect to the two existing axes. This leads to the intriguing question of how symmetry is broken in the vertebrate embryo, and how the resulting asymmetries are always orientated in the same direction.

Speculation about the existence of a chiral or 'F' molecule, which in orientating itself with the A/P and D/V axes could define left and right, began before the first asymmetrically expressed genes were identified (Brown & Wolpert, 1990; Levin et al, 1995). A common symmetry-breaking event in vertebrate embryos has yet to be defined, but several well-conserved strategies implicated in L/R patterning have now been identified. One of the essential remaining questions is whether all steps to

generate L/R asymmetry are conserved among vertebrates, particularly considering the differences in the architecture of embryogenesis that exist between species.

1.2 Asymmetry vs Laterality

Although sometimes used interchangeably in the field, asymmetry and laterality are very different concepts and distinguishing between the two is vital. Asymmetry (from the Greek meaning different measurement) can be used to describe any difference across an axis. L/R asymmetry describes differences across the left/right axis and two types are defined when considering a population of organisms. The first is randomised asymmetry, or anti-symmetry; this refers to a racemic population where 50% of individuals have an asymmetry that lies in one direction and 50% in the other. An example of anti-symmetry is found in the *Limnaea* species of snail, in which half have a sinistral (leftward) shell whorl and half have a dextral (rightward) whorl (Shibazaki et al, 2004). The second is invariant or directional asymmetry in which all members of the population have a L/R asymmetry that lies in one direction, for example the left-sided human heart. Laterality refers to the 'handedness' or direction that an asymmetry takes. These definitions become important when describing phenotypes of L/R patterning defects. An interesting question arising from the consideration of these two definitions is whether the development of asymmetry and the assignment of laterality can ever be separable processes.

1.3 Three phases to generate L/R asymmetry

It is suggested that the generation of L/R asymmetry in the embryo can be split into three conceptual phases that require different sets of genetic and epigenetic interactions (Levin, 2006). These are the initial breaking of global symmetry, the stabilisation of L/R information and it's transmission across large fields of cells and finally, relaying L/R positional information to organ primordia and co-ordinating asymmetric organogenesis. Mechanisms involved in all three processes have conserved and divergent elements among vertebrate species, and it may be the case that parallel mechanisms are operating within individual species.

1.3.1 Breaking global symmetry

There are two main hypotheses proposed to explain the initial break of symmetry in vertebrates. In the **nodal flow hypothesis,** the symmetry break occurs at post-

gastrulation stages within a spherical structure called the node and ultimately results in asymmetric gene expression in the node region. In contrast, while the **gap junction communication (GJC) model** also converges on the node, asymmetric gene expression in this region relies on L/R asymmetries generated at early cleavage stages.

1.3.1.1 Nodal flow hypothesis

In human syndromes presenting L/R patterning defects, lung, kidney and sperm functions are also often impaired. These diseases are now recognised as 'cilliopathies' and are associated with mutations in cilia proteins, motor proteins that make cilia move, or interflagellar transport (IFT) components that are necessary for building and maintaining the cilium (Fliegauf et al, 2007). Analyses of mouse cilia mutants have directly implicated node cilia in L/R patterning (Okada et al, 1999). The mouse node is an enclosed, spherical structure located at the anterior end of the primitive streak, whose ventral epithelial surface is lined with rotating monocilia. A series of experiments demonstrated a net leftward flow of fluid within the node ('nodal flow') and confirmed the lack of nodal flow in mutants with non-motile cilia (Nonaka et al, 1998, Okada et al, 1999). One particularly elegant study artificially reversed fluid flow within the node, consequently reversing organ laterality in the embryo (Nonaka et al, 2002).

Supporting a conserved role for the node, studies in the chick demonstrated that a cascade of asymmetric signals that originated at or near Hensen's node during gastrulation were sufficient to direct subsequent L/R patterning events in the embryo (Levin et al, 1995). Subtle asymmetries in gene expression around the node were also identified in the mouse embryo (Shiratori and Hamada, 2006). It has since been shown that in addition, epigenetic factors such as transient Ca^{2+} levels are asymmetric at the node in chick and mouse (Raya et al, 2004). These data supported the idea that an event occurring in the node could initiate asymmetric gene expression and direct L/R patterning.

Potentially, monocilia within the node could fulfil the criteria of the 'chiral' or 'F' molecule proposed by Brown and Wolpert. Aligned with the A/P and D/V axes and with a unidirectional rotation dictated by the chiral basal body at the root of the cilium, monocilia introduce a rotational asymmetry into a symmetric environment. This is transformed into unidirectional fluid flow, which initiates a genetic cascade on

14

one side of the node. Because cilia are always orientated in the same way, dictated by the A/P and D/V axes, symmetry is consistently broken in the same orientation without relying on any *a priori* L/R information in the embryo (Tabin, 2005).

Two mechanisms have been proposed to explain how nodal flow could break symmetry in the embryo. The first relies on the net leftward movement of a morphogen within the node, driven by the clockwise rotation of monoclilia. Accumulation of this morphogen on the left side of the node would preferentially up-regulate gene expression, or epigenetic factors, on the left of the midline. The identity of this morphogen has remained elusive, although a recent study has imaged the leftward movement of membrane-bound vesicles through the node (Tanaka et al, 2005). These 'node vesicular parcels' (NVPs) contain retinoic acid (RA) and Shh protein and are seen to break apart on contact with non-motile cilia found at the edge of the node, possibly releasing their cargo. Left-sided up-regulation of Ca^{2+} around the node is shown to be dependent on the release and leftward movement of NVPs.

The second proposed mechanism removes the need for the existence of 'morphogen X', instead relying on mechanosensory cilia, and is known as the 'two-cilia' model (Tabin, 2003). This was proposed following the observation of two populations of cilia in the node; centrally located rotating cilia and peripherally located non-motile cilia. In this model, nodal flow would increase pressure on the left side of the node, bending peripheral mechanosensory cilia and initiating an up-regulation of Ca^{2+} on the left of the midline. In opposition to the two-cilia hypothesis, recent modelling has suggested that shear-stresses generated within the node would not be asymmetric even in the presence of directional flow (Cartwright et al, 2004). However, this and other modelling studies have lent support to the idea that rotating monocilia are able to generate directional flow, by demonstrating that a posterior tilt of node cilia similar to that observed *in vivo* would be sufficient to produce a net directional movement (Cartwright et al, 2004) and that the 'drag' created by the proximity of the cilium to the ventral surface of the node would create a robust beating motion capable of generating a significant leftward movement (Buceta et al, 2005).

Conservation of nodal-flow as the initial symmetry-breaking event in vertebrates other than mouse is debateable. Ciliated structures orthologous to the node have been identified in several vertebrate species (Essner et al, 2002), including chick

(Hensen's node, Essner et al, 2002), zebrafish (Kupffer's Vesicle, Amack and Yost, 2004), *Xenopus Laevis* (gastrocoel roof plate, Schweikert et al, 2007) and rabbit (posterior groove of posterior notochordal plate, Okada et al, 2005). Mechanistic proof for the necessity of these structures in L/R patterning has been given for zebrafish and *Xenopus* in addition to mouse (Amack and Yost, 2004, Schweikert et al, 2007). However, it is known that L/R asymmetries are detectable at early cleavage stages in frogs and that genes necessary for L/R patterning are required earlier than node formation in chick and zebrafish.

1.3.1.2 Gap junction communication model

During the period that the first nodal flow experiments were being performed, studies in chick and frog were suggesting a much earlier break of symmetry. Experiments in *Xenopus* had shown that dorsal blastomeres of early cleavage stage embryos were connected by gap junctions, whereas a zone of junctional isolation existed at the ventral midline (Levin, 2006). This led Levin and colleagues to speculate that gap junctional communication (GJC) at early cleavage stages could allow the unidirectional movement of a small molecule, which would build up on one side of the zone of isolation at the ventral midline, thereby specifying left and right. Indeed, blocking GJC in dorsal blastomeres, or introducing GJC between ventral blastomeres, efficiently randomised organ situs in *Xenopus* (Levin and Mercola, 1998). Supporting this, some human patients with laterality disorders were found to carry mutations in *connexin43* (Levin, 2006), a channel subunit required for GJC.

However, unidirectional movement of a putative small molecule determinant through gap junctions necessitates an energy input. It was speculated that an electrogenic gradient could provide the required force, providing that the small molecule in question was charged. Indeed, it had already been observed that tissue on the left side of the primitive streak in chick was more depolarised than the right (Levin, 2006). Ion fluxes are needed to form voltage gradients; a large-scale pharmacological screen to identify ion channels, pumps and co-transporters required for correct L/R patterning was initiated (Levin et al, 2002). This screen identified four genes involved in H^+ and K^+ flux and one of these, the H^+/K^+-ATPase, was found to be asymmetrically localised with respect to the L/R axis at the two-cell stage in *Xenopus* (Levin et al, 2002). Pharmacological inhibition of H^+/K^+-ATPase randomises organ situs in *Xenopus,* chick and zebrafish, and in addition, the

depolarisation of the left primitive streak in chick is dependent on H^+/ K^+-ATPase function (Levin, 2006).

The multitude of data implicating ion flux and GJC in L/R patterning has been integrated into a single model, considering the embryo as an electrophoresis chamber (Levin, 2006). Here, at very early cleavage stages, the chiral nature of the cytoskeleton allows sub-cellular L/R asymmetric distribution of ion pump components (as mRNA in *Xenopus*, possibly post-translationally in chick and zebrafish). These are inherited by a single blastomere on one side of the midline. Ion exchange with the environment occurring preferentially on one side of the midline introduces a voltage gradient within the embryo. Gap junctions between cells allow exchange of a small molecule in a circumferential path around the embryo, with the ventral midline (or primitive streak) acting as a zone of junctional isolation and the voltage gradient acting as a motive force for unidirectional movement. The net result is a circumferential gradient of the small molecule, with the greatest difference in concentration being across the zone of isolation (streak in chick or ventral midline in frog blastulae). This small molecule would be at the top of a cascade of gene expression, which would occur on one side of the midline only and would convert epigenetic L/R asymmetries into stable genetic ones.

There are several candidates for the small molecule determinant, including serotonin, inositol polyphosphates and Ca^{2+}. All fit the criteria of being charged, small enough to pass through gap junctions and water soluble (lipophilic molecules would not require gap junctions to pass from cell to cell), and all have been implicated in L/R patterning (Fukumoto et al, 2005a; Sarmah et al, 2005; Raya et al, 2004). Several proteins involved in receiving, transporting and degrading serotonin have been implicated in asymmetry and a circumferential gradient of serotonin, as predicted by the model, has been demonstrated in *Xenopus* (Fukumoto et al, 2005b). Ca^{2+} levels are transiently higher on the left side of the node in mouse, chick and zebrafish (Raya et al, 2004), and inositol polyphosphates are known to be required earlier than Kupffer's vesicle formation in zebrafish (Sarmah et al, 2005).

Both the nodal-flow and GJC models have support from experimental data in a range of vertebrate systems. Although there is a confusing array of data showing both conserved and divergent elements of both models, ultimately, both converge at the node and result in stable asymmetric gene expression in the body axis.

17

1.3.2 Stabilisation and transmission of L/R information: the Nodal cassette

The second step in generating embryonic asymmetry concerns the stabilisation of transient asymmetries at the node and transmission of L/R information across large fields of cells. The pathways involved in this conceptual 'step' are very well conserved among vertebrates, and represent the most well-defined part of the L/R patterning process. Downstream of subtle asymmetries around the node, the Nodal cassette is activated on the left side of the body axis, in the lateral plate mesoderm (LPM), where it rapidly spreads as a result of it's own positive auto-regulation. Nodal ligands signal through ActRBI and ActRBII receptors phosphorylating Smads, which interact with fast/fox transcription factors to upregulate Nodal (reviewed in Tian, 2006). This positive autoregulation is offset by feedback inhibition from Lefty1 and Lefty2, which are activated by Nodal in the midline and LPM. Pitx2c, also activated by Nodal signalling, represents the output of the Nodal cassette and is expressed long after the other pathway components have been down-regulated (Bisgrove et al, 2000).

1.3.2.1 Asymmetries at the node

The initiation of Nodal pathway signalling in the LPM is dependent on transient Nodal expression around the node; whether this domain of Nodal expression is itself asymmetric varies between vertebrate species. It has recently been demonstrated that a node-specific enhancer upstream of the *Nodal* gene contains binding sites for a transcriptional mediator of Notch signalling. Indeed, it has been shown that Nodal expression at the node depends on Notch function, and that this requirement for Notch is conserved in vertebrates. Interestingly, Ca^{2+} levels have been shown to affect the binding rates of Notch to the *Nodal* enhancer, and transient increases in Ca^{2+} levels have been demonstrated on the left side of the node in mouse, chick and zebrafish embryos (Raya et al, 2004). This suggests a mechanism linking transient epigenetic asymmetries at the node, such as Ca^{2+} levels, to Nodal expression at the node, mediated by Notch signalling.

Nodal is not the only gene expressed asymmetrically in the node. In chick, for instance, there is a complex array of asymmetries on both the left and right side of the node, including members of the Hh, BMP, Fgf and Wnt pathways. Many asymmetries identified at the chick node are not found in other species, but this may reflect incomplete characterisation of other models rather than divergence in avian species.

18

For instance, the first asymmetrically expressed gene to be identified was Shh at the node in chick (Levin et al, 1995), which has recently been implicated as an asymmetrically transported morphogen contained in NVPs in the mouse node (Tanaka et al, 2005). What remains unclear is exactly how asymmetries at the node are transferred to the LPM, but Nodal and Notch expression are certainly required.

1.3.2.2 The Nodal cassette

Initial asymmetries at the node are stabilised and amplified in the LPM by the well-conserved Nodal 'cassette'. A combination of experimental and modelling approaches by Nakamura and colleagues (2006) has demonstrated that Nodal and Lefty signalling in the LPM acts as a self-enhancing and lateral inhibition (SELI) system. This system has the ability to amplify subtle differences in gene expression at the node into robust and strictly unilateral signalling in the LPM, achieved through positive autoregulation by Nodal and long-range inhibition by Lefty. In this model, small differences in an activating signal at the node results in different levels of Nodal activation in the left and right LPM. The stronger Nodal signal in the left LPM activates Lefty signalling at a high level there and at the midline, rapidly down-regulating Nodal in the right LPM. This system generates large differences in expression levels of Nodal from subtle ones, which stabilises quickly into unilateral expression and travels rapidly over large fields of cells. The SELI system model efficiently predicted mouse mutant phenotypes and was able to explain the differences in phenotype observed when various node and Nodal pathway mutant embryos are compared.

1.3.3 Asymmetric organogenesis

Little is known about the translation of genetic asymmetries into morphological ones. Pitx2c, the Nodal 'effector' is maintained longer than any other part of the Nodal pathway and is still expressed in LPM-derived mesenchyme of various visceral organs, such as the lung buds, heart and gut, at late somite stages (Shiratori and Hamada, 2006). *Pitx2c-/-* mouse mutant embryos exhibit defects in asymmetric organogenesis such as randomised heart position and right lung isomerism (Lin et al, 1999). However, some aspects are unaffected such as heart looping and expression of asymmetric genes such as *d-hand* in the heart, suggesting that while many aspects of L/R morphogenesis are Pitx2c-dependent, some are dependent on Nodal signalling that is not mediated by Pitx2c.

A recent study has demonstrated that asymmetric *pitx2c* expression in the LPM and visceral organ primordia depends on an *ASE* enhancer upstream of the *pitx2c* gene, which contains several binding sites for *foxH1* and a single binding site for *nkx2.5* (Norris et al, 2002). The *foxH1* sites are essential for initiation of asymmetric *pitx2c* expression (*foxH1* is downstream of Nodal) and the *nkx2.5* site is essential for later maintenance of *pitx2c*. The authors showed that this enhancer is functionally conserved throughout vertebrates and additionally, that *ASE*-driven *pitx2c* expression is required throughout asymmetric organogenesis.

Detailed studies of local morphogenetic movements have shed some light of events downstream of Pitx2c signalling. For example, analysis of early gut looping morphogenesis in transgenic zebrafish demonstrated that the LPM itself drives early gut looping by migrating asymmetrically (Horne-Badonovic et al, 2003). The left LPM moves dorsal to the midline gut primordium and the right LPM moves ventro-laterally, pushing endodermal tissue to the left of the midline. Migration of the left and right sides of the LPM is independently randomised when Nodal signalling is lost such that the gut loops to the left, right, or does not loop at all if the two sides of the LPM oppose each other at the same dorso-ventral level. However, like most other studies of asymmetric organogenesis, the molecular nature of the link between Nodal pathway signalling and asymmetric morphogenesis was not demonstrated.

Asymmetric organs differ in their requirement for Nodal signalling, and these differences may give clues to the mechanisms employed downstream of Nodal. For example, if randomised asymmetry is observed in the absence of Nodal signalling, this suggests that the primordium in question has the autonomous ability to develop asymmetrically and requires Nodal signalling for *situs* only. An example of this is the looping of the gut primordium in zebrafish *southpaw* morphants discussed above, where the driving force of asymmetric LPM migration occurs but is randomised. In contrast, if an organ primordium is found to be symmetric or in a midline location, this implies that Nodal signalling is directly required for it's asymmetric development or migration. The loss of normally left-sided organs, such as asplenia, or right isomerism of normally asymmetric paired structures such as lungs, implies that left identity is directly specified by Nodal signalling. In order to fully understand asymmetric organogenesis, molecular targets of *pitx2c* need to be identified that direct migration, proliferation and cell shape dynamics.

1.4 Reconciling the multitude of data from vertebrate models

A major question remaining in the field is whether mechanisms that generate asymmetry, stabilise it and translate it into asymmetric morphogenesis, are conserved among vertebrates. Early patterning steps seemed at first to be particularly divergent, but as research progresses, an increasing amount of conservation has been demonstrated. In fact, links between vertebrate and invertebrate mechanisms have been recognized and it is even suggested that plant asymmetry mechanisms may utilise similar pathways (Levin, 2006).

A major division has occurred between researchers studying the initial symmetry break in the embryo, which has led to formation of the nodal cilia and GJC 'camps'. Both models continue to gain support from recent studies in a range of vertebrate models, therefore, it seems reasonable to conclude that the later process of nodal flow is required to amplify or stabilise earlier asymmetries produced by ion flux and GJC. Mouse is the only vertebrate model that has not been demonstrated to require processes preceding nodal flow that are essential for asymmetry. There are two possible explanations for this; either that a *de novo* loss of early asymmetry mechanisms occurred in mouse and rat, or that early asymmetries exist in these embryos that remain to be identified. Indeed, the ion channel Polycystin-2 is necessary for mouse asymmetry and directly interacts with the motor protein KIF3A (Li et al, 2006), suggesting that some motor proteins assumed to be required for cilia function may also have an earlier role in localization of ion pumps.

Signaling pathways active around the node also vary between vertebrate species. Intriguingly, there are similarities between chick and rabbit peri-nodal signaling (such as Fgf8 as a right-determinant) as well as similarities in their mode of development, as a flat blastodisc. It has been suggested that the architecture of early embryogenesis may determine the pattern of signaling at the node (Fischer et al, 2002).

Eclipsing the divergence between species are the similarities in asymmetry mechanisms, suggesting that while differences in embryo shape may require modifications of some elements of the asymmetry cascade, the major structure of the cascade is conserved. Essential elements have been identified, including ion pumps, cilia, Nodal and Notch signaling at the node, transient Ca^{2+} asymmetries and buffering

by RA. These lead to activation of the highly-conserved Nodal signalling cassette in the LPM, which stabilises and transmits asymmetry in a strictly unilateral manner. Unilateral expression of Pitx2 and Nodal is in fact conserved in all chordate taxa and in echinoderms (Duboc et al, 2008).

The translation of genetic asymmetries into asymmetric organogenesis has not been studied in great depth in any system and therefore it is difficult to speculate on conservation. Studies in gut looping implicate migration of the LPM itself in providing a motive force for asymmetric morphogenesis (Horne-Badonovic et al, 2003); whereas in other primordia, such as the heart, expression of Nodal pathway genes within the developing structure itself is required for asymmetric development (Lin et al, 1999).

Decoding available clinical data for human laterality disorders is extremely challenging, but is aided considerably by comparative analysis with model systems. Human L/R patterning defects may be just one aspect of complex, multi-phenotypic disorders and data often comes from sporadic cases, where the focus of recorded information varies as much as the nomenclature. Human data is further clouded by the generation of laterality disorders by non-genetic factors such as teratogens and maternal diabetes (Bisgrove et al, 2003). However, the many similarities between human disorders and model system mutant lines has helped to elucidate genetic pathways necessary for human L/R patterning. Just as in mouse, human diseases that affect laterality often affect other ciliated structures, such as Kartegener's syndrome, where *situs ambiguus* (heterotaxia of visceral organs) and loss of function of lung cilia occur (Burdine et al, 2000). Another example is infantile nephronophthesis, which presents renal and L/R patterning abnormalities and is modelled by the *inv* mouse mutant (Peeters, 2006). These and other ciliopathies imply that nodal cilia are conserved in human embryogenesis. Human mutants in Nodal genes exist, but are rare - probably due to early lethality - suggesting that the Nodal pathway is conserved in humans as in all other chordates (Peeters, 2006). Mutations in genes required for gap junction formation have been identified in human patients with laterality defects (Levin, 2006), suggesting conservation of early symmetry breaking events as well.

Data from human patients has offered its own insights into L/R patterning; for example, data of cardiac laterality defects has shown that *situs inversus totalis* patients (complete reversal of the L/R axis) have a significantly higher risk of

complex congenital heart disease than *situs solitus* children, suggesting that while concordance of the heart with other organs is necessary for function, laterality *per se*. Subcellular asymmetries, such as asymmetric cardiac myofibre organisation, may therefore be specified independently of organ *situs* (Delhaas, 2004).

2. CNS Asymmetry

2.1 CNS asymmetry in humans

2.1.1 Functional asymmetry

Functional asymmetry in the human brain has an obvious output in handedness, which has been recognised, and in some cases stigmatised, for millennia. The words 'sinister' and 'dextrous' find their root in sinistral (left-handed) and dextral (right-handed) and demonstrate that handedness has long been linked to personality. Left-handers have encountered discrimination in many societies; for instance, in 19th century Japan, discovering your wife to be left-handed was legitimate grounds for divorce (McManus, 2002). Despite this, the rate of left-handedness has been maintained at a constant 11% throughout history and pre-history and in all cultures, suggesting that a minority of hand-use reversal is maintained as an evolutionary stable strategy (Vallortigara and Rogers, 2005).

Functional brain asymmetries were more formally recognised by Broca in the late 19th century, who observed that lesions in a particular brain region correlated with difficulty in producing coherent speech. Language has since been shown to be strongly lateralised in the brain with more than 95% of the population processing language in the left hemisphere. The left hemisphere is also known to be dominant for mathematical and logical reasoning, whereas the right is dominant for shape recognition, spatial attention, emotion processing and musical and artistic ability (Sun and Walshe, 2006). fMRI studies have demonstrated these and many further functional asymmetries, such as differences in autobiographical memory retrieval between left and right hippocampi that is dependent on remoteness of memory (Maguire et al, 2003).

2.1.2 Anatomical asymmetry

It is assumed that anatomical asymmetries underlie functional ones, however, relatively few structural asymmetries have been identified in the human brain. Several features of the planum temporal, including the posterior superior temporal sulcus and the Sylvian fissure, which separates the frontal and temporal lobes, are asymmetric and strongly lateralised among the population (Sun and Walshe, 2006). Both areas are

24

related to language processing; in fact the majority of identified asymmetries are linked to language generation or comprehension. Cellular asymmetries are much harder to detect than gross anatomical features, not least because locating exactly comparable regions between hemispheres and individuals is extremely difficult. Nonetheless, some left-right differences have been identified, such as larger and more densely packed layer 3 pyramidal cells in the left hemisphere in regions related to language processing (Hutsler, 2003). Anatomical asymmetries can also be related to handedness, for example the cortical representation of the right hand, shown by magnetic source imaging, is larger in the left primary somatosensory cortex of right-handers (Sun and Walshe, 2006).

A recent study measuring the covariance in grey matter density in a large number of subjects has demonstrated that very subtle differences exist between left and right hemispheres in terms of regional associations (Mechelli et al, 2005). If increased density in one region is correlated with an increase in another region, it is described as being positively associated. Associations can be positive or negative and are normally mirror-symmetric. However, in some cases patterns of regional covariance are asymmetric, so that a positive association may be strong in the left hemisphere, but when the same regions in the right hemisphere are compared, no association is found. For instance, the inferior frontal cortex expresses a stronger association with the pars opercularis in the right relative to the left hemisphere. Direct asymmetries in grey matter density were also found in the primary visual cortex, where left- and right-sided density variation was dissociated. Interestingly, regional associations have been shown to be disrupted in schizophrenic patients, where no mean difference in density *per se* exists between healthy and patient populations in these regions (Woodruff et al, 1997). These studies suggest that left-right differences more subtle than gross anatomical asymmetries exist and are important for lateralized functions.

2.1.3 Genetic asymmetry

Foetal brains have anatomical asymmetries comparable to those observed in adults, and appear to be lateralized at the same rate as the adult population (Hepper et al, 2005). In a study using ultrasound to assess handedness of thumb-sucking at 15 weeks (Hepper et al, 2005), it was shown that right-handed foetuses become right-handed

teenagers. These early asymmetries strongly suggest genetic control of brain lateralization; indeed, a recent study has identified *LRRTM1*, the first known human gene to be linked with an increased probability of being left-handed (Francks et al, 2007). *LRRTM1* is imprinted: an upstream haplotype associates with left-handedness, this haplotype is preferentially paternally inherited and the gene shows variable maternal down-regulation. Handedness is a complicated trait to study, not only because it does not seem to be governed by simple rules of Mendelian inheritance, but also because the definition of handedness itself is complex (Annett, 1998). It may not be a simple binary decision; our population is probably made up of a large proportion of 'mixed handers'. This does not refer to ambidexterity, but to subjects who favour either hand, depending on the task. It has been suggested that the population consists of a continuum between strongly right-handed and strongly left-handed people that is skewed toward right-hand dominance (Annett, 1999).

Two well-known theories of single gene control of brain lateralization have been postulated; the right-shift (*RS*) theory suggests that handedness is the result of a general hemispheric dominance that includes language processing, controlled by a putative *RS* gene (Annett, 1999). This theory considers handedness in the population to be a scale of hand dominance, which is achieved by variable suppression of cerebral function in the right hemisphere. In contrast, the McManus theory relies on classical Mendelian genetics and considers handedness to be either right-lateralised or randomised, controlled by two alleles, *dextral* and *chance*. Both theories can be engineered to fit actual rates of handedness; whether a single gene can control development of brain laterality remains to be seen.

A recent analysis of foetal human brains by Serial Analysis of Gene Expression (SAGE) at 12 and 14 weeks identified nearly 30 asymmetrically expressed genes (Sun et al, 2005). No genes known to be involved in regulating visceral asymmetry were identified, except for members of the Fgf pathway, but this does not rule out the possibility that earlier patterning steps require these genes. In fact, the existence of robust and varied asymmetric gene expression at 12 weeks suggests any potential whole-brain left-right patterning step would already have occurred.

2.1.4 Are brain asymmetries linked?

A crucial question when considering possible genetic control of brain laterality is

linkage - is the lateralization of all asymmetric features controlled by the same mechanism, or are regions of the brain independently lateralized? Strong correlation of left hemisphere language processing and right-handedness suggests a global mechanism; as do associations between regional covariance in grey matter density. However, confounding the idea of linkage is the fact that even though the rate is reduced compared to right-handers, the majority of left-handers (~70%) still process language in the left cerebral cortex. Annett's theory of cerebral dominance suppression and continuity of handedness resolves this problem somewhat. She suggests that the *RS* gene generally inhibits right cortical dominance, although not fully, giving a range of brain lateralization within the population, including a significant proportion of mixed- and left-handers (Annett, 1999).

Some lateralized features are more tightly linked than others; for instance, the ability to attend to local form while ignoring global form (seeing the trees and not the forest) is always reversed in left-handers (Mevorach et al, 2005). This process is not language dependent as trials involving composite forms made of both letters and shapes produced the same result. Temporary focal disruption of cortical activity slowed the process of discrimination between global and local form when applied to the left brain of right-handers and the right brain of left-handers. This study suggests that some aspects of brain lateralization, such as handedness and attention to local form, are tightly linked. If lateralization occurs in a hierarchical manner, with an early, global signal being interpreted by several different regions during development, co-ordinated reversal would occur within regions but not necessarily between regions.

2.1.5 Human disorders

Reduced or reversed brain asymmetry in humans is linked to several congenital neurological disorders including schizophrenia (Li et al, 2007), autism (Escalante-Mead et al, 2007) and dyslexia (Herbert et al, 2005). Dyslexic and autism-spectrum disorder patients often demonstrate partial or total right-sided language processing (Escalante-Mead et al, 2007).

Schizophrenia, which affects 1% of the adult population, has also been associated with reduction or reversal of cerebral asymmetries, including those of the planum temporale, the superior temporal gyrus and the medial temporal lobe (Francks et al, 2007). In addition, schizophrenic patients show fronto-temporal dissociation,

where correlations in regional grey matter densities are lost (Woodruff et al, 1997). Other known reversals associated with schizophrenia include an elevated rate of left or mixed handedness. In fact, the 'left handedness susceptibility' gene, *LRRTM1*, is linked to schizophrenia (Francks et al, 2007). Analysis of the LLRTM1 protein has shown it to have receptor-like qualities, with similar leucine repeat patterns to Nogo and Robo, suggesting a function in axon guidance. Expression in foetal and adult brains demonstrates that it is highly expressed in the dorso-medial thalamus, a region associated with schizophrenia. While expression was not found to be overtly asymmetric in foetal brains at 14 weeks, it could be subtly asymmetric, asymmetric at earlier time-points or processed in an asymmetric manner (Francks et al, 2007). The gene is imprinted, and it has been suggested that this imprinting may be restricted to certain developmental time-points in humans, where mis-regulation of *LRRTM1* imprinting may underlie it's pathology (Francks et al, 2007).

In addition to disorders related to reversal or loss of brain asymmetry, there are a number of diseases which present a lateralized pathology, such that only one hemisphere of the brain is symptomatic. An example is unilateral polymicrogyria, where an excessive number of small gyri (folds) with abnormal lamination develop on one side of the brain, which are associated with seizures and sometimes mental retardation (Chang et al, 2006). The disease is found in pedigrees, suggesting a genetic basis. In fact, a recent study identified several families with more than one affected member where all cases within the study were right-sided, indicating the possible disruption of a right-sided gene (Chang et al, 2006). Another common disease with an asymmetric pathology is Parkinson's, which presents at onset an asymmetric loss of motor control and asymmetric loss of dopamine neurons (Kittappa et al, 2007). It is suggested that genes involved in neuron survival, such as *foxa3*, may be regulated in an asymmetric manner. All these pathologies strengthen the concept of a genetic control of brain asymmetry, which in turn supports genetic model tractability.

2.2 CNS asymmetry in vertebrates and invertebrates

2.2.1 Model systems of CNS asymmetry
C.elegans - a cellular and genetic model

To consider using worm as a model system for CNS asymmetry while there are those still arguing that brain asymmetry is uniquely human (e.g. Crow, 2002) seems a giant leap through phylogeny; however, *C.elegans* shows distinct left-right asymmetries of the nervous system and has proved to be invaluable for modelling more complex brains. The worm is largely bilaterally symmetrical but shows L/R asymmetries of the gonads, gut and nervous system. Asymmetry of both body and neural features is established at the 6-cell stage and is generated via rotations of the mitotic spindle and subsequent interactions mediated by Notch signalling (Oviedo and Levin, 2007). Worm shows both anti-symmetric (e.g. AWC odorant receptor neurons, Chuang et al, 2007) and directionally symmetric (e.g. ASE taste receptor neurons, Poole and Hobert, 2006) features of the nervous system. Directional ASE asymmetries are tightly linked to the body axis and depend on A/P axis formation at the 2-cell stage (Poole and Hobert, 2006), and curiously, in the case of AWC neurons, a directionally asymmetric state precedes an anti-symmetric one (Chuang et al, 2007). AWC neurons are directionally asymmetric in their response to ion channel (*nsy-4*) and gap junction (*nsy-5*) related genes (*nsy-4* is more effective in AWCL and *nsy-5* is more effective in AWCR), however, these directional biases seem to cancel each other out in terms of their effect on competitive Ca^{2+} signalling, resulting in a stochastic allocation of cell fate (Sagasti et al, 2001).

Similar mechanisms to those generating axial asymmetry in vertebrates are employed to lateralize the *C.elegans* nervous system; generation of laterality in ASE utilises the Notch pathway, and asymmetry in AWC requires Ca^{2+} and gap junctions. AWC asymmetry requires signalling between a local neural network around a zone of isolation, similar to the chick gastrula and frog blastula and in addition, AWC neurons are already directionally asymmetric in their response to gap junction component (*nsy-5*) expression, so like in other models, gap junctions are an intermediate part of the L/R pathway in worm (Oviedo and Levin, 2007).

Worm has proved effective in deducing cell-cell interactions and genetics involved in L/R asymmetric development, but it cannot offer an inroad into complex functional asymmetries. In addition, in contrast to *C.elegans,* the generation of CNS asymmetry in higher vertebrates may be independent of lateralization of the body axis (Levin, 2006). Therefore, a range of models for CNS asymmetry have been sought, some of which are particularly attractive to functional or anatomical studies.

Primates - the behavioural model

Structural asymmetries have been observed in primate brains, for example, chimpanzees and great apes have asymmetries in Broca's area and the planum temporale (Sun and Walsh, 2006). These are both known to be regions specialised for language processing in humans, and although functional asymmetries in vocal control within these areas have not been directly demonstrated, processing of species-specific vocalizations is known to be left hemisphere dominant in rhesus monkeys and macaques (Corballis, 2008).

Handedness in captive chimps has been demonstrated for a number of complex tasks, including extracting food from a tube, throwing and gestural communication (Hopkins et al, 2004). Whether handedness in primates has been demonstrated convincingly is contentious (Crow, 2004), as it has been suggested that handedness in this context is learned and is the result of interaction with predominantly right-handed humans. Early studies of wild primate hand use failed to demonstrate handedness, but this may be due to small sample sizes and excessively simple tasks (Corballis, 2008). A recent study of wild chimps not only demonstrated a population level left-hand bias for termite fishing, but showed that this was heritable (Lonsdorf and Hopkins, 2005). The authors compared data from other studies and showed that wild chimps were right-handed for two other complex tasks, demonstrating that hand preference does exist and is lateralized depending on the task. The combination of captive and wild studies present a compelling argument that primates show handedness, but in all cases the bias was around 2:1, compared to 9:1 for human handedness (Lonsdorf and Hopkins, 2005). Several theories have arisen from this difference in rate; some have taken it as evidence to suggest that a hominid-specific mutation enhanced the bias (Corballis, 2008), while others propose that as our definition of handedness is usually based on writing, we may be more mixed-handed than we think (Annett, 1999) and rates of bias for other tasks may be lower. Interestingly, it has been proposed that communication processing and handedness may have become tied through evolution, where much expression was through manual gesture before language *per se* evolved (Corballis, 2003).

Rodents - genetically tractable 'higher' vertebrates

Like primates and humans, mice have been shown to process species-specific vocalizations predominantly in their left hemisphere (Ehert, 1987). However, it has not been possible to demonstrate population level laterality of paw-preference in rodents despite numerous studies. Tasks requiring dexterity of a single limb, such as reaching for food through a small opening, have demonstrated that paw preference can be strong in an individual, but is randomised at the population level in mice, rats, cats and dogs (Sun and Walsh, 2006). Attempts at breeding left-pawed litters from strongly left-pawed mice failed (Collins, 1991), suggesting that laterality of paw preference is allocated randomly. However, Collins did succeed in breeding mice that were strongly or weakly lateralized from parents that showed either strong or little overall paw preference, supporting a genetic basis for asymmetry. Indeed, molecular asymmetries can be related to functional asymmetries in mice - dopamine expression is asymmetric and is correlated with paw preference in an ipsilateral manner (Sun and Walsh, 2006). Expression of *LMO4*, which is consistently higher in the right human foetal cortex, is asymmetric but randomised in mouse (Sun et al, 2005). Additionally, the *LRRTM1* 'left-handed gene', which is imprinted in humans, is biallelically expressed (Francks 2007) suggesting that left-handedness is not suppressed in mice. These data suggest that anti-asymmetry preceded directional laterality during the evolution of some asymmetric features and that some features (such as processing vocal communication) became population-lateralized before others (such as forelimb preference).

Genetic studies in rodents will be useful in identifying genes required for the generation and elaboration of asymmetry. Using qRT-PCR, many genes with asymmetric expression were identified in the developing hippocampi of rats; interestingly, asymmetric genes in early (P6) brains were usually higher on the right whereas later brains (P9, P60) more often had higher left-sided expression (Moskal 2006). When classifying these genes it was noticed that many were related to synaptogenesis and axonal growth, suggesting that these processes are temporally and / or spatially asymmetric in developing rodent brains (Moskal et al, 2006). Considering that the right cortex develops before the left cortex in humans, hippocampal formation is disrupted in schizophrenics and a microarray study identified a down-regulation of synaptic vesicle proteins in schizophrenic patients

(Moskal et al, 2006), rodents will doubtless be invaluable for modelling L/R CNS asymmetry and related disorders.

Avian models - epigenetics and visual asymmetry

Birds are a popular model for studying asymmetry of the visual system (outwardly manifested as preferred eye use), and have offered insights into how genetic, epigenetic and environmental factors can be incorporated to produce directional CNS asymmetry. Many visual asymmetries are lateralised at the population level in birds, for instance, chicks are more adept at discriminating food crumbs from pebbles with their right eye when pecking (Vallortigara and Rogers, 2005). Additionally, chicks that are more strongly lateralised for this task performed better when challenged with a dual task - pecking accurately and scanning for a model predator with the opposite eye. This suggests that the strongly lateralised chicks are more effective at processing two different inputs simultaneously (Vallortigara and Rogers, 2005). In the last few days before hatching, a stereotypical turn of the chick embryo leaves the left eye occluded and the right eye facing the eggshell where it is stimulated by light. Occlusion of the right eye and stimulation of the left by light can efficiently reverse visual lateralization in chicks (Rogers, 1990), whereas incubation in the dark leads to symmetric responses (Halpern et al, 2005). This is an example of the use of external stimuli to generate an asymmetry - of course, embryo turning is intrinsic, and probably under genetic control as it is in mice (Vallortigara and Rogers, 2005).

Steroid hormone levels affect the strength of lateralization; this has been shown experimentally (e.g. Rogers and Rajendra, 1993); in vivo, variation in levels may arise from deposits of corticosterone in the egg from the mother or levels in the chick itself (Halpern et al, 2005). This is an interesting example of a variable epigenetic affect, which would result in chicks that are more or less lateralized as a result of a stressful period during incubation, allowing behaviour to be modified by the environment to enhance survival chances. There is also the possibility of a gender-based effect through eostrogen and testosterone levels, indeed, male chicks are more strongly lateralized than female chicks (Rajendra and Rogers, 1993) and this may have a role in fighting behaviours.

The relative timing of light-induced asymmetry and neural development is important - in pigeon, a different region of the brain is asymmetric (the tectofugal

system) compared to the chick (the thalamofugal visual system) as a result of a difference in developmental timing - both asymmetric structures are forming during the phase of light stimulation (Halpern et al, 2005). This is a good example of a single mechanism lateralizing totally different regions of the brain in closely related species.

Zebrafish - the genetic, developmental, anatomical, behavioural...model of choice

One of the major drawbacks of most vertebrate model systems is the need to kill and dissect the animal in order to know anything about its brain structure. Embryonic development *in utero* can only be analysed in static stages and dynamic processes are difficult to study. Not so with zebrafish, whose rapid *ex utero* development can be analysed at high resolution under the microscope. Single-cell resolution studies of brain development in transgenic zebrafish can resolve processes such as neuronal migration (Mione et al, 2008), axon path-finding (Xiao et al, 2005) and synaptogenesis (Niell et al, 2004). Movements of large groups of cells (England et al, 2006) or small nuclei (Haas and Gilmour, 2006) can be imaged in elegant timelapse studies and the genetic tractability of zebrafish allows questions to be asked in mutant and morphant contexts. Fish are also amenable to detailed behavioural studies (Miklósi et al, 2006).

Zebrafish have a conspicuously asymmetric region of the forebrain, the epithalamus, which is part of a well-conserved output pathway of the limbic system (Concha and Wilson, 2001). The limbic system is thought to function as an integrative centre and is involved in emotional responses, feeding, motivation, sexual behaviours, memory formation and response to both emotional and sensory stimuli (Concha, 2004). Asymmetries in the epithalamus are conserved among vertebrates (Concha and Wilson, 2001) and are particularly striking in lower vertebrates, which show asymmetries in the pineal complex, paired habenular nuclei and efferent connections of the epithalamus to the interpenducular nucleus (IPN). Development of an asymmetric epithalamus from a symmetric state proceeds rapidly in the zebrafish embryo, beginning with unilateral gene expression at late somite stages and presenting well-defined asymmetries within two days. Development of asymmetric structures can be imaged in live transgenic animals, and lines are available that have specific expression of fluorescent proteins in pineal complex (e.g. Concha et al, 2003) and habenular (e.g. Aizawa 2005) cells.

The laterality of asymmetries in the epithalamus are concordant, indicating that development of asymmetric structures is closely linked. The parapineal, an accessory organ to the larger, medial pineal nucleus, is located on the left of the midline and projects axons to the left habenula. The paired habenular nuclei show left-right differences in gene expression, structure and connectivity to the IPN (Fig. 1, Concha et al, 2003; Gamse et al, 2003; Aizawa et al, 2005 and others).

Particular viable mutant strains of fish show reversal or randomisation of epithalamic asymmetries, and selection of wild-type or reversed fish on the basis of transgene expression in asymmetric brain structures allows for detailed behavioural studies that relate to brain laterality (Barth et al, 2005). Although asymmetry-related behavioural studies in teleosts are relatively rare up to now (Barth et al, 2005; Dadda et al, 2007), there is potential for a wide range of studies including emotional responses to stress, eye use preference and aggression as a function of laterality or asymmetry *per se*.

2.2.2 Initiation of asymmetry and assignment of laterality in the zebrafish CNS

The earliest known asymmetry in the zebrafish brain is the left-sided expression of Nodal pathway genes in the epithalamus at late somite stages. These genes, which are also expressed unilaterally in the body axis and regulate visceral asymmetry, are expressed strictly to the left of the midline in pineal complex and habenular precursor cells (Concha et al, 2000). The Nodal ligand *cyclops* (*cyc*) and the feedback inhibitor *lefty1* are activated at around 20-22s (somites), and are expressed in a short window before being rapidly down-regulated at around 26s (Rebagliati et al, 1998). The downstream effector of Nodal signalling, *pitx2c*, is activated at 24s and is maintained until at least 26hpf (hours post fertilization, Bisgrove et al, 1999).

Shortly after Nodal signalling, at around 26hpf, parapineal precursors aggregate, and begin their leftward migration from their bilateral origin at the dorsal midline. Parapineal cells move leftward in response to signalling from left-sided habenular precursor cells (Concha et al, 2003), forming a left-sided nucleus. At early stages of parapineal migration, left-right differences in gene expression levels, correlating with differences in the rate of neurogenesis, can be observed in habenulae (Aizawa et al, 2007, Roussigne et al, 2008). Subsequently, the parapineal promotes the elaboration of left-sided differentiated character in habenular neurons, such that

the paired habenular nuclei show asymmetries in gene expression, neuropil organisation and axonal projections (Concha et al, 2003; Aizawa et al, 2005; Gamse et al, 2005). Recent studies of the genetic mechanisms underlying brain lateralisation have directly demonstrated that reversal of Nodal pathway gene expression (right-sided expression) reverses brain laterality (Carl et al, 2007), so that the parapineal migrates to the right side and the right habenula takes on 'left' characteristics. However, Nodal does not directly specify 'left character' as the loss of Nodal pathway genes (or bilateral pathway activation) does not result in a symmetric brain, but in randomised asymmetry (anti-symmetry; Concha et al, 2000). Therefore, whilst consistent laterality relies on Nodal signalling, development of an asymmetric brain *per se* is not Nodal-dependent and must be generated by other signals. It has been proposed that left and right habenulae compete across the midline to attract the parapineal laterally (Concha et al, 2003). This competition is biased to the left by unilateral Nodal signals; in the absence of Nodal, it's possible that stochastic factors determine the outcome of this competition.

2.2.3 Elaboration of CNS asymmetries in zebrafish

Habenular asymmetries can be defined in terms of gene expression, cytoarchitecture and connectivity. The left habenula of 4dpf larvae have a greater density of neuropil, as visualised by acetylated tubulin immunostaining (Concha et al, 2000). The left habenula expresses the gene *leftover* (*lov*) at higher levels than the right (Fig. 1; Gamse et al, 2003), whereas the right habenula expresses higher levels of the related gene *dexter* (*dex,* Gamse et al, 2005). Efferent connections from the left habenula project primarily to the dorsal part of the IPN, whereas axons from the right habenula project to the ventral part of the nucleus (Fig. 1; Aizawa et al, 2005; Gamse et al, 2005). These differences in connectivity reflect projections from distinct medial and lateral subnuclei within each habenula. The *lov*-positive lateral subnuclei project to the dorsal IPN and the *dex*-positive medial subnuclei to the ventral IPN. The left habenula has a larger lateral subnucleus and a smaller medial subnucleus. The reverse is the case in the right habenula and this asymmetry in relative size of subnuclei leads to the observed asymmetric pattern of efferent connectivity (Aizawa et al, 2005). Labelling of single axons in left and right habenulae demonstrated that L/R

asymmetry is encoded at the level of axon morphology as well as targeting. Both habenulae contain

Left-sided parapineal

foxD3:GFP 3dpf

Pineal complex

Lateralised structures of the zebrafish brain

left   right

Dorsal 'view' 4 dpf

Habenular nuclei

Asymmetric gene expression

leftover 3dpf

Laterotopic connectivity

Fasciculus retroflexus

IPN
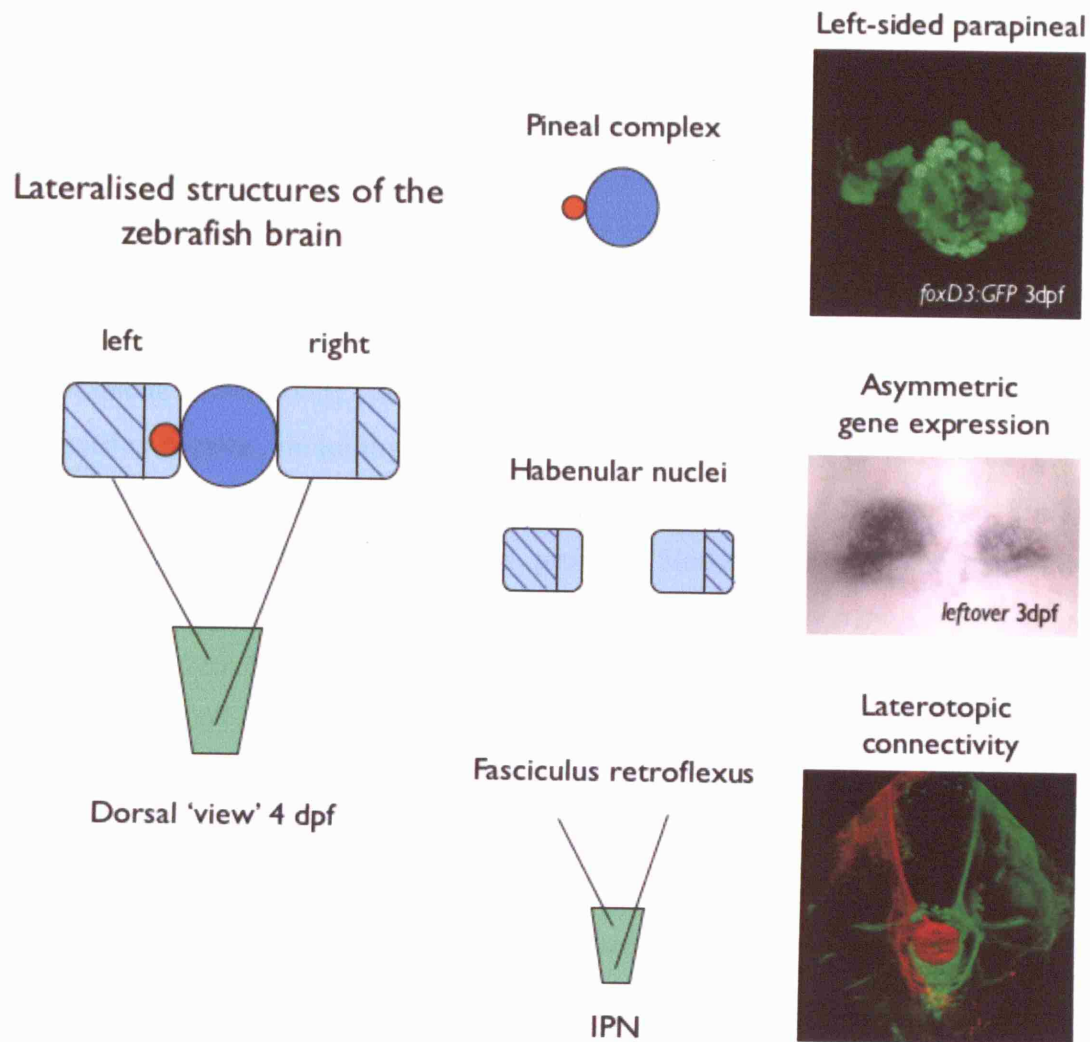
Figure 1. Zebrafish CNS asymmetries

Schematic illustrates asymmetric features of wild-type zebrafish embryos at 4 dpf, where the parapineal nucleus (red) sits to the left of the midline pineal (dark blue), sending axons to the left habenular nucleus (light blue). Gene expression is asymmetric in the habenulae (hatched blue lines), and efferent connections to a midbrain target, the interpenduncular nucleus (IPN, green) via the fasciculus retroflexus are laterotopic, such that neurons in the left habenula project predominantly to the dorsal part of the nucleus and neurons in the right habenula predominantly to the ventral part. Images that illustrate asymmetries are presented: *foxD3:GFP* in the pineal complex, *leftover* expression in the habenula nuclei and DiI and DiO fluorescent labelling of axonal projections from the habenulae to the IPN (image courtesy Isaac Bianco).

36

unipolar neurons with unique spiralling axons, but left and right neurons have different axon morphologies at the target (Bianco et al, 2008).

Epithalamic asymmetries are always concordant, such that the migration of the parapineal nucleus to the left is concomitant with denser neuropil and higher *lov* expression in the left habenula. If the parapineal migrates to the right, habenula asymmetries are also reversed. Elaboration of habenular asymmetries depends on parapineal migration, such that if the parapineal nucleus is ablated before it migrates, the left habenula fails to elaborate 'left character', *lov* and *dex* are expressed at equal levels on both sides, and both habenulae project to the ventral IPN (Bianco et al, 2008; Concha et al, 2003; Gamse et al, 2003, 2005). However, some subtle L/R asymmetries remain, including slight differences in the shape of habenular gene expression (Concha et al, 2003) and efferent axon morphology (Bianco et al, 2008). This suggests that early patterning steps, probably Nodal expression, independently affects both parapineal and habenular cells. Indeed, asymmetries in parapineal position and habenular neurogenesis appear at the same time, between 24 and 26hpf (Aizawa et al, 2007; Roussigne et al, 2008).

2.3 Linking body and brain asymmetry

Mechanisms that generate asymmetries in the body and brain are linked by lateralizing signals in the zebrafish. Recent studies have demonstrated that the Nodal ligand *southpaw* (*spaw*), which is expressed in the LPM but also affects Nodal signalling in the epithalamus (Long et al, 2003), unilaterally alleviates a bilateral repression of Nodal in the brain (Carl et al, 2007). The repressor in question is *six3*, which represses Nodal in the neural plate from late gastrulation stages (Inbal et al, 2007). This 'repression of a repressor' model had been previously suggested (Concha et al, 2003), but is now understood to be the mechanism that links asymmetries in the body and brain.

As predicted by this link between LPM and epithalamic laterality, embryos that have reversed Nodal signalling in the LPM have reversed brain structures (Barth et al, 2005). However, studies of human patients with total reversal or randomisation of body *situs* have revealed that functional asymmetries such as ear dominance and handedness are not reversed in these patients (Tanaka et al, 1999). These data suggest that unlike fish, humans do not utilize laterality signals from the body to lateralise the

brain (indeed, no evidence of lateralised Nodal signalling was found during analysis of asymmetric genes in human embryonic brains; Sun et al, 2005), leading to the theory that humans have separate head and body organisers of laterality (Levin, 2006).

2.4 Do several independent mechanisms lateralise the brain?

Studies on a line of fish with concordant reversal of visceral and epithalamic laterality (*fsi*) found that some, but not all, lateralized behaviours were reversed (Barth et al, 2005). For example, lateralised tasks such as viewing conspecifics and approaching food to bite are reversed in *fsi* fry. However, other lateralised behaviours, such as turning upon emergence in a novel environment, were not reversed (Barth et al, 2005). These data suggest that brain asymmetries underlying the lateralised behaviours that were not reversed are generated by distinct mechanisms from those that were. It is suggested that this models human brain reversals, which are often non-concordant, and that several separate organisers of laterality may be a conserved feature of the vertebrate brain (McManus, 2005). Indeed, left-handed humans always reverse processing of attention to local form but the usually do not show reversal of language processing, (Merovach et al, 2005).

An alternative way of considering non-concordance in the brain could be to imagine several sites at which a global lateralising signal has to be interpreted into lateralised structure. An inability to correctly interpret the global signal at one of these sites may reverse several linked structures (such as those underlying handedness and attention to local form), but as the other relay sites have not been affected, all other structures will be normally lateralised. This could even be imagined in *fsi* embryos; an early, global signal becomes reversed in the LPM and epithalamus, but is interpreted correctly at other relay sites in the brain.

2.4 Advantages of a lateralized brain

It is easy to imagine why asymmetry *per se* is advantageous, as it might make the brain more efficient at simultaneously processing several inputs (e.g. chicks feeding and scanning for predators), or faster at processing one (escape response in fish) (Vallitigora and Rogers, 2005). Less obvious is why population level lateralisations exist. Explanations given fall into two categories; that co-ordinated laterality is a by-

product of the need to synchronize one brain asymmetry with another (co-ordination within a brain), or that it is required for synchronization of social behaviours (co-ordination between brains). It is possible that the answer will be different depending on the asymmetry considered.

Handedness is the most frequently cited example of population level lateralisation. It is strongly lateralised in humans, weakly lateralised in primates and not at all in other mammals such as rodents, dogs or cats (Vallitigora and Rogers, 2005). It has been postulated that handedness became lateralised as a result of the evolution of gestural communication in primates (Corballis 2002, 2003). Vocal processing is lateralised to the left hemisphere in many species ranging from reptiles and birds through to mammals. When gestural and vocal communication were combined and processed together, control by the left hemisphere resulted in right-handed gesturing (Corballis, 2002). Indeed, chimps show an enhanced right hand preference when gesture is accompanied by vocalization (Hopkins and Leavens, 1998). This is an example of a 'by-product' explanation. Of course, the original lateralisation (vocal processing) itself requires explanation.

Other lateralised behaviours may be linked with the laterality of emotion processing; for example, the laterality of eye use in quail when approaching known (right eye) or unknown (left eye) conspecifics co-ordinates with a right hemisphere dominance for processing fear / caution, and a left hemisphere dominance for behaviours related to approach, exploration and courting (Zucca and Sovrano, 2008). Similar lateralisations are observed for eye use in fish (Sovrano and Andrew, 2006) and tail-wag direction in dogs (Quaranta et al, 2007). It may be impossible to distinguish whether these lateralisations are simply by-products of an original lateralised behaviour, or actively maintained by social selection. However, it is noticeable that many lateralised behaviours will be under social pressure: gestural communication, writing, courting behaviours, co-ordinated escape response in schooling fish etc.

It is certainly important to have consistent laterality of asymmetries, but perhaps some plasticity is useful. For example, left-handers are maintained at a constant percentage of the population and therefore must gain some advantage from being reversed. De-regulation of laterality may also assist adaptation to new environments, by generating novel behaviours (Barth et al, 2005).

3. Fgf8 in asymmetry

3.1 The Fgf pathway

3.1.1 Fgfs and FgfRs

Fibroblast growth factors (Fgfs) are diffusible ligands that show a high level of evolutionary conservation. Fgfs have been identified in *C.elegans* (*egl-17* and *let-756*) and *Drosophila* (*branchless*, *pyramus* and *thisbe*) (Mason, 2007) and vertebrates have gained more than 20 members through a series of gene duplications and translocations (Thisse and Thisse, 2005), with 22 FGFs identified in mouse and humans. Recent genome and *in silico* searches have identified orthologs of all human Fgfs in zebrafish (except *FGF9* which may have been lost from the genome) and several new paralogs - the zebrafish Fgf family contains at least 27 members (Itoh and Konishi, 2007). Zebrafish Fgfs can be divided into 7 subfamilies by phylogeny, which are essentially the same as in human (Itoh and Konishi, 2007).

Fgf ligands have a high affinity for heparin and signal through four tyrosine kinase receptors, FgfRs1-4. FgfRs are transmembrane receptors consisting of three Ig domains, a transmembrane domain and an intracellular tyrosine kinase domain. Situated between IgI and II are heparin binding and cell adhesion homology domains that facilitate and stabilise ligand binding (Böttcher and Niehrs, 2005). Different FgfRs are generated through expression of different genes and by alternative splicing, generating a type IIIb or IIIc C?-terminal domain of IgIII (Thisse and Thisse, 2005). Alternative splicing of FgfRs is tissue specific and dramatically affects ligand binding specificity (Dailey et al, 2005). The exceptions to this are Fgf11-14, which may signal in an FgfR-independent manner; they are located in the nucleus and have no known interaction with any FgfRs (Mason, 2007).

FgfRs exist as inactive monomers until they are bound by two Fgfs connected by a heparin sulphate proteoglycan (HSPG), which bind to the IgII and IgIII domains, initiating homodimerisation of the receptor. This induces trans-autophosphorylation of intracellular tyrosine residues, allowing binding and phosphorylation of Src homology (SH2) or phosphotyrosine binding (PTB) domain-containing proteins (Thisse and Thisse, 2005). Three pathways can be activated by Fgf-FgfR binding: Ras / MAPK, PLCγ / Ca^{2+} and PI3 kinase / Akt. The majority of signalling is through the

MAPK pathway, where briefly, activated FgfR binds a FRS2/Grb2/Sos complex, activating Ras by GTP exchange, which in turn activates Raf and the MAPK signalling cascade. The final member translocates to the nucleus and activates Ets family transcription factor encoding genes, such as *erm* and *pea3*, resulting in the transcription of Fgf-responsive genes (Böttcher and Niehrs, 2005). Target genes include several feedback inhibitors, such as *sprouty* and *sef* that negatively regulate Fgf signalling (Tsang and Dawid, 2004).

The vertebrate Fgf family is employed throughout development in many different processes; it follows that tight regulation of the pathway is necessary. This regulation occurs on several levels: at the cell surface, in the extracellular space and within the cell. For example, in HSPG-Fgf-FgfR ternary complexes at the cell surface, HSPGs function to enhance or stabilise the Fgf-FgfR interaction. Each different ligand-receptor complex requires a different HS domain that are themselves strictly spatio-temporally regulated during development; in addition, interaction with HSPGs limits the diffusion of Fgfs (Bishop et al, 2007). Feedback inhibition by *sproutys*, *sef* and *Mkps* is initiated by Fgf signalling and functions at the level of the MAPK pathway (*spry*), at the receptor level (*sef*) and in the nucleus (*Mkp1*) (Tsang and Dawid, 2004). It has also been shown that the extent of diffusion of Fgfs through the extracellular space can be restricted by endocytosis and that the rate of internalisation affects the signalling range of the ligand; thus target tissues can directly affect the availability of ligand to other target tissues (Sholpp and Brand, 2004).

3.1.2 Functions in development

Fgfs are required for multiple developmental processes and each member is used reiteratively throughout development. Fgfs pattern the embryo through regulation of cell fate (e.g. Griffin and Kimelman, 2003), cell survival and apoptosis (e.g. Raucci et al, 2008), motility and migration (e.g. Rottinger et al, 2008) and axon pathfinding (e.g. Irving et al, 2002).

A role for Fgfs in axis specification and patterning of the early embryo through mesoderm induction and maintenance is well conserved. In zebrafish, A/P patterning through posterior mesoderm specification and maintenance is regulated by Fgfs; where they act as competence factors for mesoderm induction by TGFβ signals, such as Nodal and Activin, by regulation of T-box genes (Böttcher and Niehrs, 2005).

Recent studies have indicated that t-box genes can also function upstream of Fgf signalling and that Fgfs interact synergistically with Oep in posterior mesoderm specification (Griffin and Kimelman, 2003).

Fgfs regulate cell movements in the embryo in a number of contexts. For example, Fgfs affect cell migrations during gastrulation both indirectly through regulation of other pathways, and possibly directly, as a chemotactic signal (Yang et al, 2002). In the mouse, Fgfs regulate gastrulation movements through *snail*, which probably affects migration by downregulating E-cadherins (Ciruna and Rossant, 2001). Evidence for direct chemotactic roles for Fgfs in cell migrations during gastrulation come from studies in chick embryos, where Fgf8 in the midline was shown to be chemorepulsive to anterior cells, pushing them away from the streak, co-operating with Fgf4 which is chemoattractive and directs cells toward the notochord (Yang et al, 2002). Conservation of Fgfs as chemotactic factors have been demonstrated by studies in the sea urchin embryo, where an FGFA/FGFR pathway is required for migration and differentiation of mesenchymal cells that form the skeleton of the pluteus larva (Rottinger et al, 2008). FGFA, which is restricted to lateral ectoderm by repressive Nodal signalling, acts at long range to attract the migrating cells that specifically express the receptor.

Other examples of direct chemotactic roles for Fgfs include FGF2 and FGF8 as potent chemoattractants for mouse mesencephalic neural crest (*in vitro*; *in vivo*, the role for FGF8 may be to localise FGF2 correctly; Kubota and Ito, 2000) and attraction of mesenchymal cells in the mouse limb bud by FGF2 and FGF4 (Webb et al, 1997). Also in the mouse, FGF10 is a chemoattractant for distal epithelium in lung branching morphogenesis (Park et al, 1998). Interestingly, the *Drosophila* Fgf ortholog *branchless* is necessary for tracheal branching and air sac morphogenesis (Sutherland et al, 1996), suggesting that the involvement of Fgfs in directing chemotaxis in developing airway systems is highly conserved. Recent studies in *Drosophila* have illustrated mechanisms by which Fgfs can affect migration, including the extension of cytoneme-like filopodia by migrating cells towards Fgf-expressing cells (Sato and Kornberg, 2002), and competition for lead cell position by budding tracheal epithelium based on levels of FgfR activity (Ghabrial and Krasnow, 2006).

Another general role for Fgfs during development is in regulating proliferation and differentiation. For example, a cassette of Fgfs is known to be required for limb

induction and morphogenesis, whereby Fgfs induce limb bud initiation, further Fgf expression and the formation of the apical ectodermal ridge (AER). Fgfs from the AER then maintain cell proliferation in the progress zone (Capdevila et al, 2001). Fgfs are also required to keep cells cycling in the presomitic mesoderm during somitogenesis (Dubrulle et al, 2001), and positively regulate proliferation and differentiation in osteogenesis (Raucci et al, 2008). In this context, Fgfs have different effects on stem cells depending on their age, where high Fgf signalling promotes survival in immature osteoblasts and continued signalling promotes apoptosis in mature osteoblasts, thereby regulating size of the progenitor pool (Marie et al, 2005).

Fgfs are required throughout neural development, from the earliest stages of neural induction (Sheng et al, 2003), through A/P specification of neural cells (Kudoh et al, 2004) to organiser functions at the midbrain-hindbrain boundary (Mason, 2007). Studies implicating Fgfs in axon pathfinding (Irving et al, 2002; Shirasaki et al, 2006) indicate that the Fgf family is additionally required for later stages of brain patterning.

3.2 Fgf8

3.2.1 Previously defined roles for Fgf8 in generating asymmetry

Fgf8 has been implicated in vertebrate left-right patterning in several different contexts. In mouse, rabbit and chick, FGF8 is required at the level of early asymmetric signalling at the node, but curiously, is required for Nodal expression in mouse (Meyers and Martin, 1999) and Nodal repression in rabbit (Fischer et al, 2002) and chick (Boettger et al, 1999). A recent study in fish suggests a role for Fgf8 upstream of Kupffers vesicle (KV; the equivalent of the node with respect to laterality decisions) development (Albertson and Yelick, 2005), while in human embryos, members of the FGF-pathway are asymmetrically expressed in the brain (Sun et al, 2004).

In the mouse, FGF8 hypomorphs show randomisation of organ situs, a loss of Nodal cassette genes in the LPM and a loss or disruption of peri-nodal Nodal expression (Meyers and Martin, 1999). FGF8 was termed a 'left-determinant', however, FGF8 transcripts are expressed at the midline and are not overtly asymmetric at the node. This led to the speculation that FGF8 protein is the morphogen transported to the left by rotation of nodal cilia. However, recent data

suggests that FGFs (probably FGF8 considering its pattern of expression) are required for the launch of Shh and RA-containing NVPs from microvilli in the node (Tanaka et al, 2005).

In contrast, in chick, Activin induces Fgf8 signalling on the right side of the node where it is required to repress Nodal (Boettger et al, 1999). *Fgf8* expression is asymmetric at the chick node and is downstream of other asymmetrically expressed genes such as *cActIIa* and *Fgf18* (Ohuchi et al, 2000). Ectopic Fgf8 cannot affect left-sided *Shh* expression, but represses Nodal at the node and in the LPM (Boettger et al, 1999), suggesting that it functions downstream of the initiation of nodal asymmetry.

In the rabbit, FGF8 is expressed symmetrically in the node like in mouse, but acts to suppress Nodal signalling on the right like in chick, such that inhibition of FGF8 on the right induces bilateral Nodal expression (Fischer et al, 2002). Interestingly, FGF8 asymmetries can be detected earlier than nodal flow occurs (Okada et al, 2005), suggesting that similar to chick, symmetry-breaking mechanisms in rabbit precede cilia function. It is suggested that the parallels in signalling between rabbit and chick at the node reflects their similar architecture of embryogenesis, and that this is more likely to reflect node asymmetries in human embryos as all three develop as a flat blastodisc (Fischer et al, 2002).

A number of genes related to FGF-signalling are asymmetrically expressed in human foetal cortex, including *FGFR1-3, FGF13* and several members of the MAPK signalling cascade (Sun et al, 2005), suggesting that FGFs are involved in transducing asymmetries in the developing brain. The anterior neural ridge expresses FGF8 and patterns the cortex (Fukuchi-Shimogori and Grove, 2001); it has been suggested that FGF8 from this organizer could be asymmetric, or could initiate asymmetric expression of other genes such as LMO4, which it is known to regulate (Sun et al, 2005). However, this is purely speculative.

A recent study in zebrafish has implicated Fgf8 in KV development and L/R patterning of the embryo (Albertson and Yelick, 2005). The authors observed a complete absence of KV in a large proportion of *fgf8* mutant embryos and a resulting disruption of epithalamic and LPM Nodal signalling and visceral organ *situs*. Additionally, they found that in *fgf8* mutant embryos with an intact KV, pharyngeal arch defects were asymmetric and consistently lateralised, suggesting that Fgf8 may

have a role in suppressing latent asymmetry of paired structures (Alberson and Yelick, 2005).

3.1.3 Fgf8 in zebrafish

In addition to its role in L/R patterning in the zebrafish, Fgf8 has been implicated in early D/V patterning, heart formation, somitogenesis and patterning of the limb bud (Thisse and Thisse, 2005). In particular, Fgf8 is known to be reiteratively required for patterning the embryonic nervous system (Mason, 2007). The zebrafish *fgf8* mutant *acerebellar* (*ace*) was originally identified for its lack of cerebellum and mid-hindbrain boundary (MHB) (Brand et al, 1996, Reifers et al, 1998); additionally, it is required for boundary formation between the diencephalon and mesencephalon (Sholpp et al, 2003), retinal patterning (Picker and Brand, 2005) and induction of otic and epibranchial placodes (Maroon et al, 2002; Nechiporuk et al, 2007). As such, *ace* is a pleiotropic mutant, and studies of Fgf8-dependent patterning have often required focal, or temporally regulated modulation of the pathway to properly dissect Fgf8 function (e.g. Maves and Kimmel, 2002).

3.3 This study

In this study we identify the *fgf8* mutant *ace* as an 'asymmetry mutant'. Our analysis of epithalamic structures in *ace* reveals that this normally asymmetric region of the brain is symmetric in terms of both parapineal position and habenular development. Analysis of lateralised visceral organs reveals that L/R patterning of the body axis is unaffected, as is axial Nodal signalling and KV development, suggesting that the asymmetry phenotype we observe is brain-specific. Nodal signalling in the brain is also unaffected, indicating that lateralisation mechanisms are intact. We show that in wild-type embryos, *fgf8* is expressed by the habenulae and that *fgfR4-* and *etv5-* expressing parapineal cells respond to Fgf signals during their migratory phase. This is confirmed by knocking down all Fgf signalling in a temporally controlled manner during parapineal migration. Furthermore, we rescue parapineal migration in *ace* by introducing a focal, exogenous source of Fgf8 and show that Fgf8 can direct the laterality of migration in the absence of a bias in Nodal signalling. In light of these data, we define a mechanism for breaking neuroanatomical symmetry, through Fgf8-dependent regulation of bi-stable left- or right-sided migration of the parapineal. We

propose that the combined action of Fgf and Nodal signals ensures the establishment of neuroanatomical asymmetries with consistent laterality.

Materials and Methods

1. Embryo Manipulations

1.1 Maintenance of Zebrafish

Breeding zebrafish (Danio rerio) were maintained at 28 °c on a 14 h light / 10 h dark cycle (Westerfield, 1993). Embryos were obtained by natural spawning, reared and staged according to standard procedures (Kimmel et al, 1995). Temperature shifts from 28 °c to 25 °c at tailbud stage were performed to obtain late somite stage embryos. Lower temperature shifts were never used as these can result in perturbations of laterality. Occasionally 0.002 % phenylthiourea was added to fish water from 12 hpf to prevent pigment formation.

Embryos were obtained from the wild-type lines *AB, Tübingen, and Tup Logfin. Mutant embryos were obtained from the heterozygous or homozygous crosses of the transgenic lines *Tg(foxD3:GFP)* (Gilmour et al, 2002), *Tg(flh:GFP^{711})* (Concha et al, 2003) and *Tg(ET11:GFP)* (Choo et al, 2006), and heterozygous crosses of the mutant lines *acerebellar^{ti282}* (ace^{ti282}) (Reifers et al, 1998) and maternal zygotic *one-eyed pinhead* (*MZoep*) (ref) fish. *LZoep* embryos were generated from *MZoep* mutants as described (Concha et al, 2000) by injection of *oep* RNA at the 1-cell stage (see RNA injection protocol below).

1.2 Manipulations of Live Embryos

1.2.1 Preparation of RNA for Injection

Templates for synthesis of mRNA for injection were generated by linearising pCS2+ clones at the 3' end using an appropriate restriction enzyme. Following purification of the DNA by 1x phenol:chloroform extraction, 1x chloroform extraction and precipitation with 0.1 volumes of 3MNaAc and 2.5 volumes of 100% ethanol at -80 °c for 30 min, the DNA was resuspended in ddH$_2$O. 1 μg of the linear DNA was used for the *in vitro* transcription.

In vitro transcriptions were carried out using the SP6 Message Machine Kit (Ambion). Transcription reactions were incubated for 2 h at 37 °c. The DNA template was removed by a 15 min incubation with DNase, also at 37 °c. The reaction was stopped by addition of 180 µl dH$_2$O. The RNA was extracted once with phenol:chloroform and once with chloroform and precipitated with 0.1 volumes of NaAc 3 M and 2.5 volumes of ethanol at -80°c for 30 min. The RNA was microfuged for 15 min at 4°c, washed in 70% ethanol and resuspended in 20 µl dH$_2$O. The RNA concentration was determined by spectrophotometry.

1.2.2 Preparation of DNA for Injection

DNA was linearised as described above. 1 µl was run on a gel to check for completion of digest. DNA concentration was determined by spectrophotometry and diluted appropriately.

The following DNA was injected in this study:

1. *hs_fgf8* (Halloran et al, 2000) in pBSIIKS vector, *hsp70* promoter; injected at 100ng/µl, ~1 nl/embryo

1.2.3 Preparation of Morpholinos for Injection

Various morpholinos (MOs, Gene Tools) were designed against start or splice sites and surrounding bases. The sequences and injection quantities are as follows:

1. *fgf8* MO (Draper et al, 2001) 5' - TAGGATGCTCTTACCATGAACGTCG - 3'   5 ng injected

2. *spaw* MO (Long et al, 2003) 5' - GCACGCTATGACTGGCTGCATTGCG - 3'
10 ng injected

3. *ntl* MO (Nasevicius & Ekker, 2000) 5' - GACTTGAGGCAGGCATATTTCCGAT - 3'
9 ng injected

MOs were diluted to desired concentration (ranging from 0.1mM-1mM) in 1x Danieu's medium for injection. Diluted MOs were pre-heated to 65 °c for 5 mins immediately before injection to eliminate toxic secondary structure.

1.2.4 Injection procedure for DNA, RNA and morpholinos

Embryos at the 1-2 cell stage, still in their chorions, were aligned against a glass slide in a petri dish in a small volume of fish tank water. Injections were at a volume of approximately 1-2 nl, depending on quantity required. Injections were either directly in to a single blastomere or in to the yolk, using a borosilicate glass capillary needle with inner filament (Clarke) attached to a Picospritzer (General Valve). Injected embryos were left to develop at 28 °c.

1.2.5 Blocking FgfR activity

Embryos were treated with the drug SU5402, to block FgfR activity (Mohammadi et al, 1997). Embryos, at stages and intervals listed below, were incubated at 30.5°c in 9μM ('low') or 21μM ('high') SU5402 (Sigma) dissolved in DMSO (1% final concentration) in embryo medium containing PTU. Control embryos were incubated for equivalent periods in 1%DMSO / embryo medium / PTU. At the end of the treatment period, the drug was washed out in 5 x 5 minute, gently agitated washes in 1%DMSO / embryo medium / PTU. After washes, embryos were transferred to fresh embryo medium / PTU and allowed to develop to 72 hpf, at which point they were fixed for immunostaining and imaging.

Embryos were treated at the following stages in this study:
20 - 24 hpf; 24 - 28 hpf; 36 - 44 hpf

2. Molecular Biology Techniques

2.2. Permeablisation of embryos

1. Protinase K

Store PK at -20°c at 10 mg/ml. Dilution of PK stock 1:1000 (1x) in PBTw or as directed below.

Up to tailbud, no PK; 2-10 ss, short rinse in 1x PK; 10-15 ss, 4 mins 1x PK; 16-26 ss, 5 mins 1x PK; 24 hpf, 20 mins 1x PK; 30 hpf, 30 mins 1x PK; 36-48 hpf, 1 h 1x PK; 2.5 dpf, 1 h 1.5x PK; 3 dpf, 1 hpf 2x PK; 4 dpf, 1 h 3x PK.

2. Trichloroacetic acid (TCA)

Store TCA at -20°c at 10%. Dilute to 2% with PBS before use. Permeablisation as described below followed by 2x 10 min washes; all on ice.

Up to tailbud, no TCA, 2-20 ss, short rinse; 20 ss - 24 hpf, 2 min; 2 dpf, 8 min; 3 dpf, 10 min; 4 dpf, 12 min.

2.3 Immunohistochemistry

Pre-treatment of Embryos:

Fix in 4% Paraformaldehyde (PFA) for 3 hours at room temperature or overnight at 4°c, or 2 % TCA for exactly 3 hours at room temperature. After fixing rinse twice and wash 3 x 15 mins PBTX (Phosphate buffered saline + 0.8% Triton-X) on shaker. Transfer to methanol via 5 mins rinse in 50 % MeOH / 50 % PBT. N.B. Mixing PBT and methanol produces an exothermic reaction – this solution must be made up at least 15 mins before use. Rinse twice in 100% methanol and store at -20°c for at least 30 mins, or up to 2 months.

Preparation and permeablisation:

Rehydrate embryos by rinsing in 75% MeOH/PBTw 50% MeOH/PBTw, 25% MeOH/PBTw, followed by 2x 5 mins wash in PBTw. Permeablise using Proteinase K or TCA; digestion times vary with embryo age (see table). Rinse 3x PBT. Post-fix

in 4% PFA for 20 mins at room temperature, wash 3x 5min PBT. Refix embryos in 4% PFA/PBS for 20 mins at room temperature. Rinse 3x and wash 2x5 min with PBTw.

Immunolabelling:

Pre-incubate in Immunoblock (IB) for at least 1 hour at room temp on shaker. Replace IB with IB + primary antibody overnight at 4°c on shaker. Antibody dilutions typically range between 1:200 to 1:2000, each needs to be titrated individually. The following day, remove primary antibody (can be kept at 4°c for reuse) rinse 3x in PBT. Wash at least 4 x 30min in PBT on shaker. Pre-incubate in IB for at least 1 hour at room temp on shaker. Incubate in IB + secondary antibody overnight at 4°c on shaker. The following day, rinse 3x in PBT. Wash at least 4 x 30min on shaker.

For fluorescent immunostaining:

Embryos are now ready to image. Transfer to 75% glycerol (through 25% and 50% glycerol/PBS) and mount. Keep at 4°c in the dark and image as soon as possible.

For permanent Horse Radish Peroxidase (HRP) staining:

Make up 1ml DAB solution (500μl stock in 30ml PBS) per tube of embryos. Transfer embryos to 24 well plate. Remove PBT and add 500μl DAB solution. Incubate for 20 min. Meanwhile to remaining DAB solution, add 2μl 0.3%H_2O_2 per ml. After incubation, add 500μl DAB+ H_2O_2 to each well to initiate peroxide reaction. Monitor reaction closely. When desired intensity of staining is reached, wash 3 x 10min in PBS. Fix 20 mins, room temp. with 4% PFA. Wash 3 x 10mins in PBT. Transfer to 75% glycerol (through 25% and 50% glycerol/PBS). Store at 4°c.

In situ probes used in this study were as follows:

cpd2   (Gamse et al, 2003)
cxcr4b (Chong et al, 2001)
cyc   (Rebagliati et al, 1998)
dex   (*kctd8;* Gamse et al, 2005)
erm   (Münchberg et al, 1999)
etv5   (Roussigne and Blader, 2006)
fgf8   (Reifers et al, 1998)
fgfR4 (Thisse et al, 1995)
foxa3 (Dirksen and Jamrich, 1995)

gfi	(Duforq et al, 2004)
ins	(Milewski et al, 1998)
lefty1	(Bisgrove et al, 2000)
lov	(*kctd12.1*; Gamse et al, 2003).
pax8	(Pfeffer et al, 1998)
pitx2c	(Bisgrove et al, 2000)
spaw	(Long et al, 2003)
Tag1	(*contactin2;* Warren et al, 1999)

2.4 Whole Mount *In Situ* Hybridization

Pretreatment of embryos:

Dechorionate embryos in PBTw (PBS + 0.1% Tween-20) and fix in 4% PFA/PBS for 3 hours at room temperature or overnight at 4°c. Wash once in PBS, once in 100% methanol (MeOH) and store in fresh MeOH at -20°C. Leave embryos in MeOH for at least 2 hours before use, or for up to 2 months.

Preparation and permeablisation:

Rehydrate embryos by rinsing in 75% MeOH/PBTw 50% MeOH/PBTw, 25% MeOH/PBTw, followed by 2x 5 mins wash in PBTw. Permeablise using Proteinase K (PK); dilution of PK stock 1:1000 (1X) in PBTw or as directed below. Digestion times vary with embryo age. Digestions are at room temperature with tube lying on its side. Digestions are at room temperature with tube lying on it's side. Rinse 3x PBT. Post-fix in 4% PFA for 20 mins at room temperature, wash 3x 5min PBT. Refix embryos in 4% PFA/PBS for 20 mins at room temperature. Rinse 3x and wash 2x5 min with PBTw.

In situ Hybridisation:

To prehybridize, remove PBTw and replace with prehybridization solution. allow to equilibrate replace with fresh prehybridization solution. Incubate for at least 2 hrs at 65°C. Dilute anti-sense probe in hybridisation solution as required. This needs to be individually titrated for each probe generated. Pre-heat probe mix for 3-5 mins in hot block. Remove the prehybridisation solution and add preheated probe. Incubate overnight at 65°C.

Post-hybridization washes and dioxygenin detection:

Remove probe and store at -20°C for reuse. The following washes are all carried out at 65°C: 1x 5 mins in prehybridization mix, 1x 5mins in 25%prehyb/75% 2xSSC, 1x 10 min 2x SSC, 3x 30 min 0.2x SSC. Rinse embryos 1-2x in MAB at room temperature. Incubate embryos in 500ml 2% Blocking Agent (Boehringer) in MAB (MABl) for 2-3 h at room temperature. Replace with anti-DIG-AP antibody (1:6000ml) in MABl and leave overnight at 4°C. Wash embryos at least 6 x 15 mins in MAB at room temperature. Rinse embryos twice in 0.1M Tris pH 9.5/0.1% Tween-20. Transfer embryos to a multi-well plate containing 0.5-1ml BM purple substrate, at room temperature, avoiding exposure to light. Incubate in the dark without agitation until colour reaction is complete. Chromogen can be substitute with 0.1M Tris pH 9.5 / 0.1% Tween-20 at any time for short periods of storage during development. Rinse 3x in PBS. Refix embryos 20min in 4% PFA/PBS at room temperature. Rinse 2x in PBS and replace with 70% glycerol/PBS for imaging and storage.

3. Misexpression Techniques

3.1 Focal DNA Electroporation

Mount embryos in 1.5% low melt agarose in an appropriate orientation for the tissue you wish to electroporate, in araldite well slides. Mount embryos towards left hand end of well, leaving a few mm between the embryo and well wall. Agarose should not fill more than half the length of the well. Allow agarose to set for 6 mins. Using a John Weiss surgical blade, cut a small section of agarose away to create a channel to the area you wish to electroporate. For embryos older than 16 somites, fill well with 10mg/ml pronase for a few seconds to soften skin. For embryos older than 24hrs, this can be raised to 10secs. Rinse 2x with Embryo Medium. Fill well with Embryo Medium. Pull aluminium silicate micropipettes with a tip diameter of 1-2μm using a micropipette puller. Fill needle with 2μl solution containing purified plasmid DNA resuspended in dH$_2$O. (For GFP, 0.5mg/ml is sufficient. Concentration should be no higher than 1.3mg/ml, above this is toxic). Fit needle over negative electrode, making

sure electrode is in contact with solution. Place positive electrode immediately behind embryo, making sure it is immersed in embryo medium. Stimulation parameters for DNA: 1 s long train of 1 ms square pulses at 200Hz and 45V. Trains can be delivered multiple times with 1s interval between trains. (These parameters can be modified depending on the area you wish to electroporate e.g. single or groups of cells; or for electroporation of other molecules e.g. RNA, morpholinos). Release embryos from agarose by pushing channel walls apart and return to embryo medium inoculated with antibiotic to recover. GFP can generally be visualised after 8 hours.

Constructs used for electroporation in this study are as follows:

1. α-*tubulin-GFP* (Wang et al, 1998) in pBSIIKS vector, α-*tubulin* promoter; electroporated at 0.5µg/µl

2. *fgf8* (Reifers et al, 1998) in pCS2+ vector, sCMV promoter; electroporated at 0.5µg/µl

3. *kaede* (Amalgaam, Tokyo) pKaede-MC1 vector, CMV promoter; electroporated at 0.5µg/µl

4. *lefty1* (Bisgrove et al, 2000) in pCS2+ vector, sCMV promoter; electroporated at 0.5µg/µl

5. *pCS2DsRed* (Clontech) in pCS2+ vector, sCMV promoter; electroporated at 0.5µg/µl

3.2 Fgf8 Bead Implantation

To prepare Fgf8 protein: Recombinant mouse Fgf8b from R&D systems (cat # 423-F8). Reconstitute according to R&D instructions: Dissolve protein in 100ul filter-sterilized PBS with 0.1% BSA to make 250 µg/ml stock. Aliquot & store at -80°c.

To load beads on the day of the experiment: add a drop of 'Polybead' Polystyrene 15 µm microspheres (Polysciences # 18328) solution to a 1.5ml Eppendorf tube. Divide in half and add to another tube. Spin both tubes in table-top microfuge. Remove buffer, add 100 µl filter-sterilized PBS to each tube, agitate and spin down beads again. Repeat wash 2 more times, remove PBS. Add 20 µl 0.5mg/ml

heparin in f/s PBS to precoat beads (heparin – Sigma cat # H5284), agitate on shaker at room temp for 20 mins. Spin down, remove heparin. Add 10ul 250ug/ml Fgf8 to one tube and 0.1% BSA to the other (these are your control beads) and agitate at RT for 2 hours. Spin down, remove protein / BSA, add 50ul f/s PBS to rinse. Chill until use. Bead implantation: mount embryos in 2% low-melt agarose / fish water in glass rings, with the area you wish to implant into facing up. Cover the exposed agarose with fish water inoculated with 1% penicillin / streptomycin antibiotic. With a micropipette, transfer a few microlitres of beads onto the agarose. Puncture skin with tungsten needle and push bead into the hole. The wound should heal immediately. Beads are more easily manipulated if squashed slightly with forceps. This can be done when you move beads close to your embryo, making sure beads are never exposed to the air. Allow embryos to recover for at least 1 hour before releasing from agarose. Then photograph, fix or move to multiwell plate innoculated with antibiotic for further growth.

4. Microscopy and Image Manipulation

Fluorescent labelling was imaged by confocal laser-scanning microscopy (Leica SP2) using x25 oil immersion and x40 water immersion objective lenses. z-stacks were typically acquired at 1-2μm intervals. 3D-projections were generated from the stack of images using Volocity (Improvision) software. Live embryos were imaged under x20 water-immersion DIC or fluorescent optics (Axioskop 2 FS microscope, Carl Zeiss). *In situ* hybridisation stainings were photographed using a Jentopix C14 digital camera attached to a Nikon Eclipse E1000 compound microscope. For presentation, image manipulation was performed using Photoshop CS2 (Adobe) software.

5. Statistics

Statistics were performed using InStat software (Graphpad). Categorical data was analysed using Fisher's Exact test, where the p-value is two-tailed. Confidence is denoted by *p for <0.05 and **p for <0.01.

6. Solutions

DAB stock: Sigma D5637; 25mg/500μl dH$_2$O, store aliquots at -20°c and thaw immediately before use.

DAB solution: 500μl stock in 30ml PBS.

Danieau solution: 58 mM NaCl, 0.7 mM KCl, 0.4 mM MgSO4, 0.6 mM Ca (NO3)2, 5 mM HEPES, pH 7.6)

Hybridisation solution: 50% formamide, 5x SSC, 0.1% Tween-20, 5 mg/ml torula (yeast) RNA, 50 μg/ml Heparin. Adjust pH to 6.0 by adding 92μl 1M Citric acid per 10ml solution.

Immunoblock (IB): 10% goat serum, 1% DMSO, 0.8% Triton-X in PBS.

Malic Acid Buffer (MAB): 150mM NaCl, 100mM Malic Acid. Adjust with NaOH to pH 7.5, higher pH required to get MA in solution.

Malic Acid Buffer Block (MABl): Use Blocking Reagent (Boehringer Mannheim): make up as 10% stock in MAB, heat to solublise. Store frozen aliquots at -20ºC.

Prehybridisation solution: 50% formamide, 5x SSC, 0.1% Tween-20. Adjust pH to 6.0 by adding 92 μl 1M Citric acid per 10 ml solution.

Torula RNA: prepared by proteinase K digestion of RNA with subsequent phenol-, phenol/chloroform-, and chloroform-extraction. RNA is precipitated and dissolved in RNase-free water.

Trichloroacetic acid (TCA): Dissolve 500 g of TCA in 227 ml distilled water, this is 100% stock. Dilite to 10% in PBS and store aliquots at -20°c.

Chapter 1 - Nodal signalling directs parapineal laterality

1. Introduction

It has previously been shown that mutations affecting Nodal signalling randomise CNS laterality (Concha et al, 2000) and that Nodal genes are asymmetrically expressed in the epithalamus (Bisgrove et al, 2000). However, it has not been demonstrated that epithalamic Nodal signalling can directly influence laterality decisions. Habenula ablation experiments have revealed that left and right habenular nuclei compete across the midline to attract the parapineal laterally (Concha et al, 2003), where this competition is probably biased to the left by Nodal signalling. To add further support to this theory and to determine whether the Nodal pathway has a direct role in lateralisation of the epithalamus, we sought to unilaterally abrogate Nodal signalling on the right side of the brain in embryos that have bilateral Nodal expression, to see if parapineal cells migrate to the contralateral side of the brain.

2. Results

2.1 Local Modulation of Nodal Signalling Directs Parapineal Laterality

(This work was carried out in collaboration with Marcel Tawk.)

Nodal expression is bilateral and the laterality of the epithalamus in *ntl* morphants is normally randomised, such that morphants are equally likely to show a rightward parapineal migration as a leftward one (Concha et al, 2000). We wanted to ask whether unilateral mis-expression of *lefty1*, which encodes a potent secreted antagonist of Nodal signalling, could bias migration of the parapineal to one side in this context through introducing a LR bias in Nodal signaling. To achieve this we used a technique novel to zebrafish, focal electroporation (Haas et al, 2001), to deliver DNA constructs to small groups of cells in the brain.

Early electroporation trials, following the published protocol developed in *Xenopus* (Haas et al, 2001), resulted in large groups of cells being electroporated with the reporter construct (Fig. 1). Preferring single, or small groups of cells to express exogenous protein (in case large quantities of Lefty1 adversely affected pineal complex development or the
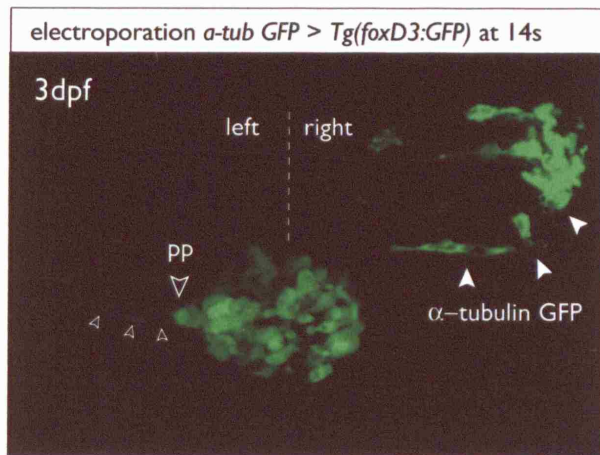
Figure 1. Local mis-expression of proteins in the brain can be achieved by focal electroporation

Dorsal view of a 3dpf (days post fertilization) *Tg(foxD3:GFP)* embryo, with a large group of electroporated cells expressing the reporter α-tubulin-GFP (white arrowheads). The parapineal is visualised as a distinct group of cells to the left of the pineal organ (large white-edged arrowhead), projecting axons towards the left habenula (small white-edged arrowheads).

pp, parapineal nucleus.

ability of parapineal cells to migrate), we modulated the protocol to obtain this outcome (see Methods section).

Once we were able to consistently achieve electroporation in small numbers of cells, we proceeded with mis-expression of *lefty1* in *ntl* morphants. *ntl* morpholino was injected into *Tg(foxD3:GFP)* embryos, in which pineal and parapineal cells are visualised. Cells were either electroporated with a fluorescent reporter construct (*α-tubulin-GFP* or *pCS2DsRed;* Wang et al, 1998, Finley et al, 2001) or a reporter construct plus a *lefty1* construct (Bisgrove et al, 2000). Cells elecporated with *α-tubulin-GFP* were easily distinguished from pineal complex cells as expression of *α-tubulin-GFP* is membranous, whereas *Tg(foxD3:GFP)* is cytoplasmic (Fig. 2e, compare white-edged arrow with white arrow). Electroporated cells were also always lateral to the pineal complex (Fig. 2c-e). Embryos were electroporated at 14s (somites), in order to allow sufficient time for transcription and translation from the exogenous construct before endogenous Nodal expression and parapineal migration is initiated.

58

After electroporation, high levels of exogenous *lefty1* mRNA expression could be detected in small numbers of cells on the right side of the epithalamus (40hpf, Fig. 1a,c), co-localising with the site of *α-tubulin-GFP+* clones (Fig. inset 1b). As Lefty1 can signal at a distance from its site of expression (Chen and Schier 2002), then it is likely that Lefty1 activity spreads beyond the immediate vicinity of the electroporated cells.

All *ntl* morphant embryos electroporated with *lefty1* on the right showed a leftward migration of parapineal cells (n = 10/10, 100%; Fig. 1e). Conversely, co-electroporation of *α-tubulin-GFP* and *pCS2DsRed* constructs had no effect on laterality and parapineal migration remained randomised (left parapineal = 52%, right = 48%, n = 29; Fig. 1d).

This data shows that local modulation of Nodal signalling is able to impose laterality on embryos that would otherwise develop randomised CNS asymmetries. It also suggests that competition by left and right sides of the brain to attract the parapineal laterally can be biased to one side by a bias in Nodal signalling levels.

This work was published as part of a larger study in *Neuron* **39** 423-438 (2003).
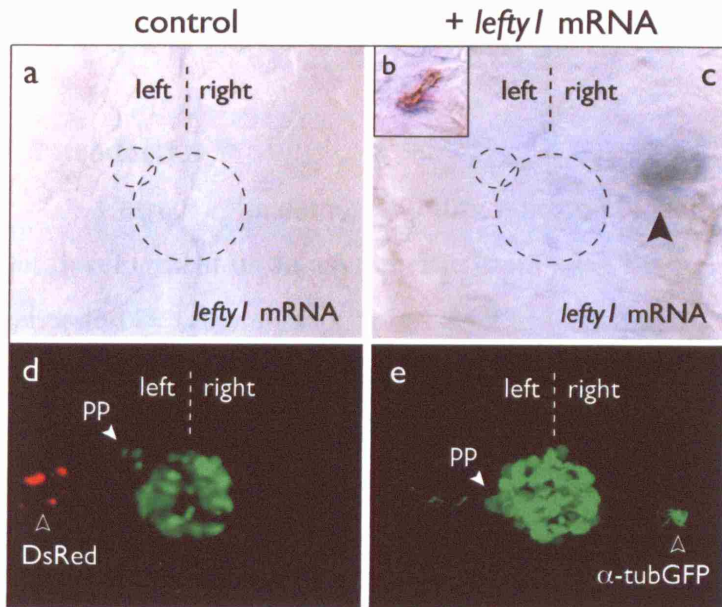
Figure 2. Electroporation of *lefty1* in the epithalamus directs parapineal migration

(a-e) Dorsal views of *ntl*MO / *Tg(foxD3:GFP)* embryos, with anterior to the top. Embryos were electroporated with *α-tubulin-GFP* + *pCS2DsRed* in the left epithalamus (a,d), or *α-tubulin-GFP* + *lefty1* in the right epithalamus, at 10 - 14ss (b-d).

     (a-c) Whole-mount *in situ* hybridisation for *lefty1* mRNA at 40hpf. Exogenous *lefty1* mRNA is detected after *lefty1* DNA electroporation (arrowhead in c), co-localising with α-tubulin-GFP+ cells (brown immunostaining, inset b).

     (d,e) Epithalamic expression of *foxD3:GFP* transgene (pineal and parapineal organs), electroporated DsRed (arrowhead in d) and electroporated α-tubulin-GFP (arrowhead in e) in live embryos at 48hpf (d) and 72hpf (e).

α-tub-GFP, α-tubulin-GFP; DsRed, pCS2DsRed; pp, parapineal.

Chapter Two - Fgf8 is required for CNS asymmetry

1. Introduction

Correct epithalamic laterality relies on Nodal signalling (Concha et al, 2000), but development of an asymmetric brain *per se* is not Nodal-dependent and must be generated by other signals. It has been proposed that left and right habenulae compete across the midline to attract the parapineal laterally (Concha et al, 2003). This competition is biased to the left by unilateral Nodal signals; in the absence of biased Nodal signalling, stochastic factors must determine the outcome of this competition. To elucidate the genetic basis underlying this competition, which initiates the break of epithalamic symmetry, we screened lines of fish for mutant phenotypes in which the epithalamus appeared symmetric.

2. Results

2.1 Parapineal nuclei are found at the midline in 3 dpf *ace* embryos

In a shelf-screen, we observed that the *fgf8* mutant *acerebellar*[ti282] (*ace*) (Reifers et al, 1998) has a midline located parapineal organ that fails to migrate to the left of the pineal (Fig. 1a-h). This was confirmed using several markers, including the parapineal specific marker *gfi* (Duforq et al, 2004), which labels the left-sided parapineal in wild type embryos at 60hpf. In *ace* mutants we found most embryos to have a midline located parapineal nucleus (Fig. 1a,b). The transgene *Tg(ET11:GFP)* is expressed after 60hpf in parapineal cells (Choo et al, 2006). Using the nuclear marker TOPRO-3 to distinguish habenulae and pineal stalk, we can locate the parapineal within the epithalamus in *Tg(ET11:GFP)* embryos. In 3dpf *Tg(ET11:GFP)* embryos, the parapineal nucleus is positioned to the left of the pineal nucleus and projects axons to the left habenula, which arborise in a space surrounded by habenula cell bodies (Fig. 1c). Parapineal cells in *ace* / *Tg(ET11:GFP)* are located at the midline, anterior to the pineal stalk in most embryos (Fig. 1d). Few axons can be visualised; most mis-project posteriorly, remaining close to the pineal stalk. These data suggest that the parapineal primordium is unable to migrate to a left-sided position in *ace* embryos. To exclude the possibility that the midline location of the parapineal at 3dpf in *ace* embryos is the result of a delayed or mis-directed migration, we analysed parapineal cell behaviour at a range of stages.
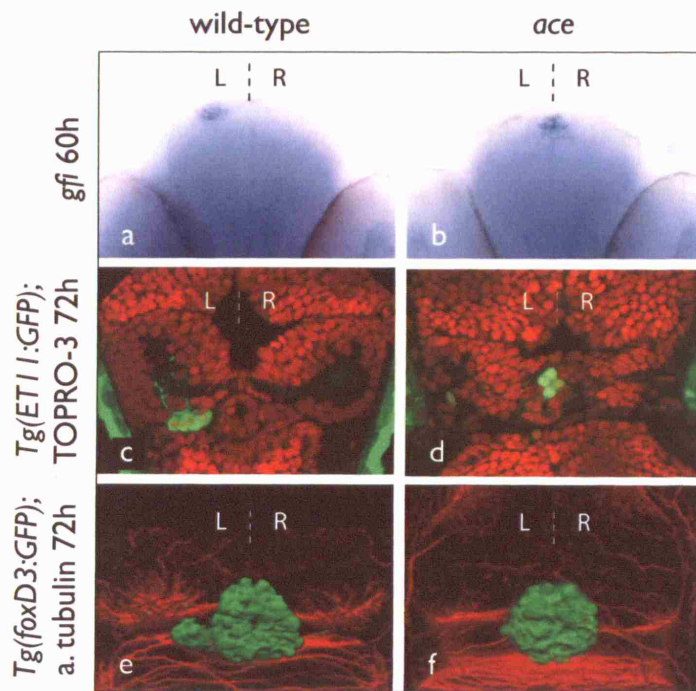
Figure 1. The *fgf8* mutant *ace* has a midline located parapineal

(a-b) Frontal view of parapineal-specific *gfi* expression in wild-type and *ace* 3 dpf embryos, with dorsal to the top. Parapineal cells are at the midline in *ace* (b).

(c-f) Dorsal views of confocal images of the epithalamus in wild-type and *ace* 3 dpf embryos, with anterior to the top.

(c-d) The parapineal-specific marker *Tg(ET11:GFP)* is present (green), but expressing cells remain at the midline in the *ace* embryo compared to the wild-type embryo at 3 dpf. Brain morphology is visualised using the nuclear marker TOPRO-3 (red). A single *z*-slice is presented for each example.

(e,f) 3D reconstructions of pineal/parapineal nuclei and axons (green; *Tg(foxD3:GFP)*) and neuropil of the habenular nuclei (red; anti-acetylated tubulin) are visualised. The parapineal nucleus is located to the left of the pineal in wild-type (e), but cannot be visualised in ace as it is located midline and ventral to the pineal nucleus (f).

L, left; R, right.

2.1 Parapineal cells remain static at all stages in *ace* embryos

The transgenic line *Tg(foxD3:GFP)* expresses GFP in pineal and parapineal cells (Fig. 1e). Parapineal cells start to express GFP shortly after they begin to migrate leftwards, allowing us to image their movements over time in live embryos. In order

to determine whether parapineal cells make any migratory movements in *ace* embryos, we analysed GFP expression at several time-points between 30 and 96hpf in *Tg(foxD3:GFP)* and *ace / Tg(foxD3:GFP)* embryos (Fig. 2). Actively migrating parapineal cells expressing a low level of GFP are visualised anterior and to the left of the pineal nucleus at 30hpf in *Tg(foxD3:GFP)* embryos. By 36hpf the parapineal nucleus is more condensed and expresses higher levels of GFP. At 48hpf it reaches the furthest lateral point in its migration pathway, and by 60hpf begins to move medially, and ventral to the pineal nucleus. Axonal projections to the left are first observed at around 42hpf (Concha et al, 2003; this study), and a tightly fasciculated bundle of axons that arborises in the left habenula is observed from 60hpf. Most *ace / Tg(foxD3:GFP)* embryos do not show migration of a parapineal nucleus at any time point. If cells do migrate, they tend to do so singly or as small groups of 2 or 3 cells, often migrating to aberrant positions rostral or caudal to the pineal nucleus (see arrowheads, Fig. 2). Very rarely, a cohesive group of parapineal cells migrates laterally in *ace* embryos, but these nuclei project few axons and most do not move ventral to the pineal nucleus. We found that at 3dpf, similar to the other markers we have analysed, most *ace / Tg(foxD3:GFP)* embryos had a midline parapineal organ. This midline nucleus lies ventral to the pineal at 3dpf and cannot be distinguished from a dorsal aspect (e.g. Fig. 1h), but can be visualised using 3D-rendering techniques.

In order to quantify parapineal migration in *ace*, we imaged large numbers of *ace / Tg(foxD3:GFP)* embryos at 3dpf, 3D-rendered the images and grouped embryos into 3 classes based on parapineal position. Parapineal cells were distinguished by virtue of their lateral and / or ventral position with respect to the pineal nucleus and by their stereotypical axonal projections. Class I comprises *ace* embryos that have a migrated parapineal, similar to wild-type embryos (Fig. 3b). A nucleus consisting of 4 or more cells that is found lateral to the pineal and is visible from a dorsal aspect was considered to approximate wild-type migration and was included in this class. We find 14% of *ace* embryos fit into this category (n = 3/22). Class II comprises embryos that have 1, 2 or 3 parapineal cells that have moved lateral to the pineal (Fig. 3c). This was the most abundant class (11/22; 50%). In many cases where there was more than one lateral cell, cells had moved independently of each other and were found far apart, often on opposite sides of the midline (see arrow heads, Fig. 3c). Rotation of
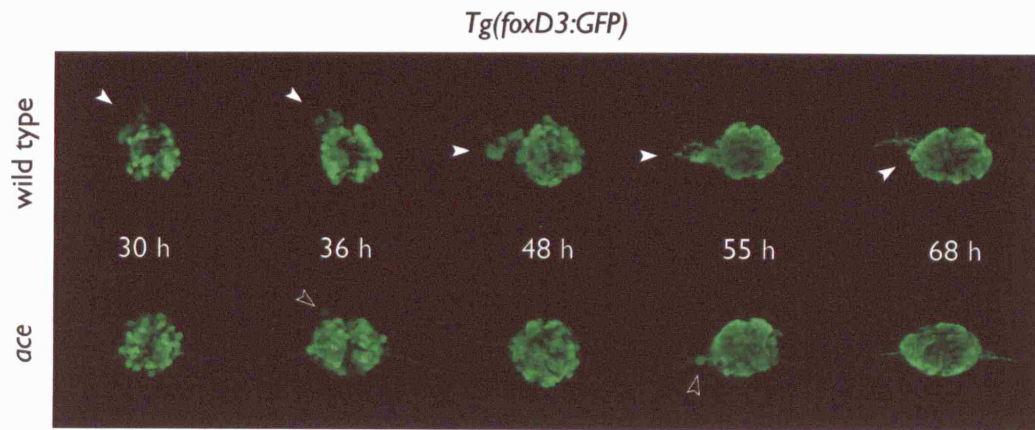
Figure 2. Parapineal cells remain static at all time-points in ace embryos

Parapineal migration is tracked over time in wild-type *Tg(foxD3:GFP)* embryos (top row; white arrowheads). Parapineal cells move from the left of the anterior midline at 30hpf, to occupy a left lateral position at 48hpf. By 68hpf, cells have moved medially and ventral to the pineal nucleus. *ace* embryos do not show migration of a cohesive parapineal nucleus at any time point (bottom row) but sometimes show movement of single cells away from the pineal nucleus (white-edged arrowheads).

3D-reconstructions reveal the majority of parapineal cells to be clustered at the midline in these embryos, ventral to the pineal nucleus. Class III embryos had no lateral parapineal cells at all (Fig. 3d) and were the second most frequent type (8/22; 36%). Parapineal nuclei in these embryos were always ventral to the pineal nucleus and were positioned at, or close to, the midline. Classes II and III represent embryos without parapineal migration and total 86% of *ace* embryos. Together, these data demonstrate that the majority *ace* mutant embryos have ventral, midline located parapineal cells, which is the result of a defect in migration.

Previous studies have demonstrated a close correlation between the asymmetric development of diencephalic structures (Halpern et al, 2003). Crucially, parapineal and habenula lateralities are always concordant, and ablation of the parapineal primordium leads to a loss of overt habenula asymmetry (Gamse et al, 2003). Therefore we next wanted to address whether habenula asymmetries develop normally in *ace* embryos.
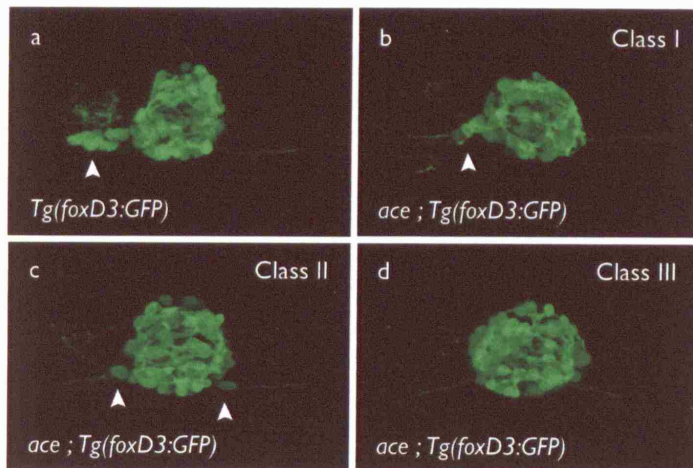
Figure 3. Most *ace* embryos do not show parapineal migration

(a) All 3dpf wild-type embryos (98%) have a left-sided parapineal.

(b-d) *ace* embryos can be classified according to parapineal migration phenotype:

> (b) Class I embryos (14%) show 4 or more parapineal cells in a cohesive group to the left of the pineal (white arrowheads), approximating wild-type migration.

> (c) Class II embryos (50%) show migration of 1, 2 or 3 cells away from the pineal nucleus (white arrowheads), usually to different locations, often opposite sides of the midline.

> (d) Class III embryos (36%) do not show migration of any parapineal cells away from the pineal nucleus.

In Class II and Class III embryos (totalling 83% of *ace* embryos), rotation of 3D images reveals parapineal nuclei are located at the midline, ventral to the pineal nucleus.

2.3 Asymmetric habenular markers are symmetric in *ace* embryos

Left and right habenulae show distinct patterns of gene expression and structure in wild-type embryos by 4dpf (Concha et al, 2003; Gamse et al, 2003, Gamse et al, 2005, Aizawa et al, 2005). Analysis of the paired habenula nuclei in *ace* revealed that they do not exhibit these normal left-right differences (Fig. 4). All markers examined in *ace* embryos were reduced and predominantly symmetric in their expression. *Leftover* (*lov*, recently renamed *kctd12.1* to conform with human gene nomenclature), a member of the *KCTD* (potassium channel tetramerisation domain containing) gene family, is expressed at higher levels in the left habenula than the right in wild-type embryos, and its asymmetric expression is known to be dependent on parapineal migration (Gamse et al, 2003). Analysis of *lov* expression in *ace* embryos revealed

65
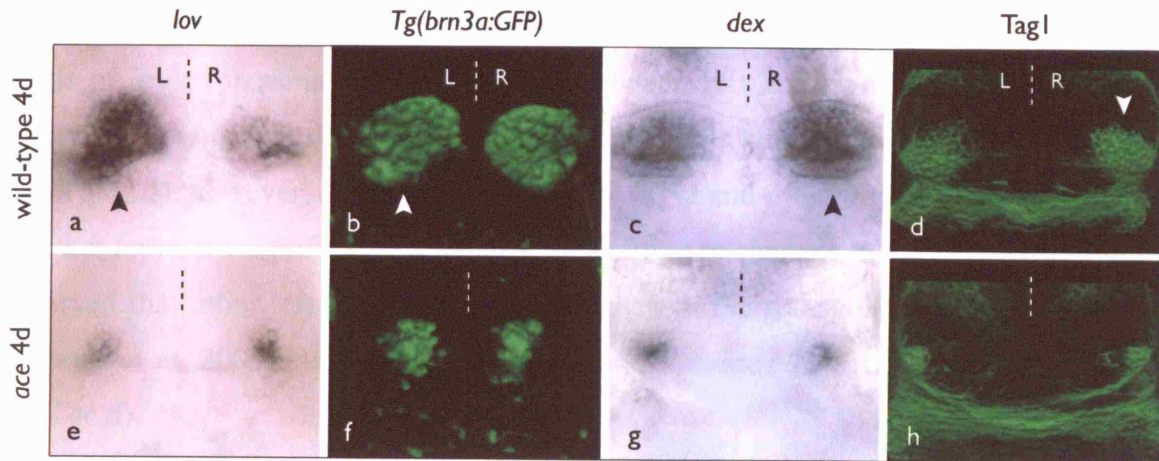
Figure 4. *ace* embryos do not develop habenular asymmetries

(a-d) Dorsal views of asymmetric habenular markers in 4dpf wild-type embryos; *lov* and *Tg(brn3a:GFP)* are expressed at higher levels on the left, *dex* and Tag1 at higher levels on the right (arrowheads denote larger habenula nucleus).

(e-h) Dorsal views of 4dpf *ace* embryos; all markers are reduced and symmetric.

L, left; R, right.

Table 1. Habenula laterality in *ace*

		L>R	R>L	E	sL>R	sR>L	sE	None
lov	wild-type (n=352)	96%	4%					
	ace (n=112)				27%	14%	54%	6%
dex	wild-type (n=129)	5%	90%	5%				
	ace (n=84)				53%	21%	26%	
tubulin	wild-type (n=146)		94%	4%	2%			
	ace (n=98)				34%	9%	55%	2%

Table displaying *n* values and percentages of habenular laterality in *ace* and WT embryos as visualised by asymmetric markers *lov* and anti-tubulin (left-sided in wild-type) and *dex* (right-sided in wild-type). E, equal; L, left; L>R, left habenula expression domain is larger than right; R, right, R>L, right habenula expression domain is larger than left; s, small habenulae compared to wild-type.

that it is reduced and symmetric at 4dpf (Fig. 4a,b). Occasionally slight differences in levels of *lov* expression can be observed between left and right habenulae. More embryos showing this slight asymmetry have higher levels on the left than the right (see Table 1), however, as differences are very slight and often difficult to score, this may not represent significant asymmetry. In addition to changes in *lov* expression, we observed that other left-lateralised markers, such as the transgene *Tg(brn3a:GFP)* (Aizawa et al, 2005), are reduced and symmetric in *ace / Tg(brn3a:GFP)* embryos (Fig. 4c,d).

A small domain of *lov* expression is characteristic of right habenula nuclei in wild-type embryos and is concomitant with a larger domain of *dexter* (*dex*, recently renamed *kctd8* to conform with human gene nomenclature) (Gamse et al, 2005), also a member of the *KCTD* gene family. We considered the possibility that the reduced *lov* expression we observe in *ace* mutants reflects an expanded domain of *dex* expression in both habenulae. We find that this is not the case and that *dex* has a reduced and symmetric expression pattern, which is similar to *lov* (Fig. 4e,f; compare to Fig. 4a,b). This is also true of the GPI-anchored protein *Tag1* (*contactin2;* Warren et al, 1999) in *ace* embryos (Fig. 4g,h), which is expressed at slightly higher levels on the right in wild-type habenulae at 4dpf (Carl et al, 2007).

Medial neuropil is denser in the left habenula than the right in wild-type embryos at 4dpf, as visualised by anti-acetylated tubulin immunostaining (Fig. 5a, white dashed brackets; Concha et al, 2000). This medial neuropil is found within the *lov*-positive domain (Gamse et al, 2003) and is therefore contained within the medial habenular sub-nucleus (Aizawa et al, 2005, Gamse et al, 2005). In order to find out whether all features of the medial sub-nucleus are affected in a similar way, we examined neuropil in *ace*. We find that it is greatly reduced in both habenulae, to the extent that in many embryos the medial neuropil tufts are missing altogether, leaving only small, symmetric lateral tufts (Fig. 5b, white-edged arrows; Table 1). The remaining embryos show only a very slight asymmetry in neuropil density between left and right sides, where similar to *lov* expression, left lateralisation is more common than right. This asymmetry arises from a small medial tuft of neuropil, which is almost always concordant with parapineal axon projections (Fig. 5c, arrow; Table 1). We find it unlikely that these medial tufts arise as a result of parapineal axon projections, as after ablation of the parapineal, neuropil asymmetries remain (Concha

et al, 2003). This is also true in the case of parapineal axotomies that have been performed before axons synapse with habenular neuropil (I.H.Bianco, personal
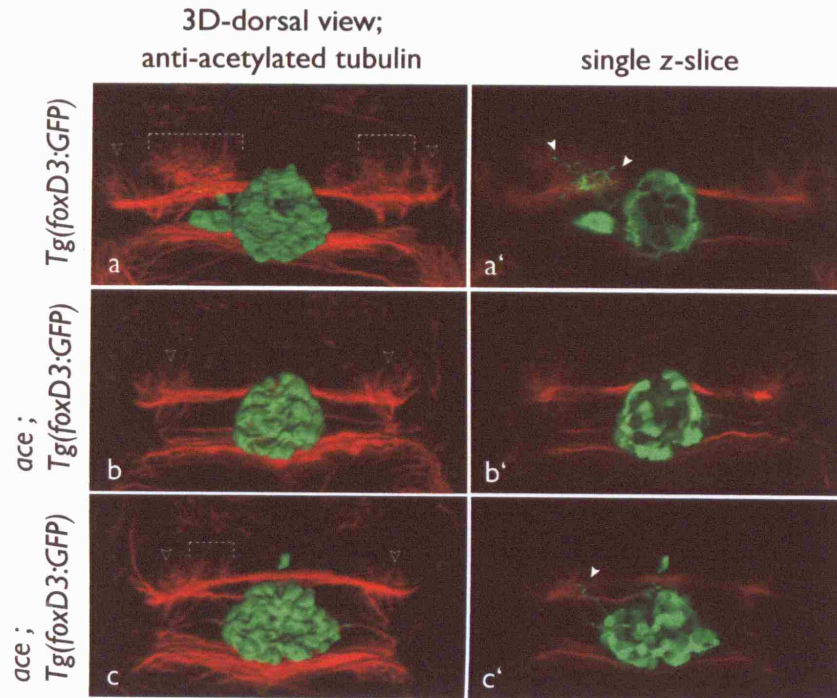
Figure 5. Asymmetries in neuropil density are lost in most *ace* embryos

(a-c) 3D-reconstructions of dorsal views of the pineal complex (α-GFP, green) and surrounding axons and neuropil (α-acetylated tubulin, red) in 3dpf *Tg(foxD3:GFP)* embryos.

(a'-c') Single *z*-slice from the stack of images, allowing visualisation of axon projections from the parapineal to habenular neuropil.

Wild-type *Tg(foxD3:GFP)* embryos have higher density medial neuropil on the left (a; dashed brackets), coinciding with parapineal axon terminations (a'; white arrowheads). Most *ace* embryos only have small lateral neuropil tufts remaining (b; white-edged arrowheads), which do not receive any parapineal axon projections (b'). A few *ace* embryos show a small amount of asymmetric medial neuropil (c; dashed bracket), which usually coincides with one or two parapineal axon terminations (c'; white arrowhead).

communication). Therefore we speculate that axons are attracted towards any remaining medial neuropil in the *ace* mutant.

The loss of asymmetry in habenular markers could in part be due to defective parapineal migration as ablation of parapineal cells has been shown to result in both

habenulae displaying a 'right-sided' phenotype (Gamse et al, 2003). In order to assess whether Fgf8 is required for habenula development *per se*, we next analysed symmetric habenular markers.

2.4 Symmetric habenular markers are reduced in *ace* embryos

Markers labelling all habenular neurons, such as *cpd2* (Gamse et al, 2003), are expressed symmetrically in left and right wild-type habenulae at 3dpf (n = 48; Fig. 6a). We observe that *cpd2* expression is reduced in both habenulae in *ace* embryos (n = 35; Fig. 6b). This is also true of the marker *cxcr4b* (wild-type n = 83, *ace* n = 51; Fig. 6c,d), which labels an undefined population of cells, thought to be habenula neuron precursors (Roussigne et al, 2008). The bilaterally reduced expression of both asymmetric and symmetric markers suggests that Fgf signalling is required during the maturation of both left and right habenulae.
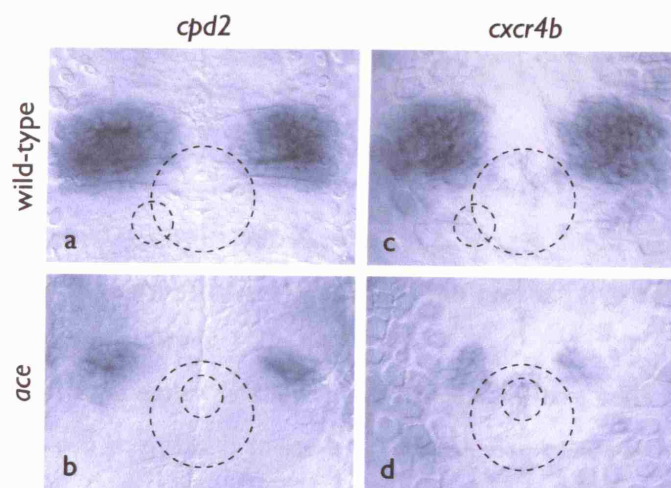
Figure 6. Symmetric habenular markers are reduced in *ace* embryos

(a,b) The bilateral marker *cpd2* is symmetric in wild-type embryos at 4dpf (a); expression of this marker remains symmetric in *ace* but expression level and area is greatly reduced (b).

(c,d) Similarly, the *cxcr4b* is bilaterally symmetric in 4dpf wild-type embryos (c) but is severely reduced in *ace* (d). Dashed lined indicate pineal (large circle) and parapineal (small circle) position.

It has been proposed that early asymmetries in habenula development precede, or are concomitant with, the earliest stages of parapineal migration, and that such differences may determine the laterality of parapineal migration (Aizawa et al, 2007). We considered the possibility that early defects in habenula development could account for the lack of parapineal migration in *ace*. Therefore, we were interested to analyse early habenula markers, such as *cxcr4b*, in *ace* embryos.
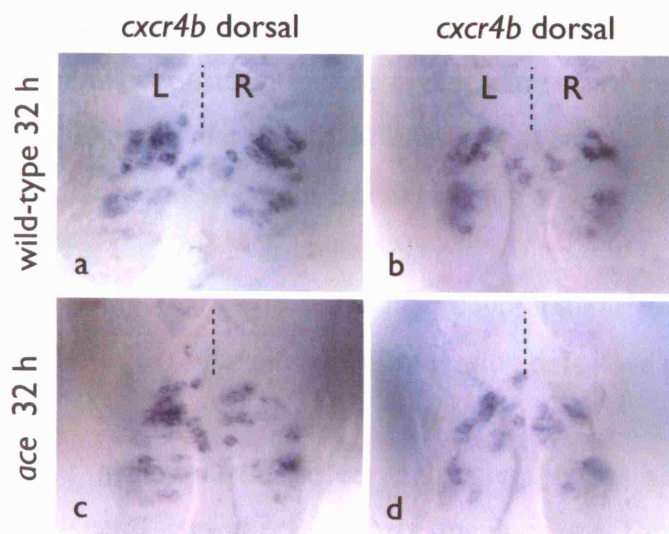
Figure 7. Early *cxcr4b* expression is largely unaffected in *ace* embryos (M. Roussigne)
Dorsal views of *cxcr4b* expression in presumptive habenulae of 32 hpf wild-type (a,b) and *ace* (c,d) embryos.

Wild-type embryos show more *cxcr4b*-positive cells on the left than on the right, although this can be difficult to see by eye (a,b). Expression is largely unaffected in most *ace* embryos (c,d), where L-R asymmetry still occurs (c). A small number of *ace* embryos show a slight delay (d), such that fewer cells express *cxcr4b* at 32 hpf.

L, left; R, right.

2.5 Early markers of habenula neurons are largely unaffected in *ace* embryos
(this work was done by **Myriam Roussigne**)

cxcr4b is expressed by what are thought to be habenula neuron precursors and represents the earliest asymmetric habenular marker (Roussigne et al, 2008). Although a few *lov*-expressing cells can be detected at 28hpf in wild-type embryos

and differences in numbers of expressing cells between left and right sides are observed, these differences are not significant (Aizawa et al, 2007). Conversely, at least 1.5-fold differences in *cxcr4b*-expressing cell number can be observed at 28h in wild-type embryos (Roussigne et al, 2008), with the higher number of cells on the left side. When we analysed *cxcr4b* expression in *ace* at 32 hpf, we found that it was similar to wild-type in most embryos; that is, expressed bilaterally in the region of presumptive habenula, with a higher number of expressing cells on the left side (Fig. 7a-d). Asymmetries are sometimes difficult to see by eye; cell-counting experiments have confirmed that wild-type embryos (Roussigne et al, 2008) and *ace* embryos (data not shown) consistently have higher numbers of cells on the left compared to the right side. The only detectable difference between *ace* and wild-type was a slight delay in some *ace* embryos, such that expression at 32 hpf resembled a wild-type embryo at 30 hpf (e.g Fig. 7d). Altogether, *cxcr4b* expression is largely unaffected in *ace* embryos, suggesting that early habenular development proceeds normally and may not be responsible for the parapineal migration defect we observed.

Mutations that affect brain laterality can also affect asymmetric development of visceral structures if early mechanisms for left-right axis specification are disrupted. For instance, mutations in pathways involved in development of dorsal forerunner cells, Kupffer's vesicle or midline structures can affect global laterality (Amack and Yost, 2004, Essner et al, 2005, Rebagliati et al, 1998). Fgf8 is involved in many aspects of embryonic development (Thisse and Thisse, 2005) and as such, *ace* is a pleiotropic mutant. Therefore we next wanted to analyze visceral development in *ace* embryos to determine whether axial left-right development is affected by loss of Fgf8 signalling.

2.6 Laterality of visceral asymmetries is normal in *ace* mutant embryos

Heart looping of the ventricle to the right and atrium to the left in wild-type embryos is preceded by a leftward 'jog', such that the whole heart primordium is displaced to the left side of the midline from around 24hpf. Fgf8 is required for normal heart development (Reifers et al, 2000), such that *ace* embryos have small, straight heart tubes with ventricle defects, which have often developed severe odeama by 60hpf. Therefore we considered the earlier phenotype, heart jogging, to be preferable to heart

looping as an indicator of cardiac laterality in *ace*. When we scored heart jogging at 28hpf, we found that almost all wild-type embryos, as expected, showed a leftward heart jog (98%, n = 352; Table 2). In accordance with mutant screening data (Chen 1996), we find heart jogging to be unaffected in most *ace* embryos, with 88% showing a normal leftward laterality (n = 112; Table 2). Of the remaining embryos, 7% showed rightward and 5% showed no jogging (primordium positioned at the midline). As the laterality of gut looping and heart jogging are both governed by signals initiating from the lateral plate mesoderm (LPM; Bisgrove 2000), we next wanted to analyse whether the position of the liver and pancreas, both of which arise from the gut primordium, are affected by loss of Fgf8 signalling.
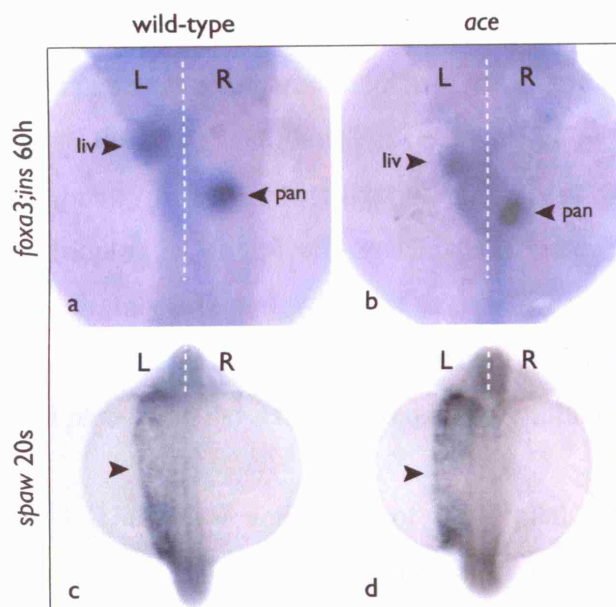
Figure 8. Visceral asymmetry and Nodal expression in the body axis is unaffected in *ace* embryos

(a,b) *foxa3* labels the liver primordium and *ins* labels the pancreas in 60hpf embryos. The liver is positioned to the left of the midline and pancreas to the right in wild-type embryos (a); laterality of viscera is unaffected in *ace* embryos (b).

(c,d) *spaw* is expressed unilaterally on the left at 20s in wild-type embryos (c; black arrowhead). Expression is unchanged in *ace* (d; black arrowhead).

Liv, liver; pan, pancreas; L, left; R, right.

Gut looping follows a stereotypical pattern in zebrafish embryos (Horne-Badovinac et al, 2003): an initially straight, solid rod of endodermal cells formed during mid-somitogenesis curves to the left at 26hpf. This leftward bend occurs at the anterior end, the region which gives rise to the esophagus, intestinal bulb and liver. Following this is the bend to the right of a more posterior region that gives rise to the pancreas. By 60hpf, the liver primordium is clearly to the left of the midline and the pancreas to the right. Using *foxa3* (Dirksen and Jamrich, 1995) as a marker for liver position and *preproinsulin* (*ins;* Milewski et al, 1998) as a marker for pancreas position, we were able to assess the laterality of endodermal viscera in *ace* (Fig. 8a,b, Table 2). We found that positioning of the liver is completely unaffected in *ace* embryos, whereby 100% of mutants had a left-sided liver primordium (Fig. 8b; n = 84, compare to wild-type where 100% were left-sided, Fig. 8a; n = 129). Similarly, pancreas position was unaffected: 97.5% of ace embryos (Fig. 8b; n = 84) had a right-sided pancreas compared to 98% of wild-type embryos (Fig. 8a; n = 129).

These data suggest that Fgf8 signalling is not required for generating visceral asymmetry or for correct lateralization. Liver and pancreas positioning, arising from gut looping, is completely unaffected in *ace*. Positioning of the heart primordium is only slightly affected, with just over 10% of mutants showing reversed or no jogging. It is possible that this slight perturbation of cardiac laterality is linked to early heart field patterning defects observed in *ace* mutants (Yelon, 2001).

Unilateral activation of the Nodal pathway in the left LPM is known to regulate visceral laterality in the embryo (Bisgrove et al, 2000). Our results indicate that left-right patterning of viscera is largely unaffected by loss of *fgf8* signalling and so we assume that Nodal signalling is similarly unaffected. However, our data contradicts a recent report suggesting Fgf8 acts upstream of Nodal signalling, by modulating Kupffer's Vesicle (KV) development, resulting in laterality defects of visceral structures in a high proportion of *ace* embryos (Albertson and Yelick, 2005). In light of this, and in order to confirm our findings, we analysed KV development and LPM Nodal signalling in *ace* mutants.

Table 2. Visceral laterality in *ace*

			left	right	midline
heart jog	wild-type	(n=352)	98%	2%	0%
	ace	(n=112)	88%	7%	5%
liver position	wild-type	(n=129)	100%	0%	0%
	ace	(n=84)	100%	0%	0%
pancreas position	wild-type	(n=129)	2%	98%	0%
	ace	(n=84)	2.5%	97.5%	0%

Table displaying *n* values and percentages of visceral lateralities in *ace* and WT embryos as visualised by markers *foxa3* (liver, 60 hpf), *ins* (pancreas, 60 hpf) and in live embryos at 24 hpf for heart position.

2.7 Unilateral Nodal signalling in the LPM and development of Kupffer's Vesicle is normal in *ace* mutant embryos

The earliest gene expressed unilaterally in the left LPM is the Nodal ligand *southpaw* (*spaw;* Long et al, 2003). Asymmetric expression is first observed at 10 - 12s, in posterior LPM aligned with the tailbud, with expression rapidly spreading anteriorly. By 20s, left-sided expression is broad and robust and reaches as far anteriorly as the level of the hindbrain. When we analysed *spaw* expression in *ace* embryos at 20s, we found it was restricted to the left LPM (97%, n = 73; Fig. 8d), as it is in wild-type embryos (99%, n = 175; Fig. 8c).

Kupffer's vesicle is an enclosed, spherical structure, lined with monociliated epithelial cells, analogous to the Node in mouse and Hensen's Node in chicken (Essner et al, 2002). Gene-knockdown specific to dorsal forerunner cells that leads to disruption of KV formation has directly linked this structure to lateralization of the embryo (Amack and Yost, 2004). It first appears at early somite stages (1-3s) in the tailbud and has usually disappeared by 14s. We scored KV presence by DIC-imaging in live wild-type and *ace* embryos at 3s (Fig. 10), then sorted them and re-confirmed scoring at 6s to eliminate the effects of developmental asynchrony. We found that most *ace* embryos have a KV of wild-type dimensions at 3s (85%, n = 112; Fig. 9, compare a and b). The remaining *ace* embryos were divided into two classes; those

with a small or fragmented KV (12%; Fig. 9c) and those with no visible KV (3%; Fig. 9d). Given that left-sided *spaw* expression depends on KV function and *spaw* is left-sided in 97% of *ace* embryos, we suggest that even the small or fragmented KVs we observe are sufficient to direct laterality of Nodal signalling. Altogether, we find Kupffer's vesicle formation and *southpaw* expression in the left LPM to be largely unaffected by loss of Fgf8 signalling.
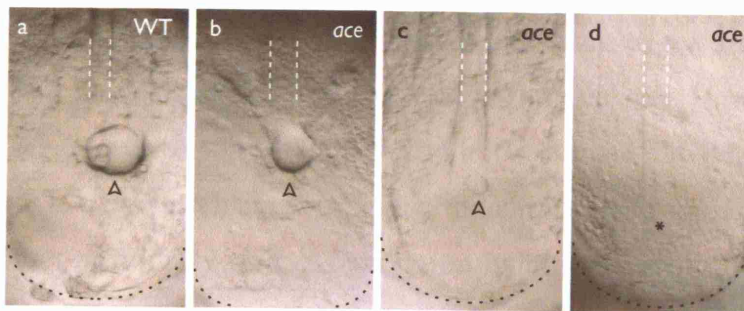
Figure 9. KV development is largely unaffected in ace embryos
(a-d) DIC-images of 3s tail-bud (black dashed lines denote tail end). In wild-type embryos (a), a spherical KV (black-edged arrowhead) is positioned caudal to the posterior end of the notochord (white dashed lines). A normal KV is observed in most *ace* embryos (b, black-edged arrowhead); in a small number of *ace*, the KV is reduced (c) or absent (d).

Our observations of normal KV development, Nodal signalling and visceral laterality in *ace* mutants suggest that the defects in brain asymmetry are specific to the CNS and do not represent a secondary phenotype of a global asymmetry defect. Therefore, we next wanted to examine the specificity of Fgf8 signalling in the diencephalon, and whether loss of the pathway affects epithalamic Nodal signalling.

2.8 Nodal signalling is slightly affected in the epithalamus of *ace* mutants
The Nodal 'cassette' is highly conserved across species and expression domains (Tian and Meng, 2006), and comprises the Nodal ligand (*cyclops* (*cyc*) in the zebrafish epithalamus), the essential co-factor *one eyed pinhead* (*oep*), the feedback inhibitors *lefty1&2* and the downstream effector, *pitx2c*. All members of the pathway are expressed unilaterally on the left of the brain in wild-type embryos, except for *oep*,

which is expressed bilaterally, as is the case in the body axis. Expression of *cyc, oep* and *lefty1* is confined to a short window, which begins at around 22s and ends when they are rapidly down-regulated at 26s (Bisgrove et al, 2000). The downstream gene *pitx2c* is expressed later than the other members of the pathway, from 24s until at least 26hpf (Essner et al, 2000). When we examined the expression of the Nodal ligand *cyc* in *ace* (Fig. 10a-c'), we find that although the majority of *ace* embryos have normal left-restricted expression of *cyc* (63%, n = 73; Fig. 10b,b'), around a quarter of embryos have 'left-biased' bilateral expression (stronger and broader on the left than on the right; 27%; Fig. 10c,c', black-edged arrows) and a small proportion (8%) have equal bilateral expression (not shown). However, it is important to note that *cyc* expression is not perfectly left-restricted in wild-type embryos, where we find 9% to have 'left biased' or 'equal' bilateral expression.

Similarly, *lefty1* expression is slightly perturbed by loss of Fgf8 signalling (Fig. 10g-k): most embryos have left-sided expression (75%, n = 24; Fig. 10h) but in the remaining quarter, expression is either reversed (8%; Fig. 10i), bilateral (13%; Fig. 10j) or absent (4%; Fig. 10k).

pitx2c can be considered the 'output' of the Nodal pathway (Essner et al, 2000) and is in fact more robustly unilateral than the other members of the cassette, such that all wild-type embryos we examined showed left-sided expression in the epithalamus (100%, n = 42; Fig. 10d,d'). *pitx2c* expression is less affected than other Nodal genes in *ace* embryos, with almost all showing left-restricted expression (90%, n = 31; Fig.10c,c') and the remaining showing bilateral expression that is strongly biased to the left, with only a few *pitx2c*-positive cells on the right (10%; Fig. 10c,c', black edged arrows). These results suggest that although expression of *lefty* and *cyc* is disturbed in a proportion of *ace* embryos, downstream genes such as *pitx2c* are nevertheless left-restricted in almost all embryos. Considering these data, we find it unlikely that the loss of asymmetry we observe in *ace* is due to any slight changes in Nodal signalling, particularly as bilaterality or loss of the Nodal pathway in other mutant backgrounds does not affect any aspects of asymmetric development except handedness (Concha et al, 2000; Concha et al, 2003; Gamse et al, 2003 and others). To further assess the specificity of Fgf8 signalling in epithalamic development, we carefully analysed Fgf-pathway expression in the dorsal diencephalon of wild-type embryos.
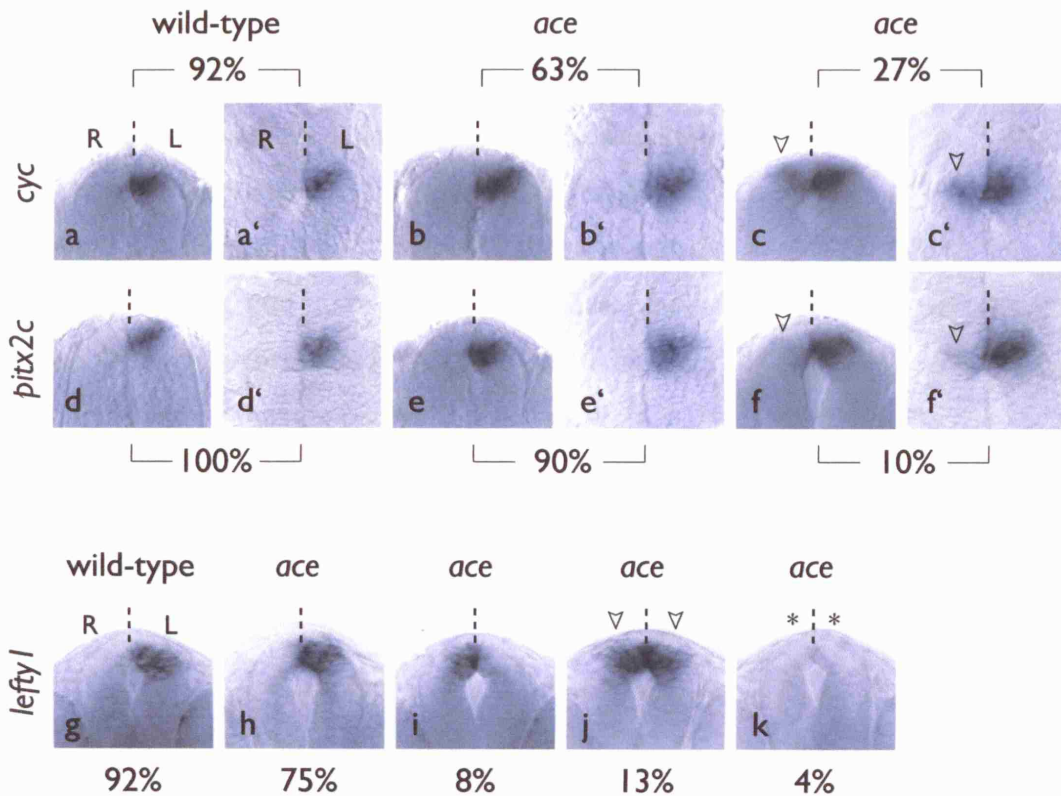
Figure 10. Epithalamic Nodal signalling is slightly perturbed in *ace* embryos

Frontal (a-k) and dorsal (a'-f') views (anterior to the top) of Nodal pathway gene expression in the epithalamus.

(a-c') *cyc* expression at 24s is left-restricted in wild-type embryos (a,a') and in most *ace* embryos (b,b'). A quarter of *ace* embryos have bilateral expression that is stronger on the left (c,c'; black edged arrowheads); a small number have equal bilateral expression (not shown).

(d-f') *pitx2c* expression at 26s is left-restricted in all wild-type embryos (d,d') and the majority of *ace* embryos (e,e'). 10% of *ace* show left-biased expression with a small number of *pitx2c*-positive right sided cells (f,f'; black edged arrowheads).

(g-k) *lefty1* expression at 22s is left-restricted in most wild-type embryos (g), and the majority of *ace* embryos (h). A quarter of *ace* embryos have aberrant *lefty1* expression including right-restricted (i), bilateral (j) and absent (k).

L, left; R, right.

2.9 *fgf8* is expressed in the epithalamus during development of asymmetric structures

fgf8 is expressed bilaterally in the epithalamus from stages prior to the leftward migration of parapineal cells, throughout the development of habenular asymmetries, until at least 4 dpf (Fig. 11). At earlier stages, expression appears to be in the region of neuroectoderm that gives rise to habenula neurons (e.g. 22s, 24hpf; Fig. 11a,b; Concha 2003 for fate-mapping). From 36hpf onwards, habenular structure is more defined and *fgf8* expression is clearly restricted to anterior and anterior-medial regions of left and right habenula nuclei (Fig 11d-f).
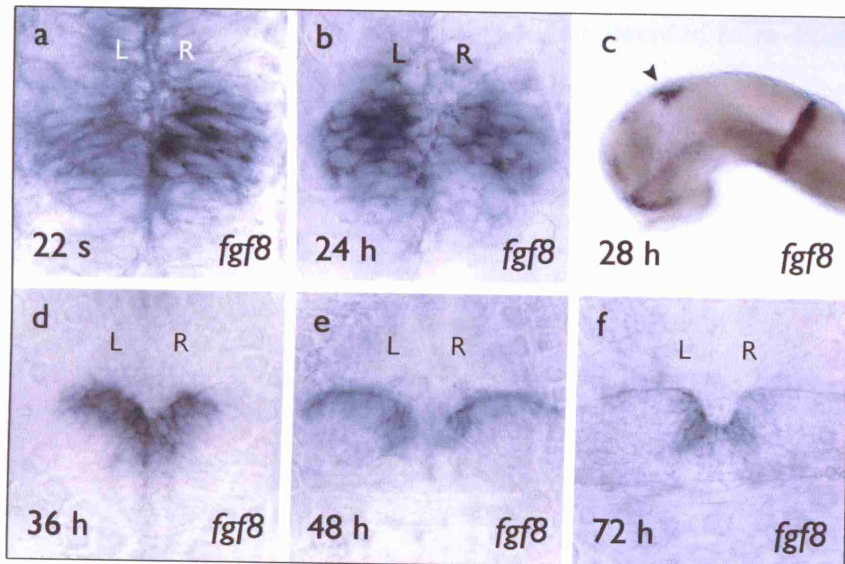
Figure 11. *fgf8* **is expressed bilaterally in the epithalamus throughout asymmetric development**

(a-f) *fgf8* expression in wild-type embryos, dorsal views with anterior to the top, except (c), which is lateral. Expression at 22s (a) and 24hpf (b) is in presumptive habenula. Later expression (d-f) is in anterior-medial habenula. Expression is higher on the right at 22s (a) and higher on the left from 24hpf onwards (b,d-f). L, left; R, right.

In order to locate *fgf8* expression more accurately with respect to the pineal complex, we performed in situ-hybridisation for *fgf8* in *Tg(flh:GFP)* and *Tg(foxD3:GFP)* embryos, followed by immuno-staining for GFP, at several stages (Fig. 12). At 22 s (n = 9; Fig. 12a,b), *fgf8* expression extends anteriorly to the pineal complex (Fig. 12a;

dashed bracket), and lateral views show that expression also lies ventral to the anterior third of the pineal complex (Fig. 12b; black edged arrow heads). This corresponds with the region that has been fate-mapped as presumptive habenula (Concha et al, 2003). Using these detection methods, it was unclear whether ventral *flh:GFP-*expressing pineal complex cells also express *fgf8*. Expression at 24hpf is also observed in cells anterior and ventral to the pineal complex (n = 6; Fig. 12c; dashed bracket), but at higher levels than at 22s. Double staining in 60hpf embryos revealed that medial habenular cells express *fgf8*, with expression decreasing progressively in more lateral anterior cells. We noted that in 3 dpf embryos, expression of *fgf8* is higher on the left than the right (n = 8; Fig. 12d; black edged arrowhead), corresponding with left-sided parapineal location (black arrowhead). In light of the asymmetries observed in 3dpf embryos, we decided to re-examine *fgf8* expression at all stages to look for asymmetry at other time-points.
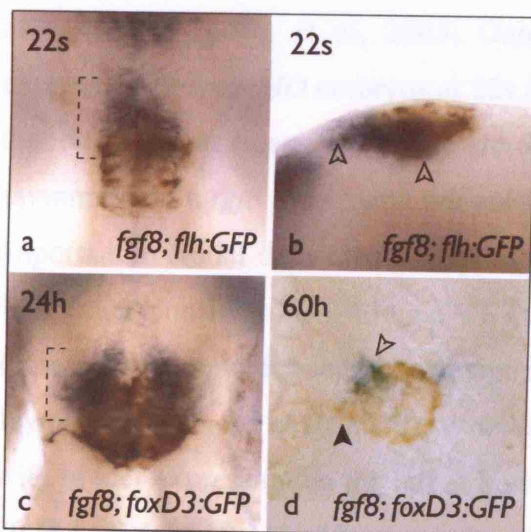
Figure 12. *fgf8* is expressed rostral and ventral to the pineal nucleus

(a-d) *fgf8* expression (blue) with respect to pineal cells (brown), marked at 22s (a,b) by *Tg(flh:GFP)* and at 24 and 60hpf (c,d) by *Tg(foxD3:GFP)*.

At 22s, dorsal (a) and lateral (b) views confirm that *fgf8* is expressed in neuroectoderm rostral (a, black dashed brackets) and ventral (b, black edged arrowheads) to pineal cells, in the region of presumptive habenula. At 24hpf (c) bilateral expression remains rostral and ventral to the pineal (black dashed brackets). By 60hpf (d) expression is restricted to cells proximal to the pineal. Expression is higher on the left (black edged arrowhead), concordant with parapineal position (black arrowhead).

2.10 Asymmetries in *fgf8* expression are Nodal-dependent

When we re-examined *fgf8* expression in embryos at earlier developmental stages, we found that there are slight, but consistent differences in expression levels between left and right sides. At 22s, we find expression is higher on the right in most embryos (Fig. 11a). Expression of *fgf8* at this stage is dynamic, with each individual embryo showing variation in expression levels, area, and rostral limit. Despite these variations, more intense staining on the right is usually visible. By 24hpf, expression level is more often higher on the left and remains so at all later stages examined (Fig. 11b, Table 3).

Considering that the Nodal pathway is responsible for lateralising all other known epithalamic asymmetries, we were interested to know what happens to *fgf8* expression in embryos where Nodal signalling is either bilateral or absent. To generate conditions of absent Nodal signalling, we injected wild-type embryos with the *southpaw* morpholino (*spawMO,* Long et al, 2003). These embryos have no expression of Nodal pathway genes in the epithalamus and show randomised viscera and brain asymmetries (Long et al, 2003; Gamse et al, 2005). When we examined *fgf8* expression in *spawMO* embryos at 22s and 28hpf, we found that expression levels on the left and right sides are equal in almost all cases (Table 3). This suggests that overt asymmetries in *fgf8* expression are not required for parapineal migration, but may be important in Nodal-dependent lateralisation.

To further confirm our findings, we analysed *fgf8* expression in 24hpf and 30hpf *LZoep* embryos, which lack Nodal signalling in the brain and have randomised brain asymmetry (Concha et al, 2000). Whereas wild-type embryos are usually asymmetric with higher expression on the left at both stages; (24 hpf, 75 % L>R (n = 16); 30 hpf, 80 % L>R (n = 10); Fig 13a,c), we found no differences between left- and right-sided expression in all *LZoep* embryos we examined, at both stages (24 hpf, 100% equal (n = 8); 30 hpf, 90 % equal (n = 10); Fig. 13b,d). It is clear that embryos lacking a Nodal bias also lack any obvious bias in *fgf8* expression levels between left and right sides of the brain, but wild-type *fgf8* asymmetries are not as clear-cut. The proportion of wild-type embryos with stronger left-sided expression at 28hpf is not as high as the proportion observed with Nodal genes, for example, and while this may reflect our inability to score more subtle differences, there are a number of embryos that have higher *fgf8* expression on the right (Table 3). Scoring whole-mount *in situ*

hybridisations by eye is by no means a perfect method for estimating expression levels or indeed *fgf8*-positive cell number. It would be necessary to measure fluorescence levels and count cells using confocal imaging techniques in order to accurately quantify subtle asymmetries in *fgf8* signalling. However, we can surmise from this data that the majority of wild-type embryos have higher levels of *fgf8* expression on the right at 22s and higher levels on the left at 24hpf and at all stages thereafter, and that these differences are dependent on unilateral Nodal signalling.
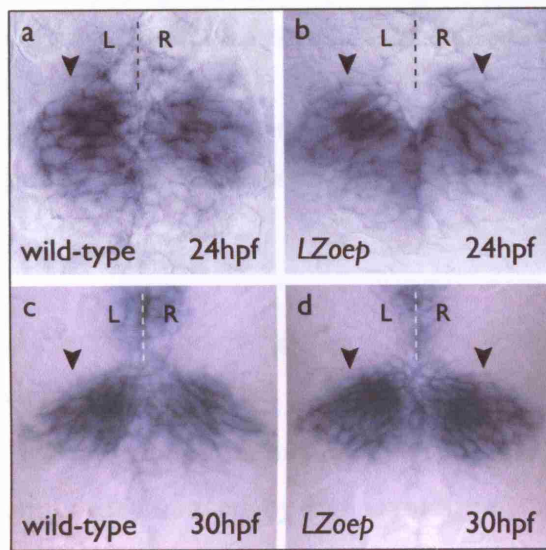
Figure 13. Asymmetries in *fgf8* expression are Nodal-dependent
Wild-type embryos at 24hpf (a) and 30hpf (c) show a left-sided bias in *fgf8* signalling (black arrowheads) This bias is lost in *LZoep* embryos at both stages (b,d; black arrowheads) where expression levels on left and right sides are equal.

L, left; R, right.

Several genes have been identified that are expressed in response to Fgf signalling (Tsang and Dawid, 2004), so we next wanted to analyse the specificity of these genes in the epithalamus, and to look for any asymmetries in expression.

Table 3. *fgf8* expression in wild-type and Nodal-modulated embryos

		L > R	R > L	E
fgf8 at 22ss	wild-type (n = 32)	5%	81%	14%
	spawMO (n = 27)	5%	7%	88%
fgf8 at 28hpf	wild-type (n = 24)	76%	11%	13%
	spawMO (n = 29)	12%	5%	83%

Table displaying *n* values and percentages for *fgf8* expression levels in wild-type and Nodal modulated embryos (*spawMO* = absent epithalamic Nodal; *ntlMO* = bilateral epithalamic Nodal) at 22ss and 28hpf.

E, equal; L, left; L>R, left epithalamic expression domain is larger than right; R, right, R>L, right epithalamic expression domain is larger than left.

2.11 Fgf-responsive genes are expressed in habenulae; *erm* is up-regulated in the parapineal

The transcription factors *pea3* and *erm* and the feedback inhibitors *sef* and the *sprouty* family are induced by Fgf signalling (Raible and Brand, 2001; Tsang et al, 2002, Furthauer et al, 2002; Minowada et al, 1999). When we analysed expression of Fgf-responsive genes in the epithalamus of wild-type embryos, we find that they are expressed bilaterally, in a pattern similar to that of *fgf8*. *pea3*, *sef*, *spry2* and *spry4* are expressed in presumptive habenula at 24hpf, and later in medio-lateral habenula cells (data not shown). We could not detect any left-right asymmetry in the expression of these genes. When we analysed the expression of the transcription factor *erm*, we found that it is also expressed in presumptive habenula at early stages and bilaterally in anterior and medial habenula at later stages (e.g 32hpf, Fig. 14a-c). Frontal views show that *erm* expression extends more laterally than *fgf8* expression (Fig. 14b, black arrowheads), which may reflect the range travelled by Fgf8 protein (Sholpp and Brand, 2004), or the expression of another Fgf. Expression of *erm* appears to be excluded from pineal cells (Fig. 14b white dashed line and Fig. 14c black dashed line). There is an area to the left of the midline in which *erm* is up-regulated that probably corresponds with medial habenula cells (Fig. 14b,c; black-edged arrowheads). When we examined *erm* expression in *ace* embryos, we find that

although it is significantly down-regulated, a low level of expression is visible in the epithalamus (Fig.14d-f). It is possible that another Fgf family member is expressed in this region. No left-sided up-regulation of *erm* expression could be detected in *ace* embryos (Fig. 14e,f). Expression of *pea3*, *sef*, *spry2* and *spry4* is also dramatically reduced in *ace* (data not shown).

Altogether, this data suggests that Fgf8 is responsible for the majority of Fgf-pathway signalling in the epithalamus, particularly the left-sided up-regulation of *erm*, which is likely to be in habenular cells. To better understand which cells are able to respond to Fgf8 signals, we next analysed the expression of the four known Fgf receptors in this region.
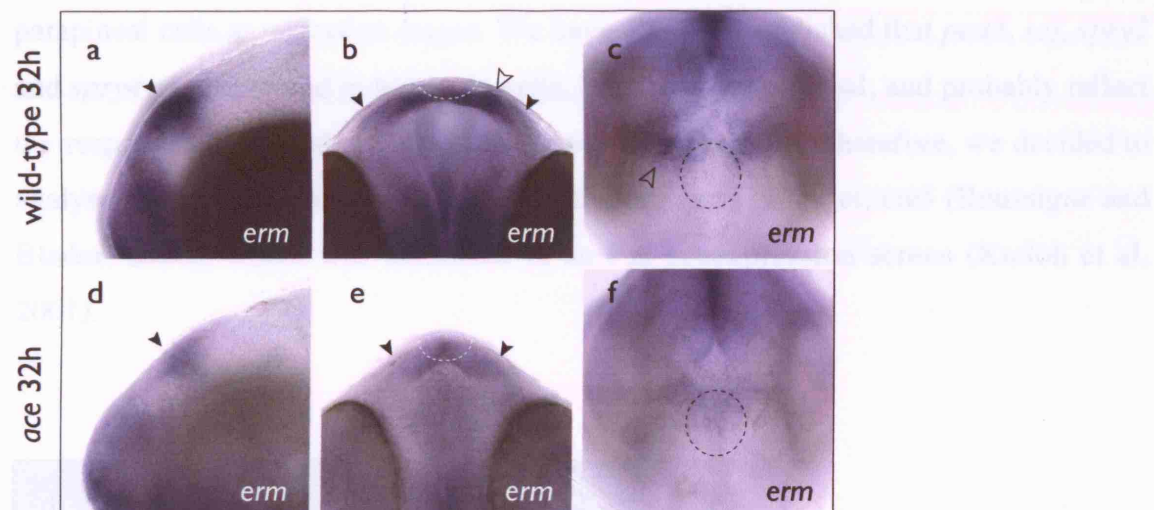
Figure 14. *erm* signalling is asymmetric in wild-types and is dramatically down-regulated in *ace*

(a-c) Wild-type expression of *erm* at 32hpf is in habenula cells, but is largely excluded from the pineal (b,c; dashed lines). Expression is more intense on the left than the right (b,c; black edged arrowheads).

(d-f) *erm* is considerably down regulated in *ace* embryos at 32hpf, although a small amount of bilateral expression remains (d,e; black arrowheads). Asymmetry in *erm* expression is lost in *ace* (e,f).

2.12 *fgfR4* is expressed specifically in the parapineal primordium

Although all four FgfRs are widely expressed in the epithalamus (data not shown), *fgfr4* shows elevated levels of expression specifically in parapineal cells (Fig. 15; this work was done in collaboration with **Myriam Roussigne**). At early stages of parapineal migration, *fgfr4* expression in parapineal cells and at the midline in the pineal is clearly visible (Fig. 15a,b; white dashed circles denote pineal and parapineal). By 48hpf, expression of *fgfr4* is more widespread and specific expression in the parapineal becomes harder to detect, however, it is usually possible to locate a group of *fgfr4*-expressing cells on the left side (Fig. 15c; small white dashed circle). We never detect *fgfr4* transcripts in habenular cells. This data suggests that parapineal cells can receive Fgf signals through Fgfr4 during their migratory phase. Considering this data, we found it likely that an *fgf*-responsive gene would be expressed in parapineal cells at migration stages. We have already established that *pea3*, *sef*, *spry2* and *spry4* are expressed in habenula cells, but not the parapineal, and probably reflect the response of habenular cells to their own Fgf signalling. Therefore, we decided to analyse the epithalamic expression of another known Fgf target, *etv5* (Roussigne and Blader, 2006), which was identified in an Fgf-synexpression screen (Kudoh et al, 2001).
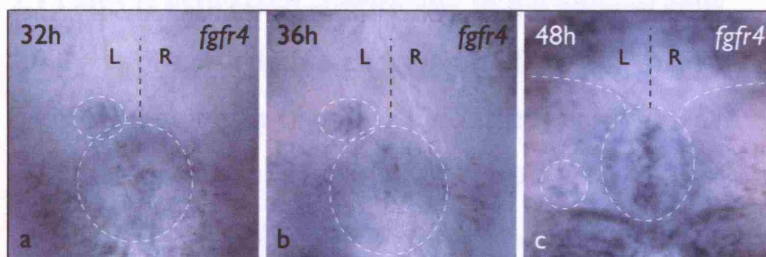
Figure 15. *fgfr4* is expressed in parapineal cells throughout migratory phase
At 32hpf (a) and 36hpf (b), *fgfr4* is clearly expressed in parapineal cells (small dashed white circle) and within midline pineal cells. Bilateral expression flanking the pineal nucleus is probably too posterior to be habenula nuclei. By 48hpf (c), *fgfr4* is more broadly expressed; although parapineal cells are difficult to resolve, expression is visible in several cells within the nucleus (c; small dashed white circle).
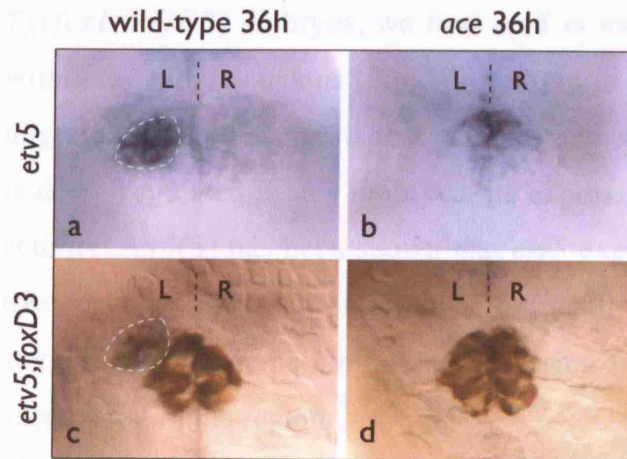
Figure 16. *etv5* **is expressed specifically in parapineal cells**

(a,b) *etv5* is expressed in 36hpf wild-type embryos in a left sided group of cells that corresponds to parapineal position (a, white dashed circle). expression is down-regulated in 36hpf *ace* embryos; remaining expression is found in midline cells (b), similar to other parapineal marker expression in *ace*.

(c,d) Double-labelling of *etv5* (blue) and *Tg(foxD3:GFP)* (brown) shows that left-sided parapineal cells express *etv5* (blue and brown labelling contained within dashed white circle). Not all parapineal cells express *Tg(foxD3:GFP)* at this stage, so *etv5*-positive, *Tg(foxD3:GFP)*-negative cells may be parapineal.

2.13 *etv5* is expressed specifically in parapineal cells

Analysis of epithalamic expression of *etv5* in wild-type embryos at various stages revealed that unlike the other Fgf target genes we have examined, it is not expressed in habenular cells. However, we find that a region to the left of the midline, corresponding to parapineal position, strongly up-regulates *etv5* between 24 and 40hpf (Fig. 16a, 36hpf). We find *etv5* expression is maintained in *ace* embryos, although at a lower level and in a midline position (Fig. 16b). In order to establish whether *etv5* is expressed by parapineal cells, we analysed transcript expression in *Tg(foxD3:GFP)* embryos (Fig. 16c,d). We find that *etv5* expression (Fig. 16c; blue cells within white dashed circle) and *foxD3:GFP* expression (brown cells within white dashed circle) are concomitant and therefore conclude that *etv5* is expressed by parapineal cells. Not all *etv5* expressing cells were *GFP* positive, nevertheless, these may be parapineal cells as *Tg(foxD3:GFP)* is not expressed in the entire parapineal primordium at early migration stages. When we examined *etv5* in *ace /*

Tg(foxD3:GFP) embryos, we find *etv5* is expressed is by the anterior-most cells within the pineal nucleus (Fig. 16d), likely to be parapineal cells that have failed to migrate. This data suggests that *etv5* is expressed by parapineal cells, and although it is down-regulated in *ace* embryos, its expression is not entirely dependent on Fgf8 activity. As it is has been shown that *etv5* expression is completely lost in embryos treated with drugs that block all Fgf signalling (Roussigne and Blader, 2006), we suggest that the remaining *etv5* expression in *ace* embryos reflects signalling by another Fgf in the region.

Our analysis of habenular- and parapineal-specific expression of Fgf8 pathway components, together with the *ace* mutant phenotype indicates that initiation and maintenance of parapineal migration specifically requires Fgf8. We wanted to further confirm this specificity by abrogating Fgf signalling in a temporally controlled manner.

2.14 Drug knockdown of Fgf-signalling reveals a critical window for Fgf signalling in parapineal migration

(This work was carried out in collaboration with **Claire Russell**, a former post-doc in the Wilson lab, who performed the drug-treatment experiments and imaging).

The SU5402 drug inhibits all Fgf signalling by inhibiting the kinase activity of FgfRs and preventing downstream pathway activation (Mohammadi et al, 1997). The drug can simply be added to embryo medium, as it efficiently penetrates the zebrafish embryo. Washing out the drug permits a rapid recovery of Fgf signalling, thereby allowing knock-down of signalling during specific time windows. We blocked Fgf signalling in *Tg(foxd3:GFP)* embryos in a four-hour treatment window between 24 and 28hpf, 'washing out' the drug at 28 hpf and allowing embryos to develop to 3 dpf. Two levels of the drug were used (see Methods), 21μM ('high') and 9μM ('low'); control embryos were treated for the same period in the solvent DMSO only. We observed that parapineal migration was disrupted with most cells remaining at the midline (0% in controls (n = 9), 20% at 9μM (n = 10), 100% at 21μM (n = 10); Fig. 17a-b'). Primordia were often disaggregated such that a few cells were scattered to the left or right of the midline, but these never migrated laterally as a cohesive group and remained ventral to the pineal nucleus. This largely phenocopies the parapineal
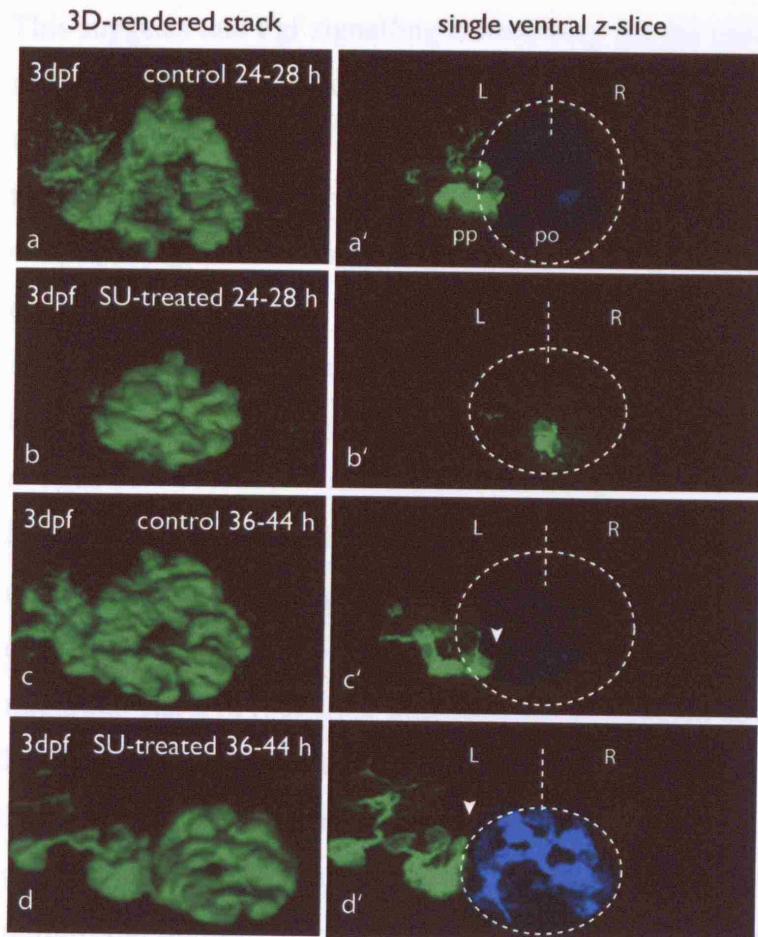
Figure 17. Temporally controlled abrogation of Fgf signalling identifies a critical window for Fgf-dependent parapineal migration

(a-d) 3D reconstructions and (a'-d') single *z*-slices of dorsal views of the epithalamus in control- (a,a',c,c') and SU5402- (b,b',d,d') treated *Tg(foxD3:GFP)* 3dpf embryos, with anterior to the top. Pineal cells have been pseudo-coloured in blue in single *z*-slices (a'-d'). SU5402-treatment at 24 - 28 hpf completely abolished the initial leftward migration of the parapineal to lateral and dorsal positions (b,b'). Treatment at 36 - 44 hpf abrogated later translocation of the parapineal to ventral and medial locations relative to the pineal nucleus and parapineal cells remain at dorso-lateral positions in the pineal complex (white arrow heads).

po, pineal nucleus; pp, parapineal nucleus.

migration defect of *ace* mutants although the extent of disaggregation of the parapineal primordium was more severe following SU5402 treatment (data not shown).

This suggests that Fgf signalling is necessary for the initiation of parapineal migration and that embryos treated during this short time window are not able to recover migratory behaviour. In addition, blocking signalling during the migratory phase led to arrest of parapineal migration. For instance, in embryos treated between 36 and 44hpf (an eight-hour treatment window, 'washing out' the drug at 44 hpf and allowing embryos to develop to 3 dpf), parapineal cells fail to move ventral to the pineal nucleus, remaining lateral to (Fig. 17c',d'; white arrowheads), and at the same dorsal level as, pineal cells (Fig. 17d'; note blue pineal cells; 0% in controls (n = 11), 100% at 9μM (n = 11); 21μM treatments were not performed due to an increased lethality at higher concentrations at this stage). This suggests a continuous requirement for Fgf activity during migration. However, if SU5402 was applied to embryos earlier in development, at 20 - 24 hpf, where 'washing out' is performed at 24 hpf before migration starts (a four-hour treatment window, again allowing embryos to develop to 3 dpf), parapineal migration proceeded as normal and epithalamic laterality, including left-sided Nodal signalling, was undisturbed (100% in controls (n = 11), 100% at 9 μM (n = 8), 100% at 21μM (n = 7)). These data support the idea that parapineal cells require Fgf signalling to initiate and maintain their migration, and as all migrations were directed to the left in treated embryos, that unilateral Nodal signalling does not require Fgfs.

Altogether, our data demonstrates that parapineal migration and subsequent development of epithalamic asymmetries requires Fgf8 signalling. We find that in *ace* mutants the parapineal nucleus is specified, but fails to migrate, and that habenulae remain largely symmetric. Examination of visceral asymmetries revealed that these are correctly lateralised in *ace*, suggesting that asymmetry defects are restricted to the brain. We demonstrate that loss of asymmetry in the brain in *ace* is not via disruption of epithalamic Nodal signalling, as this is only slightly affected. The requirement for Fgf8 signalling in parapineal migration is supported by the specificity of *fgf8* expression in medial habenulae and *fgfr4* expression in parapineal cells, which also up-regulate the Fgf target gene *etv5*. We find subtle asymmetries in *fgf8* expression and show that these are dependent on unilateral Nodal signalling. These subtle asymmetries may reflect early habenular lateralisation, but are not required for parapineal migration. By blocking all Fgf signalling using drugs we demonstrate the

requirement for Fgfs during the initiation and continued migration of the parapineal nucleus.

Chapter 3 - Fgf8 breaks symmetry in the brain and directs laterality in the absence of a Nodal bias

1. Introduction

We have shown that the epithalamus is symmetric in the *fgf8* mutant *ace*, such that the parapineal fails to migrate to the left of the midline and later habenular asymmetries fail to elaborate. Analysis of lateralised viscera demonstrated that the asymmetry defects we observe are restricted to the brain. We have shown that *fgf8* is expressed by habenula cells and that parapineal cells can likely respond to Fgf signalling through expression of *fgfR4*. The Fgf-response gene *etv5* is expressed by parapineal cells during their migratory phase. In addition, blocking all Fgf signalling allowed us to identify a critical window for Fgf-dependent parapineal migration. To further test the hypothesis that it is the local activity of Fgf8 that is required for the parapineal primordium to move leftward from its initially symmetric location we next wanted to provide *ace* embryos with a focal source of exogenous Fgf8 protein. Rescue of migration by exogenous Fgf8 in *ace* would confirm the specificity of *fgf8* signalling in generating brain asymmetry and has the possibility to address questions about the action of Fgf signals on parapineal cells.

2. Results

2.1 Mis-expression pilot 1: single cell electroporation

Previously, we have successfully generated targeted mis-expression of *lefty1* in the epithalamus by means of single cell electroporation, efficiently biasing the direction of parapineal migration (Chapter 1). We considered the possibility that the same technique could be used to mis-express *fgf8* in the epithalamus. We attempted to introduce *fgf8* and *kaede* DNA to single cells or small groups of cells rostral to the pineal complex in *Tg(foxD3:GFP)* and *ace / Tg(foxD3:GFP)*, and to assess the effect exogenous Fgf8 has on parapineal migration. Kaede is a photoconvertable fluorophore that changes from green to red on exposure to light (Ando et al, 2002) and was chosen because it is much brighter than conventional RFPs.
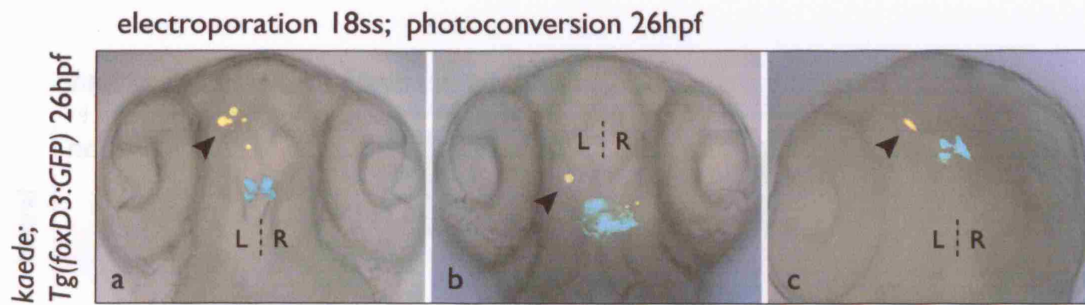
Figure 1: Single cell electroporation in *Tg(foxD3:GFP)* embryos

(a-c) Red photoconverted Kaede-positive cells (black arrowheads) are visible in the left forebrain of 24hpf *Tg(foxD3:GFP)* embryos after electroporation of *kaede* DNA at 18s.
Dorsal views, anterior to the top. R, right; L, left.

Following electroporation of *fgf8* and *kaede* DNA constructs, or *kaede* alone, into *ace / Tg(foxD3:GFP)* embryos at 14-18ss, we observed *kaede*-positive groups of cells rostral to the pineal at 24hpf (Fig. 1). Some electroporated cells were not close enough to the pineal (Fig. 1a), or had a rounded cell-shape that is indicative of cell death (Fig. 1a,b). Nevertheless, some *kaede*-positive cells were well-targeted and of an elongated shape typical of neurons (Fig. 1c). Unfortunately, these successful electroporations were not generated at a rate that would allow meaningful interpretation of data. Electroporation after 24hpf is relatively productive and is a useful method for labelling cells (Aizawa et al, 2005), however, younger embryos are much less rigid and electroporation causes involution of the head so that targeting is less accurate. Additionally, fewer cells take up DNA at earlier stages (data not shown) and we speculate that this is because neuroepithelial cells are much less tightly packed than at later stages. Indeed, in order to mis-express *lefty1* (Chapter 1), electroporation of several hundred 10-14ss embryos was required to produce 10 successfully electroporated specimens. Altogether, although single cell electroporation is an elegant method for focal mis-expression of genes or labelling of single cells, it was not a viable choice for this particular question.

2.2 Mis-expression pilot 2: mosaic heatshock

Injection of single cell embryos with DNA causes mosaicism, so that at later stages of development, small clones of cells expressing the injected construct can be observed,

hs:fgf8; Tg(foxD3:GFP) 60hpf
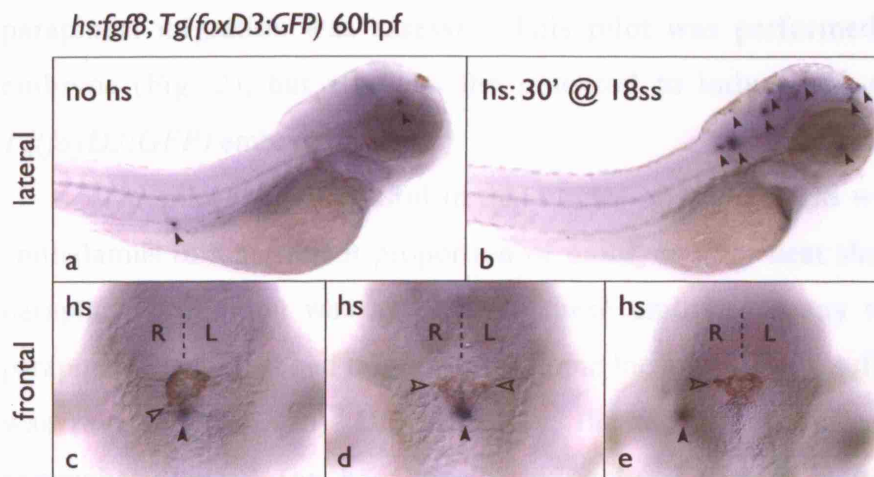
Figure 2. Mosaic clones of *hs_fgf8* can affect migration of the parapineal in *Tg(foxD3:GFP)* embryos

(a-e) 60hpf *Tg(foxD3:GFP)* subjected to ISH for *fgf8* (blue) and immuno-labelling for GFP (brown).

(a,b) Lateral views of untreated and heat-shocked embryos. Clones are induced spontaneously at a low rate in embryos not subjected to heat shock (a, black arrowheads) and at a higher rate in embryos heat shocked for 30' at 18s (b, black arrowheads).

(c-e) Dorsal views of epithalami in heat-shocked embryos. Ectopic *fgf8* clones (black arrowheads) are concomitant with rostral (c; n = 3), split (d; n = 2) and right-sided (e; n = 9) parapineal nuclei (black-edged arrowheads).

hs, heat shock; R, right; L, left.

randomly distributed throughout the embryo. We took advantage of this mosaicism by injecting *fgf8* DNA under the control of a heat shock promoter (*hs_fgf8*, Halloran et al, 2000) at very low concentrations into 1-cell embryos. The small clones of cells containing the construct should not transcribe *fgf8* until the embryo is subjected to heat shock, thus allowing temporal control of the induction of ectopic *fgf8*. By injecting large batches of *Tg(foxD3:GFP)* embryos with the *hs_fgf8* construct we were able to generate significant numbers of embryos with *hs_fgf8* clones in the region of the epithalamus. A 42°c heat shock for 30 minutes at 18s induced *fgf8* expression in the clones. We considered this time-point to be sufficiently early to allow translation of Fgf8 before the initiation of parapineal migration at 26-28hpf. At

2dpf, *hs_fgf8* clones were detected by ISH and their position was recorded, and parapineal migration was assessed. This pilot was performed in *Tg(foxD3:GFP)* embryos (Fig. 2), but also has the potential to induce mis-expression in *ace / Tg(foxD3:GFP)* embryos.

The pilot was successful in that clones of ectopic *fgf8* were generated in the epithalamus in a sufficient proportion of embryos after heat shock (Fig. 2b). When parapineal migration was assessed in these embryos, many were found to have parapineal nuclei that had migrated to ectopic locations (Fig. 2c,d), or whose laterality was reversed (Fig. 2e). Unfortunately, the *hs_fgf8* construct was found to be somewhat 'leaky' (as has been previously reported, Bajoghli et al, 2004), spontaneously transcribing *fgf8* in a small number of clones in embryos that were not subjected to heat shock (Fig. 2a), even when embryos were raised at 25°c. This could have been disregarded, as spontaneous rates of induction were fairly low (average *n* clones in non-hs = 2 ± 2.5 from 54 embryos; vs average *n* clones in hs = 18 ± 5.3 from 63 embryos) and did not appear to affect parapineal migration. However, we observed abnormal development of some embryos preceding heat shock (data not shown), suggesting that ectopic *fgf8* was being transcribed at early stages, or that injection of the construct, even at low doses, was toxic to the embryo. In addition, when we subjected heat-shocked embryos to ISH for *fgf8*, endogenous *fgf8* was not detected, or was only detected at low levels. Embryos with fewer clones had a higher level of endogenous *fgf8*. Uninjected embryos in the same batch had normal *fgf8* detection by ISH, suggesting that high levels of exogenous *fgf8* were probably not affecting detection methods. The apparent suppression of endogenous *fgf8* by exogenous *fgf8* made our results very difficult to interpret. Nonetheless, this may prove to be a feasible method for mis-expression in other contexts, particularly in light of development of non-leaky, bi-cistronic constructs that express *fgf8* and *GFP*, strictly on induction by heat shock (Bajoghli et al, 2004).

2.3 Mis-expression pilot 3: bead implantation

Implantation of protein-soaked beads is a classic method used in developmental biology to introduce a focal source of exogenous protein. It offers the advantage of being almost instant (the time of effect depends on diffusion of the protein away from the bead, compared to the delay of several hours imposed by transcription and

translation of exogenous DNA or RNA constructs) and the source is easy to locate. Fgf8, as a diffusible signalling molecule, is a perfect candidate for binding to beads. Numerous studies have utilised bead implantation techniques in zebrafish (e.g. Reifers et al, 2000) including several that have used Fgf8-loaded beads (e.g. Shinya et al, 2001). Studies have moved away from using the large, heparin-coated resin beads traditionally used in chick, to using smaller (<50μm), polystyrene beads that can be pre-soaked in heparin solution (Maves et al, 2002).
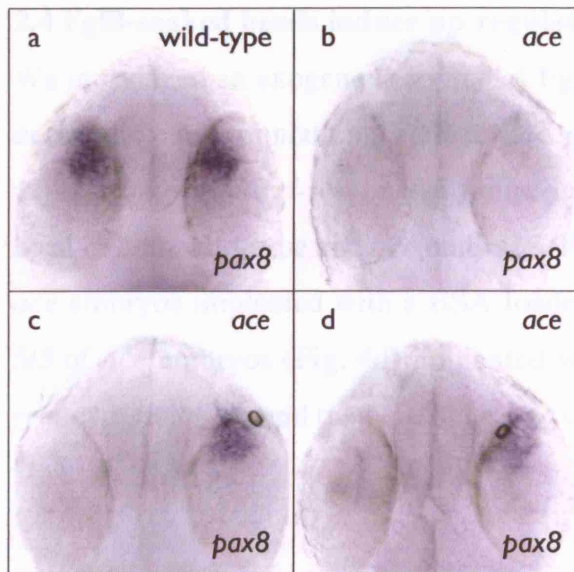
Figure 3. Implantation of Fgf8-loaded beads can rescue *pax8* expression in *ace* mutant embryos

(a-d) Ventral views of 24hpf wild-type and *ace* embryos subjected to ISH for *pax8* (blue)

      (a,b) Wild-type embryos show *pax8* expression in the presumptive optic stalk in the ventral region of the eye (a); this expression is lost in *ace* embryos (b).

(c,d) *ace* embryos implanted with an Fgf8-loaded bead in the left eye show rescued expression of *pax8* close to the bead.

In order to test the efficacy of Fgf8-loaded bead implantation in our hands, we attempted to rescue *pax8* expression in the presumptive optic stalk in the anterior eye of *ace* mutant embryos, which is usually lost in the mutant (after Picker and Brand, 2005). We loaded recombinant mouse Fgf8b protein (rmFgf8b) on to beads that had been pre-soaked in heparin (after Maves et al, 2002, see Methods). We used 10-15μm

beads, which to our knowledge, are the smallest beads ever used for this type of implantation experiment. Using a tungsten needle, beads were implanted into the ventro-nasal part of the eye at 20ss; embryos were grown for 5 hours and fixed at 24hpf for ISH. *pax8* expression in the eye was rescued at the site of bead implantation in 3/3 *ace* embryos (Fig. 3c,d). BSA-loaded beads did not induce expression of *pax8* in *ace* embryos (n = 2). In light of these results, we decided to use Fgf8 micro-bead implantation to introduce exogenous Fgf8 into the forebrain of *ace* mutants to assess its affect on parapineal migration.

2.4 Fgf8-soaked beads induce up-regulation of the Fgf-target gene *erm*

We introduced an exogenous source of Fgf8 protein to the forebrain of wild-type and *ace* embryos by implanting Fgf8-loaded polystyrene beads. We were able to induce expression of the Fgf-responsive transcription factor *erm* in a broad ring around the bead in both wild-type and *ace* embryos (Fig. 4), such that 0/4 of wild-type and 0/4 of *ace* embryos implanted with a BSA-loaded bead, and 7/8 of wild-type (Fig. 4c) and 5/5 of *ace* embryos (Fig. 4d) implanted with an Fgf8-loaded bead showed a ring of *erm* expression around the bead. The ring of up-regulated erm expression is broad,
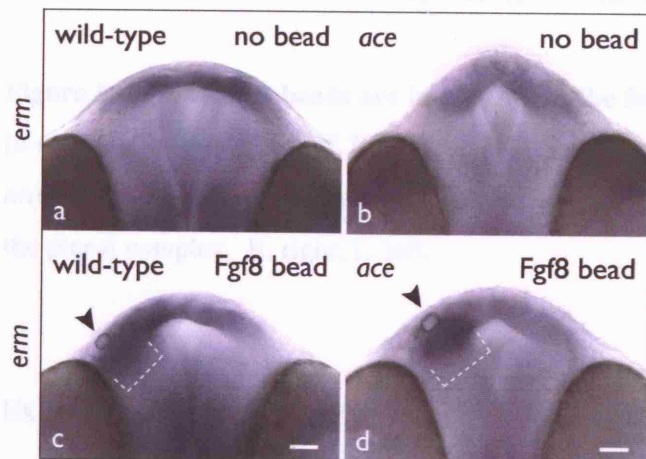
Figure 4. Fgf8-loaded beads induce target genes in wild-type and *ace* embryos
(a-d) Frontal views of wild-type and ace embryos subjected to ISH for the Fgf-target gene *erm* (blue). *erm* is up-regulated in a ring around the bead (white dashed brackets) in embryos at 30 hpf after Fgf8-bead implantation (black arrowheads) at 26s (c,d).
Scale bars = 30μm

usually with a radius of at least 30μm (e.g. Fig. 4c,d, note scale bars). We infer from this that Fgf8 protein from a bead placed within this distance from the pineal complex would reach parapineal cells.

2.5 Exogenous Fgf8 efficiently rescues migration of the parapineal nucleus in *ace*

In order to provide *ace / Tg(foxD3:GFP)* embryos with an exogenous source of Fgf8, we implanted Fgf8-loaded micro-beads rostral to the pineal complex at 24hpf, before migration of the parapineal nucleus begins. Beads were implanted either at the midline or to the left or right of the midline within 30μm of the pineal (Fig. 5). Embryos were selected on the basis of implantation accuracy with respect to GFP-expressing pineal cells, and were bathed overnight in antibiotic-inoculated embryo medium. Parapineal migration was analysed in live embryos at 2dpf and recorded; embryos were fixed at 3dpf for immuno-staining and confocal analysis.
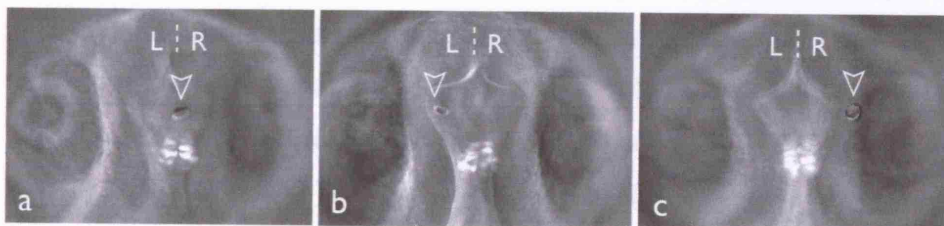
Figure 5. Fgf8-loaded beads are implanted in the forebrain of *Tg(foxD3:GFP)* embryos (a-c) Dorsal views of 24hpf *Tg(foxD3:GFP)* implanted with Fgf8-loaded beads (white-edged arrowheads); implantation is at the midline (a), to the left (b) or to the right (c) and rostral to the pineal complex. R, right; L, left.

Exogenous Fgf8 efficiently restored lateralised parapineal migration in *ace* mutants such that by 3 dpf, 56 % of *ace* embryos with an implanted Fgf8 bead showed a migrated parapineal nucleus (Fig. 6c,c', Table 1; **p = 0.0015 for *ace* + Fgf8 where 29/52 migrated; vs *ace* + BSA where 3/21 migrated) whereas BSA-soaked beads had no effect on parapineal migration (Fig. 6b,b', Graph 1, Table 1). Parapineal nuclei were considered to have approximated wild-type migration if a cohesive group of 4 or more cells migrated laterally to the pineal complex and could be distinguished as distinct from the pineal (e.g. Fig. 6c,c'). Migration in BSA-bead implanted embryos
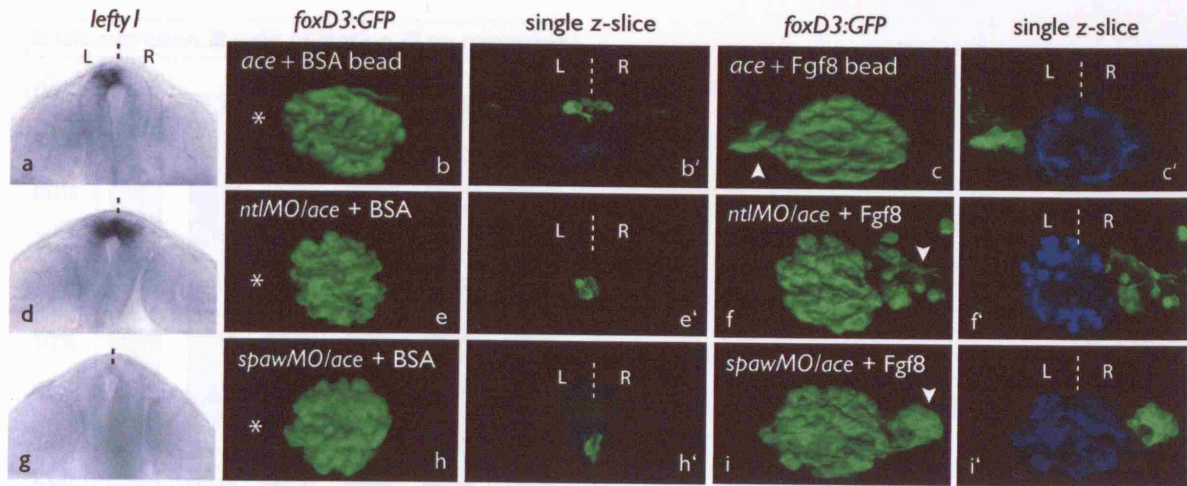
Figure 6. Local provision of Fgf8 restores parapineal migration in *ace* embryos and directs laterality of migration in the absence of a Nodal signalling bias

(a, d, g) frontal views of *lefty1* expression (as a marker of Nodal signalling) in *ace* (a), *ntlMO/ace* (d) and *spawMO/ace* (g) embryos at 20 hpf, with dorsal to the top.

(b, b', c, c', d, d', e, e', f, f', h, h', i, i') 3D reconstructions and single *z*-slices of dorsal views of the epithalamus in *ace* (b-c'), *ntlMO/ace* (e-f') and *spawMO/ace* (h-h') *Tg(foxD3:GFP)* embryos at 3 dpf implanted with BSA- (b, b', e, e', h, h') or Fgf8- (c, c', f, f', i, i') loaded beads. Pineal/parapineal complex (green) is visualised by α-GFP immuno-staining. Pineal cells have been pseudo-coloured in blue in single *z*-slices.

was found to be at the similar rate as in embryos without a bead implant (p = for 3/21 migration in *ace* + BSA vs 1/11 migration in non-implanted *ace*; Table 1).

2.6 Migrating cells in *ace* embryos are parapineal cells

We wanted to confirm that the lateralised cells we observed in Fgf8 bead-implanted *ace* embryos were parapineal cells, and not pineal cells that had been induced to delaminate. We used the marker *gfi*, which is specifically expressed in parapineal cells (Dufourq et al, 2004), to distinguish the position of the parapineal primordium in rescued embryos. We first recorded the position of 'non-pineal' *foxD3:GFP*-expressing cells in live 3 dpf embryos, 2 days after Fgf8-loaded beads were implanted. These cells were either lateral or ventral to the pineal organ and are the cell type we have assumed to be parapineal. Embryos were immediately fixed and subjected to whole-mount ISH for the marker *gfi*. The position of *GFP*-expressing

left migration ■ right migration □ no migration

100%
90%
80%
70%
60%
50%
40%
30%
20%
10%
0%

ace + L BSA   ace + M BSA   ace + R BSA   ace + L Fgf8   ace + M Fgf8   ace + R Fgf8
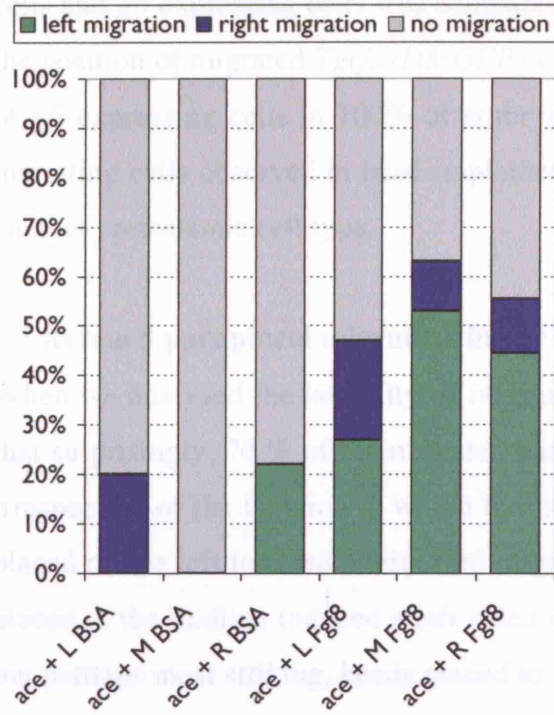
Graph 1. Implantation of Fgf8-soaked beads rescues parapineal migration in *ace* mutant embryos

Graph representing proportions of embryos with right (blue), left (green) or static (gray) parapineal nuclei after epithalamic implantation of BSA- and Fgf8-loaded beads in *ace* embryos. The majority of rescued parapineal migration is to the left.

Tg(foxD3:GFP) 3dpf   *gfi* 3dpf

a   L   R   b   R   L
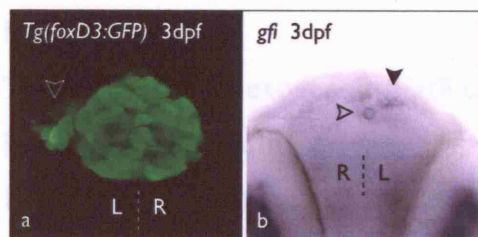
Figure 7. Migrating cells in rescued *ace* embryos are parapineal cells

(a) dorsal view of live 3dpf *Tg(foxD3:GFP)* implanted with an Fgf8-loaded bead. Non-pineal, GFP-positive cells denoted by white-edged arrowhead

(b) frontal view of the same embryo, fixed and subjected to ISH for the parapineal-specific marker *gfi* (black arrowhead), Fgf8-bead denoted by black-edged arrowhead.

R, right; L, left.

cells and *gfi* expressing cells was compared in each individual embryo. We found that the position of migrated *Tg(foxD3:GFP)*-expressing cells correlated with the position of *gfi* expressing cells in 100% of embryos (n = 5; Fig. 7). This data confirms that migrating cells observed in bead-implanted *ace* embryos are parapineal cells and not another epithalamic cell type.

2.7 Rescued parapineal migration in *ace* is biased to the left

When we analysed the laterality of migration in bead-implanted embryos, we found that surprisingly, 76 % of the migrated parapineal nuclei were positioned on the left, irrespective of the location at which the bead was placed (Graph 1, Table 1). Beads placed on the left induced a left-ward migration in 57 % of embryos (n = 4/7); beads placed at the midline induced a left sided migration in 83 % of embryos (n = 10/12), but perhaps most striking, beads placed to the right of the midline also induced a left-biased migration pattern (80 % migrated left, n = 8/10). This suggests that additional signals influence the direction of migration once movement is initiated. An obvious candidate is the Nodal signalling pathway, particularly considering that it is expressed unilaterally on the left in most *ace* embryos (Fig. 6a; Chapter 2 Fig. 10). We speculate that exogenous Fgf8 is allowing parapineal cells to migrate and that Nodal signals are directing this migration to the left. We therefore next wanted to analyse the effect of Fgf8-bead implants in embryos with no Nodal bias.

2.8 Exogenous Fgf8 directs parapineal migration in *ace* embryos with no Nodal bias

To assess whether exogenous Fgf8 can instruct laterality in *ace* embryos that lack biased Nodal signalling, we generated conditions of symmetric Nodal signalling. Embryos with bilateral and absent Nodal signalling were obtained using *ntl* (Concha et al, 2000) and *spaw* (Long et al, 2003) morpholinos, respectively (Fig. 6d,g). In both morphants, parapineal migration occurs normally but with randomised directionality (Concha et al, 2000; Gamse et al, 2003). We injected *ntl* and *spaw* morpholinos into *ace* mutants to obtain embryos lacking both Fgf8 signalling and biased Nodal signalling.

In *ace* embryos where Nodal signalling is either bilaterally symmetric or absent, we find that exogenous Fgf8 is sufficient to direct migration of the parapineal
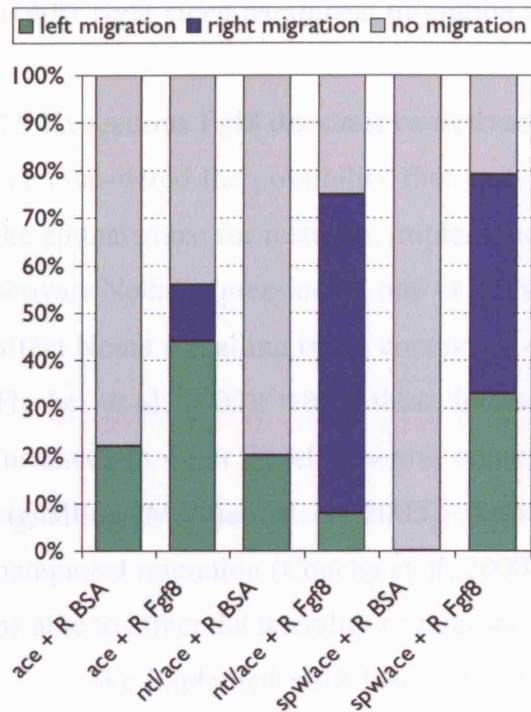
Graph 2. Fgf8-soaked beads direct migration in *ace* embryos without a Nodal bias
Graph representing proportions of embryos with right (blue), left (green) or static (gray) parapineal nuclei after epithalamic implantation of BSA- and Fgf8-loaded beads in *ace* embryos *ntlMO/ace* embryos and *spawMO/ace* embryos. Most parapineal nuclei migrate left in *ace* embryos implanted with a right sided bead, in contrast, in *ace* embryos with unbiased Nodal implanted with a right sided bead, most migration is to the right.

primordium. In *ntl*MO / *ace* embryos in which Fgf8-loaded beads were transplanted rostral and to the right of the parapineal, 8 of 9 parapineal nuclei that migrated (9/12 showed migration) did so towards the position of the bead (Fig. 6e-f'; Graph 1; Table 1). Similarly, in *spawMO / ace* embryos, rescued parapineal migration was usually towards the bead (n = 7/10 from 15 cases; Fig. 6h-i'; Graph 2; Table 1). The most parsimonious explanation of these results is that Fgf8 can break initial symmetry by inducing parapineal migration and in addition, has the potential to influence the laterality of the asymmetry by acting as an attractive signal for migrating cells. The

100

lateralising influence of right-sided Fgf8 beads in *spawMO* embryos (Graph 2; Table 1) is not as effective as observed in *ntlMO* embryos. We assume this is because injection of *spawMO* at non-toxic levels does not completely abolish Nodal signalling in our hands, such that we observe a consistent population laterality of 60% left-sided to 40% right-sided parapineal migration in *spaw* morphants.

2.9 Exogenous Fgf8 does not re-activate Nodal signalling

We considered the possibility that exogenous Fgf8 could affect Nodal signalling in the epithalamus; for instance, implantation of an Fgf8-loaded bead at 24hpf might re-activate Nodal expression on one or both sides of the midline. Fgf8 has been shown to affect Nodal signalling in the context of asymmetries at the node (Boettger et al, 1999, Fischer et al, 2002); whilst these interactions are of an inhibitory nature, there are instances in other developmental contexts when Fgfs can promote Nodal pathway signalling (Mathieu et al, 2003). Although Nodal signalling is not required for parapineal migration (Concha et al, 2000), re-activation of Nodal expression may well be able to affect the laterality of migration.

We implanted Fgf8-loaded beads into wild-type embryos at 24hpf and fixed them 4 hours later to check for expression of *pitx2c* in the epithalamus. 0/4 embryos implanted with a BSA-loaded bead and 0/4 embryos implanted with an Fgf8-loaded bead had *pitx2c* expression in the epithalamus (Fig. 8a,b; ventral *pitx2c* expression acted as an internal control for the ISH probe). This suggests that exogenous Fgf8 does not affect parapineal migration through modulation of Nodal signalling.

2.10 Exogenous Fgf8 does not rescue lateralised gene expression in habenulae

One possible explanation for the migration of parapineal cells observed in *ace* embryos implanted with an Fgf8-loaded bead is that habenular asymmetries are rescued by the exogenous Fgf8 source, and these asymmetries then act to attract parapineal cells laterally. Although we have shown that early habenular asymmetries appear to be intact in *ace* embryos (such as *cxcr4b* expression at 26s, Chapter Two, Fig. 7), later asymmetric gene expression, such as *lov*, is reduced and bilateral (Chapter 2, Fig. 4). We find the prospect that parapineal rescue is secondary to habenular rescue unlikely, as beads implanted on the right side in *ace* usually result in a leftward migration (Graph 1). However, it is possible that signalling from rescued

habenulae on the right side, in combination with Nodal signalling on the left, results in a leftward migration; or even that Fgf8 from a right-sided bead crosses the midline and affects left habenular development. Therefore we next analysed expression of the asymmetric gene *lov* in 3dpf Fgf8 bead-implanted embryos.
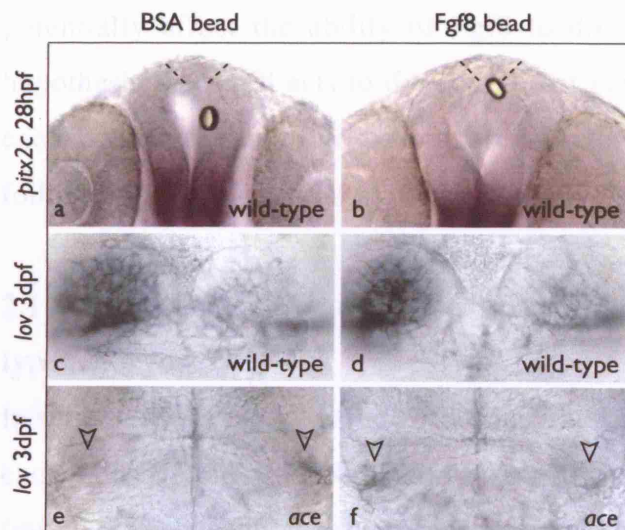
Figure 8. Fgf8-loaded beads do not re-activate Nodal signalling in the epithalamus or rescue asymmetric *lov* expression

(a,b) Nodal signalling is not re-activated in the epithalamus (black dashed lines) at 26 hpf by implantation of BSA- (a) or Fgf8- (b) loaded beads at 26s as demonstrated by lack of *pitx2c* staining in all embryos; ventral *pitx2c*-positive domain acted as an internal control.

(c-f) *lov* expression at 3dpf is not altered by BSA- (c,e) or Fgf8- (d,f) loaded beads at 26s in wild-type (c,d) or *ace* (e,f; black-edged arrowheads) embryos.

Expression of *lov* in *ace* embryos at 3dpf is unaffected by introduction of an exogenous Fgf8 source at 24hpf, whereby expression is weak and bilateral or absent as observed in *ace* embryos implanted with a BSA-loaded bead (n = 3/3 unaffected by right-sided Fgf8 bead, n = 3/3 unaffected by left-sided Fgf8 bead; Fig. 8c,d). Wild-type *lov* expression was similarly unaffected, whereby implantation of an Fgf8-loaded bead did not change the expression pattern or intensity (n = 3/3 unaffected by right-sided Fgf8 bead, n = 2/2 unaffected by left Fgf8 bead; Fig. 8a,b). These results suggest that introducing an exogenous Fgf8 source at 24hpf does not affect

asymmetric *lov* expression in either wild-type or *ace* embryos and that rescue of parapineal migration in *ace* is probably not via rescue of lateralised gene expression in habenulae. Additionally, these results suggest that the defects in *lov* expression we observe in the *ace* mutant are secondary to another phenotype or reflect a requirement for Fgf8 signalling at another time-point.

As we do not know if migratory substrates are abnormal in *ace*, which could potentially affect the ability of Fgf8 to direct migration, and to further test the hypothesis that Fgf8 acts to directly attract parapineal cells, we next asked whether exogenous Fgf8 can influence migration in embryos where parapineal cells are able to follow their normal migratory pathways.

2.11 Exogenous Fgf8 can re-direct parapineal cells to ectopic locations in wild-type embryos

In support of the idea that Fgf8 can direct migrating parapineal cells, we found that an exogenous source of Fgf8 rostral to the parapineal primordium of wild-type embryos (midline bead) could, in some cases, direct parapineal cells away from their normal leftward trajectory towards the bead ($*p = 0.0111$ for wild-type + Fgf8 where 7/33 migrated ectopically vs wild-type + BSA where 0/31 migrated ectopically; Fig. 9, Table 1).

Analysis of wild-type embryos implanted with a BSA bead confirmed that individual parapineal cells never move away from the cohesive, leftward-migrating primordium (Fig. 9b,b'). In Fgf8 bead implanted embryos, ectopic migration of parapineal cells ranged from one or two cells breaking from the main group and moving rostrally towards the bead, to a split parapineal where one group of cells has migrated left and the other group has moved rostrally (Fig. 9c,c'). In the most extreme cases, the entire parapineal migrated ectopically towards the rostral bead (Fig. 9e-f'). In all cases, parapineal cells still projected axons towards the left habenula (e.g. Fig. 9f'). This data shows that wild-type parapineal cells can be attracted to an exogenous source of Fgf8; however, most cells continue to migrate leftward under the influence of endogenous Nodal and Fgf8 signalling.

This data further supports the hypothesis that endogenous Fgf8 acts as a chemoattractant for the parapineal primordium. To further address this possibility, we
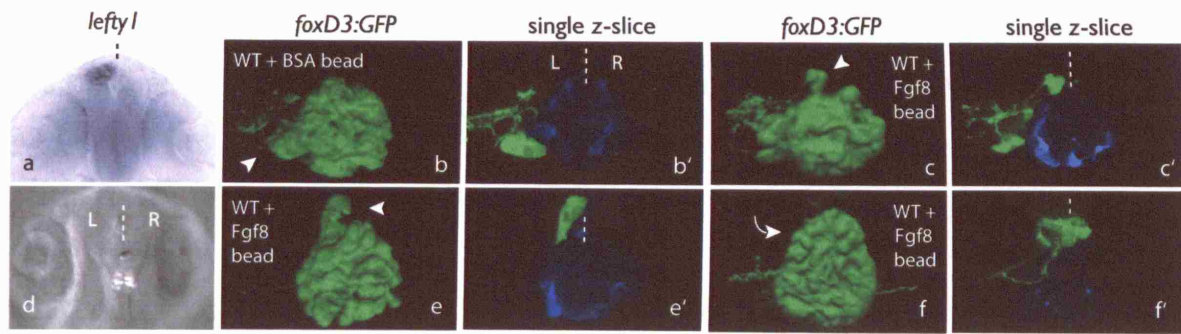
Figure 9. Exogenous Fgf8 induces ectopic migration of wild-type parapineal cells

(a) frontal view of left-sided *lefty1* expression (as a marker of Nodal signalling), with dorsal to the top.

(d) dorsal view of live embryo showing Fgf8-soaked bead implanted at the midline and rostrally to the pineal complex visualised by *Tg(foxD3:GFP)* expression.

(b, b', c, c', e, e', f, f') 3D reconstructions and single *z*-slices of dorsal views of the epithalamus in *Tg(foxD3:GFP)* embryos at 3 dpf implanted with BSA- (b, b') or Fgf8- (c, c', e, e', f, f') loaded beads. Pineal/parapineal complex (green) is visualised by α-GFP immuno-staining. Pineal cells have been pseudo-coloured in blue in single *z*-slices. Rostral beads induced ectopic, rostral migration of several parapineal cells (c,c'; white arrowheads), or the whole parapineal nucleus (e-f'; white arrowheads).

next implanted Fgf8 beads into embryos without a Nodal bias, to see if we could consistently direct migration of the whole parapineal primordium.

2.12 Fgf8 levels determine the laterality of parapineal migration

In *spaw* morphant embryos, Nodal signalling is absent, but all other epithalamic signalling pathways are likely to be intact, as parapineal cells migrate normally, but with randomised laterality (Gamse et al, 2003). We previously demonstrated that endogenous *fgf8* expression is present in the absence of Nodal signalling, and is found at equal levels on either side of the midline (Chapter 2, Fig.13). We were able to effectively direct the laterality of parapineal migration in *spawMO* embryos by raising the level of Fgf8 protein on one side of the midline. We implanted Fgf8 beads in the right side of the epithalamus of *spawMO* embryos at 20 - 22 s, a stage we considered early enough to ensure that endogenous Fgf8 signalling had not yet committed parapineal cells to migration to either left or right. Almost all embryos implanted with

a right-sided Fgf8 bead had a right-sided parapineal nucleus (*p = 0.0172 for Fgf8 bead where 11/14 had a right parapineal vs BSA bead where 3/11 had a right parapineal; Graph 3).

Interestingly, parapineal migration was biased to the left in embryos implanted with a BSA bead on the right (8/11 migrated left). We speculate that this may be due to the effect of bead implantation on endogenous Fgf8 levels on the right. If Fgf8 levels are very similar on either side of the midline in *spawMO* embryos, as we have observed with RNA levels, then parapineal cells may be sensitive to small changes in signalling levels on either side. Therefore, if our bead implantation has acted as a focal ablation, killing a few, or disrupting signalling from, *fgf8*-expressing cells on the right of the epithalamus, Fgf8 levels will be higher on the left. This difference may be sufficient to cause the bias in migration laterality that we observe.
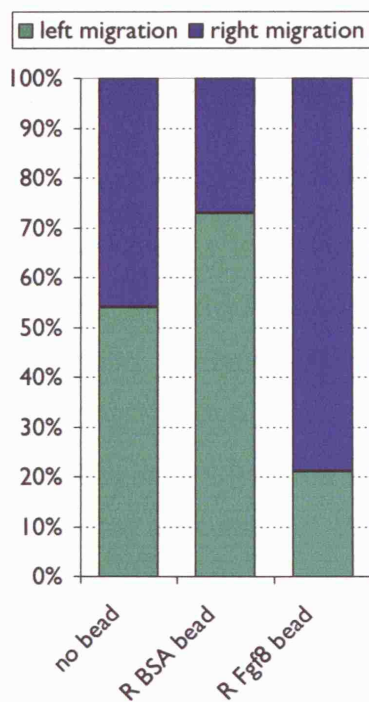
Graph 3. Fgf8 levels determine the laterality of parapineal migration
Graph representing proportions right (blue) or left (green) parapineal nuclei in *spawMO/ace* embryos with no bead or after epithalamic implantation of BSA- and Fgf8-loaded beads. Most *spawMO/ace* embryos implanted with a right sided bead showed a rightward migration.

embryo class	bead loading	bead position	implant (n)	migration (n)	Lpp % (n)	Rpp % (n)	Mpp % (n)	Npp % (n)
ace	Fgf8	left	15	7	27% (n=4)	20% (n=3)	0% (n=0)	53% (n=8)
		right	18	10	44% (n=8	11% (n=2)	0% (n=0)	44% (n=8)
		midline	19	12	53% (n=10)	11% (n=2)	0% (n=0)	37% (n=7)
	BSA	left	6	1	0% (n=0)	17% (n=1)	0% (n=0)	83% (n=5)
		right	9	2	22% (n=2)	0% (n=0)	0% (n=0)	78% (n=7)
		midline	6	0	0% (n=0)	0% (n=0)	0% (n=0)	100% (n=6)
	no bead	n/a	11	1	9% (n=1)	0% (n=0)	0% (n=0)	91% (n=10)
ace /ntlMO	Fgf8	right	12	9	8% (n=1)	67% (n=8)	0% (n=0)	25% (n=3)
	BSA	right	5	1	20% (n=1)	0% (n=0)	0% (n=0)	80% (n=4)
	no bead	n/a	10	2	10% (n=1)	0% (n=0)	10% (n=1)	80% (n=8)
ace /spawMO	Fgf8	right	15	10	20% (n=3)	47% (n=7)	0% (n=0)	33% (n=5)
	BSA	right	5	1	20% (n=1)	0% (n=0)	0% (n=0)	80% (n=4)
	no bead	n/a	12	4	25% (n=3)	8% (n=1)	0% (n=0)	67% (n=9)
spawMO	Fgf8	right	14	14	21% (n=3)	79% (n=11)	0% (n=0)	0% (n=0)
	BSA	right	11	11	73% (n=3)	27% (n=8)	0% (n=0)	0% (n=0)
	no bead	n/a	28	28	54% (n=15)	46% (n=13)	0% (n=0)	0% (n=0)

Table 1. Bead implantation raw data

n-values and percentages where appropriate for all bead implants. Implants in *ace, ace / ntlMO* and *ace / spawMO* were performed at 26 s - 24 h and implants in *spawMO* were performed at 20 - 22 s. Lpp, left parapineal; Rpp, right parapineal; Mpp, midline anterior parapineal; Npp, midline ventral parapineal (no migration).

In summary, we have identified bead implantation as an efficient method for providing embryos with a focal source of exogenous Fgf8 in the epithalamus. Using this method, we have rescued migration of the parapineal in *ace* mutant embryos, supporting the notion that Fgf8 is specifically required for migratory behaviour. Regardless of the position of the bead, we find that migration is usually to the left, presumably directed by left-sided Nodal signalling. In situations where Nodal signalling is bilateral or absent, exogenous Fgf8 is able to direct migration of parapineal cells in *ace* embryos. We show that rescue of migration in *ace* is not via modulation of Nodal signalling or via rescue of habenular asymmetries. Further supporting the idea that Fgf8 can direct migration of parapineal cells, we can attract parapineal cells to ectopic locations in wild-type embryos by implanting Fgf8-loaded beads. In addition, LR differences in Fgf8 activity imposed by exogenous Fgf8 are sufficient to direct the laterality of asymmetries in *spaw* morphants that would usually show randomisation.

Discussion

1. Local modulation of Nodal signalling directs parapineal laterality

Laser-ablation experiments have shown that the parapineal is required for the development of epithalamic asymmetries. For example, expression levels of *leftover* (*lov*) in habenulae and laterotopic connectivity from the left and right habenulae to the IPN become largely symmetric in parapineal ablated embryos (Aizawa et al, 2005; Concha et al, 2003; Gamse 2003 and 2005). Additionally, ablation of left habenula cells randomises parapineal migration, suggesting that the habenulae initially compete to attract the parapineal laterally (Concha et al, 2003). Usually the competition is left-biased but in the case of left-ablated embryos, this bias is removed making the outcome of the competition less certain, sometimes resulting in right-sided parapineal migration and corresponding habenular laterality (Concha et al, 2003).

These experiments suggest a mechanism whereby an initial asymmetry between the left and right sides of the brain is amplified by parapineal migration. This initial asymmetry is probably related to Nodal signalling, as left-sided expression of Nodal precedes left-sided parapineal migration, and mutants that lack Nodal signalling show randomised parapineal migration (Concha et al, 2000). Using a focal electroporation technique, we showed that *ntl* morphant embryos that have bilateral epithalamic Nodal and usually show randomised migration of the parapineal were efficiently left-lateralized by right-sided exogenous Lefty1, a potent antagonist of Nodal signalling. This was the first time epithalamic Nodal signalling had been directly modulated in the brain and confirms that Nodal signalling directs the laterality of parapineal migration (Chapter 1; Concha et al, 2003).

Nodal signalling is not required for parapineal migration or development of later asymmetries, however, as these processes still occur, albeit with randomised laterality, in the absence of Nodal signalling. In fact, embryos lacking epithalamic Nodal (such as rescued maternal zygotic *oep* mutants, *LZoep*) are viable and develop to adulthood, suggesting that brain patterning is relatively normal, even in reversed-brain embryos. This suggests that a mechanism generating asymmetry exists independently of lateralization by the Nodal pathway.

Studies on mutants lacking Nodal signalling suggest a competition occurs between left and right sides of the brain to acquire 'left' character (parapineal

migration, habenular innervation by parapineal axons, high *lov* expression, dorsal connectivity at the IPN) and generate an asymmetric brain. Epithalamic isomerism is not seen in mutants with unbiased Nodal signalling, suggesting that if one side adopts 'left' character, the other is unable to do so (Concha et al, 2003). Conceptually, this could be achieved in two ways. Either, via mutual inhibition, where one side inhibits the other from becoming 'left' (Concha et al, 2003), or, by a physical constraint ensuring that there can only be only one 'winner' in the competition. Usually, this competition, whatever its nature, is biased to the left by unilateral Nodal signalling, but in the absence of Nodal, the outcome must be determined stochastically. We wanted to elucidate the nature of this competition and the signalling pathways responsible, so we therefore screened for mutants in which the epithalamus appeared symmetric.

2. Fgf8 is required for epithalamic asymmetry

We have identified Fgf8-signalling as essential for generating asymmetry in the epithalamus. Our analysis of the *ace* mutant revealed that parapineal cells require Fgf8 signals from habenula cells to initiate and maintain their leftward migration. Asymmetric habenular markers were found to be reduced and predominantly symmetric in *ace*, suggesting that Fgf8 may have a role in generating habenular asymmetry, or an indirect role dependent upon parapineal migration. In addition, symmetric habenular markers are also reduced in *ace*, indicating that Fgf8 has a role in development of both left and right habenular nuclei. Therefore, the habenula phenotype we observe may reflect several combined defects. Early markers of habenular asymmetry are only slightly reduced at stages when parapineal migration should be initiated in *ace*, suggesting that habenular defects increase over time.

In accordance with the mutant phenotype, we observed *fgf8* expression in the epithalamus throughout development of lateralised structures. Expression at early stages of parapineal migration appeared to be restricted to habenula precursor cells and at later stages to antero-medial habenulae. In addition, *fgfR4* and the Fgf-response gene *etv5* are expressed specifically in parapineal cells during their migration. These data strongly suggest that Fgf8 signals from habenula cells are received by *fgfR4*-expressing parapineal cells, which in turn activate *etv5* expression during their

migratory phase. Indeed, we found that *etv5* expression was reduced in *ace* mutant parapineal cells.

etv5 expression is not entirely lost in *ace* mutants, and as *etv5* requires Fgf-signalling for its expression (Roussigne and Blader, 2006), this suggests that another Fgf is expressed in the epithalamus. Knocking down all Fgf-signalling using small-molecule inhibitors phenocopied the *ace* parapineal migration and habenular development defects, indicating that Fgf8 is the Fgf-pathway member required for brain asymmetry. However, an additional parapineal cohesion defect was identified, suggesting that at least one other Fgf is expressed in the epithalamus and could be responsible for the remaining *etv5* expression we observed. Indeed, *fgf3* is expressed in the epithalamus, in a similar pattern to *fgf8* (data not shown). Preliminary analyses of the *fgf3* mutant *lia* (Herzog et al, 2004) have revealed that relatively normal, left-lateralised asymmetries develop in the absence of Fgf3 signalling; however, parapineal nuclei appear to be less cohesive during migration (data not shown and personal communication, Claire Russell and Myriam Roussigne).

Altogether, these data fit with a model where Fgf8 signalling from the habenulae is required for the migration of parapineal cells, possibly via FgfR4 and Etv5; migration is in turn required to activate downstream asymmetric development.

3. Generation of asymmetry and lateralization are distinct processes in the brain and are uncoupled in *ace*

As generation of epithalamic asymmetry does not depend on lateralisation, we considered the possibility that despite the asymmetry defects in *ace*, lateralisation mechanisms may be intact. Analysis of Nodal pathway gene expression in the epithalamus and body axis showed that this was the case in the majority of *ace* embryos. This is in direct contradiction to the only other study of asymmetry in *ace* (Albertson and Yelick, 2005), which found that epithalamic *pitx2c* was perturbed in over 70% of *ace* mutant embryos. The same study also showed that Nodal signalling in the body axis is affected in *ace* and that visceral organ situs is randomised. The authors conclude that this is a direct effect of a requirement for Fgf8 in Kuppfer's Vesicle (KV) development, as they show that a large proportion of *ace* embryos lack a visible KV.

There are several possibilities that could explain the differences between our findings and those of Albertson *et al*. Genetic background may affect sensitivity to loss of Fgf8 in KV development; although both studies use the same *ace* mutant allele, the background and wild-type lines used in the published study are not specified. Alternatively, the authors may have grown embryos at a lower temperature, in order to obtain appropriately staged embryos. Raising embryos at temperatures lower than 25°c is sufficient to randomise Nodal in the LPM and epithalamus (unpublished observation) and we consider it likely that low temperatures are having an effect at the level of DFC migration or KV cilia function. As wild-type embryos in the published study were lateralised normally, it is possible that *ace* mutants are more sensitive to temperature change upstream of KV development / function.

Despite the findings reported by Albertson *et al*, we conclude that Nodal signalling is largely normal in *ace* mutants and therefore, mechanisms to generate asymmetry and consistent laterality are independent and are uncoupled in *ace*. Intact Nodal signalling in *ace* is sufficient to explain the low levels of lateralisation that we see with habenular markers in some embryos; where remaining *lov* and neuropil asymmetries are more often left-sided (Chapter 2, Table 1). This may be similar to slight remaining asymmetries in the *lov* expression domain observed in embryos after parapineal ablation (Concha et al, 2003), suggesting that in both cases a low level of asymmetry is specified in early habenulae by Nodal signalling (Roussigne et al, 2008), which fails to be amplified in the absence of parapineal migration.

4. Fgf8 generates asymmetry by inducing parapineal migration

We were able to efficiently rescue parapineal migration in *ace* mutants by providing an exogenous source of Fgf8 rostral to the pineal, confirming that local Fgf8-signalling is required for parapineal migration. When we examined *lov* expression in *ace* embryos with exogenous Fgf8, we found that it was unaffected, suggesting that parapineal migration is not sufficient to rescue *lov* asymmetry in *ace* and that Fgf8 must therefore be required at other time-points for habenular development. We showed that *cxcr4b*, which is thought to label habenular progenitors (Roussigne et al, 2008), to be slightly reduced at early stages in *ace*. Therefore, we consider it a possibility that Fgf8 regulates the size of the habenular progenitor pool at early stages, similar to the effect of FGF2 on mouse osteoblast precursor cells (Marie et al, 2005),

resulting in a habenular phenotype that is compounded over time and cannot be rescued by exogenous Fgf8.

Although exogenous Fgf8 does not appear to rescue asymmetric gene expression or habenular development in *ace*, we cannot be absolutely sure whether the effect of Fgf8 on parapineal migration is direct, modulating migratory behaviour in parapineal cells, or indirect, affecting habenular cells that signal to the parapineal. However, a variety of results suggest that Fgf8 is likely to act directly on parapineal cells to mediate migration. Fgfs act directly as chemoattractants in various developmental contexts including mesencephalic neural crest cell migration (Kubota and Ito, 2000), tracheal and lung branching morphogenesis (Sutherland et al, 1996; Park et al, 1998), and migration of mesenchymal cells in the limb bud (Webb et al, 1997). If Fgf8 is chemoattractive to parapineal cells, we would expect the parapineal primordium to move towards an exogenous source of the protein. However, we were surprised to find that most rescued parapineal nuclei in *ace* migrated to the left, regardless of the position of the Fgf8 source. This indicates that signals that lateralise the epithalamus are still intact in *ace* mutants, and indeed, we have already shown that Nodal signalling is relatively unaffected in *ace*. It also makes the prospect that parapineal rescue is secondary to habenular rescue seem unlikely, as beads implanted on the right side in *ace* usually resulted in a leftward migration. However, it is possible that signalling from rescued habenulae on the right side, in combination with Nodal signalling on the left, results in a leftward migration; or even that Fgf8 from a right-sided bead crosses the midline and affects left habenular development.

However, in light of our results showing specific expression of *fgfR4* and the Fgf-response gene *etv5* in the parapineal, we consider it is likely that Fgf8 acts directly on parapineal cells. Supporting the idea that Fgf8 can direct migration we found that midline Fgf8-soaked beads could sometimes induce ectopic migration of wild-type parapineal cells and furthermore, migration was always directed rostrally towards the implanted bead. Because the source of Fgf8 in these experiments was in a region that did not contain habenular cells, and because migration was ectopic to normal pathways, we conclude that the effect on migration is probably direct and attractive.

It is possible that Fgf8 is able to modulate parapineal migration in two ways - as a chemoattractant directing migration, and to promote migration *per se*. It is clear

111

that Nodal signalling has a dominant effect on migration laterality, overriding any chemotropic action of Fgf8, however, the requirement for Fgf8 in promoting migration is not dispensable. There are some examples where Fgfs act to promote migration without affecting the direction of migration, such as the downregulation on E-cadherin levels by FGFs during mouse gastrulation mediated by *snail* (Ciruna and Rossant, 2001). Also, FGF8-loaded beads implanted into the dorsal cortical plate of mouse cortical slices induced translocation of radial glial cells from the ventricular zone to the cortical plate, in the absence of chemotropic movement toward the bead (Smith et al, 2006).

5. Fgf8 is sufficient to determine laterality in the absence of Nodal signals

Several lines of evidence allow us to conclude that exogenous Fgf8 is sufficient to induce parapineal migration and direct laterality in the absence of a bias in Nodal signalling. Firstly, exogenous Fgf8 in *ace* embryos lacking a bias in Nodal signalling (*ace / spawMO* and *ace / ntlMO*) rescues parapineal migration and biases the laterality of migration in favour of the bead-implanted side. Secondly, even in the presence of unilateral Nodal signals, ectopic Fgf8 is able to direct some cells away from their usual migratory pathway in wild-type and *ace* embryos.

As Fgf8 is both necessary for parapineal migration and can positively influence the direction of migration, we speculate that it is the signal driving the 'competition' between left and right sides of the brain to attract the parapineal and induce asymmetric development in the epithalamus. If this is the case, then asymmetrically modulating endogenous levels of Fgf8 in embryos that have no Nodal bias should be sufficient to bias parapineal migration in one direction. For technical reasons, we could not perform this exact experiment, but when we implanted Fgf8-beads in the right side of the brain in *spaw* morphants, which we have shown to have bilateral, equal *fgf8* expression and usually show randomisation of brain asymmetries, we efficiently biased parapineal migration to the right, supporting our hypothesis that small, stochastic differences in endogenous Fgf signalling may be sufficient to attract the parapineal and break symmetry in embryos without biased Nodal signalling.

6. How might Fgf8 and Nodal signalling be integrated in the epithalamus?

It is attractive to speculate that in wild-type embryos, Nodal signalling directs parapineal migration by up-regulating *fgf8* expression on the left side of the epithalamus. We have shown that *fgf8* expression levels are higher on the left from 24h in wild-type embryos and that embryos lacking Nodal signalling have bilateral *fgf8* with no detectable asymmetry. Nodal and Fgf pathways interact in several other developmental contexts, for example, Fgf8 inhibits Nodal on the right side of the node in rabbit and chick (Fischer et al, 2002; Boettger et al, 1999) and is required for left-sided expression of Nodal at the mouse node (Meyers and Martin, 1999). Fgf is also thought to amplify and propagate Nodal signalling during mesoderm formation in zebrafish by inducing *oep* in response to Nodal (Mathieu et al, 2004).

However, some of our results do not fit easily with a simple model of Nodal directing migration through up-regulation of *fgf8*. For example, the fact that the majority of parapineal nuclei migrate left in response to right-sided exogenous Fgf8 in *ace* suggests that Nodal directs laterality of migration through a parallel mechanism. Asymmetries in *fgf8* expression may simply reflect different rates of neurogenesis between the left and right habenulae (Aizawa et al, 2007; Roussigne et al, 2008).

It is possible that a parallel mechanism for Nodal requires Fgf8: for example, Fgf8 could act as a competence factor for Nodal signalling, similar to interactions between Fgfs and TGFβ signals in mesoderm specification (Griffin et al, 2003). In this scenario, Fgf8-signalling alone promotes and directs migration, but in the presence of Nodal, Fgf8 promotes migration and additionally, acts as a competence factor for Nodal signals that have an overriding effect on migratory direction. There are other events during development where Fgf-signalling is required for two distinct processes at the same time, for example, mesoderm specification and morphogenetic movements during gastrulation in *Xenopus*. These are co-ordinated by signalling through different downstream pathways that are regulated by different feedback inhibitors: mesoderm specification through the Ras/ERK pathway, negatively regulated by Spreds, and morphogenetic movements through Ca^{2+} and PKCδ pathways, negatively regulated by Sproutys (Sivak et al, 2005). It's possible that different roles for Fgf8 in the epithalamus (migration, competence for Nodal) are executed by signalling through distinct pathways, and that both are rescued in *ace* by exogenous Fgf8, allowing leftward migration of the parapineal.

On the other hand, the observation that *ace* parapineal nuclei are rescued to the left in response to right-sided exogenous Fgf8 may be explained by the timing of bead implantation relative to early parapineal movements. Current studies have observed parapineal cells moving from a bilateral position at 24h to a position on the left of the midline, but still adjacent to it, by 28h (Concha et al, 2003; Roussigne et al, 2008 and others). During this period, condensation of the parapineal nucleus occurs, where a flat, bilateral group of cells aggregates to form a rosette with greater D-V depth, sitting to the left of the midline (M. Concha, personal communication). Following this, the parapineal detaches from the pineal nucleus and migrates laterally. It seems possible that parapineal cells condense to the left side in response to Nodal-dependent habenular asymmetries and subsequently commence their Fgf8-dependent migration. If moving to the left of the midline is an Fgf8-*in*dependent process, it's possible that *ace* parapineal nuclei are already situated slightly to the left of the midline when they receive exogenous Fgf8 signals and cannot re-cross. Our experiments suggest that trophic factors (e.g. Fgf8) can cross the midline in the epithalamus, as right-sided beads can initiate and maintain a leftward migration of the parapineal, though it is unclear what kind of barrier it represents to migrating parapineal cells.

To understand better whether condensation, moving to one side of the midline, detachment and migration are separate processes under distinct regulation, it will be interesting to closely analyse *ace* and Nodal mutant parapineal cell behaviour at these stages, a study already underway (M. Concha, personal communication).

7. Fgf8 and Nodal signals co-operate to establish neuroanatomical asymmetry with consistent laterality

We present a model whereby generation of asymmetry and consistent laterality are achieved by separate mechanisms, dependent on Fgf8 and Nodal signalling, respectively. These processes can be uncoupled and are not inter-dependent, but occur in parallel and probably require cross-talk for their co-ordinated actions. In wild-type embryos (Fig. 1a), lateralisation signals from the Nodal pathway constitute the earliest asymmetry and therefore, conceptually, break symmetry in the brain. These signals quickly establish lateralised asymmetry in habenular neurogenesis (Roussigne et al, 2008) and *fgf8* levels. Fgf8-dependent parapineal migration amplifies early habenular asymmetries, where later habenular development is Fgf8-dependent. In the absence of

114

Nodal signalling (Fig. 1b), asymmetries in habenular neurogenesis do not exist (Roussigne et al, 2008) and stochastic differences - probably in Fgf8 levels - between the left and right sides determine the laterality of parapineal migration, which fixes and amplifies the initial stochastic asymmetry. In the absence of Fgf8 (Fig. 1c), asymmetric Nodal signals exist, as do initial habenular neurogenesis asymmetries. However, the parapineal is not able to migrate, remains in a midline position and cannot amplify initial, Nodal-dependent asymmetries, resulting in an essentially symmetric epithalamus.
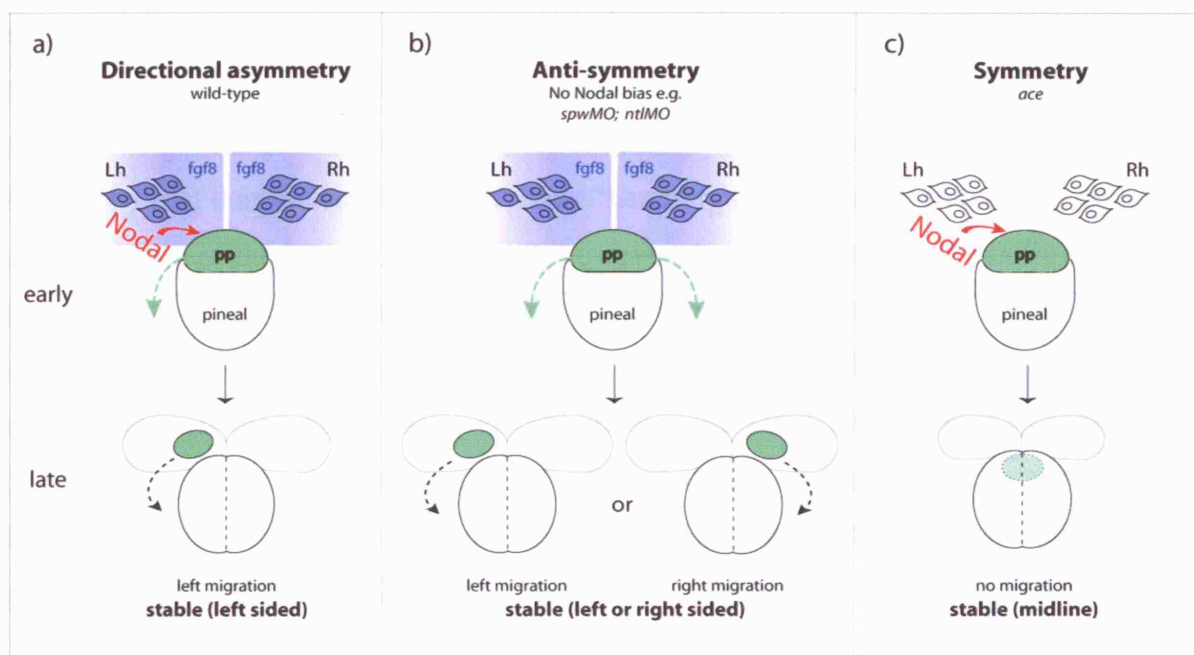
Figure 1. The role of Fgf8-signalling in the generation of neuroanatomical asymmetry

8. Is the parapineal a bi-stable switch and the epithalamus an organiser?

If asymmetric Nodal signals and probably asymmetric habenular neurogenesis precede parapineal migration, can this migratory event really be considered the 'switch' that establishes asymmetry in the epithalamus? Recent experiments have shown that in embryos with bilateral Nodal signalling, most embryos have symmetric habenular neurogenesis (Roussigne et al, 2008). However, in a small proportion of embryos, early habenular asymmetry can be detected and it is not always concordant with parapineal migration (Roussigne et al, 2008). In contrast, late habenular

asymmetries (*lov*, *dex*, laterotopic projections to the midbrain) are always concordant with parapineal position. This suggests that if early habenular asymmetry and parapineal migration are uncoupled for some reason, parapineal migration subsequently dictates laterality, as it does in embryos that have no early asymmetries. As epithalamic asymmetry becomes canalised at the level of parapineal migration, it is possible to consider parapineal migration from the midline as a 'bi-stable switch' that establishes downstream asymmetries; bi-stable because of its ability to 'flip' in either direction in unbiased contexts.

The epithalamus may constitute a 'head organiser' in fish, in terms of CNS asymmetry and laterality, as all asymmetries identified so far are connected with the epithalamus and are concordant with parapineal position. Of course, it is possible that the epithalamus only lateralises one region of the brain, although asymmetries in structure or gene expression have not been identified anywhere else in the CNS. It has been suggested that humans have a separate 'head organiser' that lateralises the brain independently of the body (Levin, 2006), however, brain and body may not be linked by lateralizing signals like the zebrafish as *situs inversus totalis* patients do not show reversal of most functional asymmetries (Sun and Walshe 2005). Although it is unclear whether higher and lower vertebrates use the same mechanisms to achieve consistent brain laterality, acquisition of a lateralizing mechanism may be a general feature of social animals that need to co-ordinate asymmetric behaviours within a group (Concha and Wilson, 2001).

9. Fgf8-dependent anti-symmetry may be an evolutionarily older process than directional asymmetry in the brain

Our studies support the idea that the evolution of directional asymmetry from a symmetric ancestral structure is likely to proceed in two steps (Palmer, 2004): the first induces asymmetry without a directional bias (anti-symmetry) and the second biases this asymmetry in one direction. Loss of the pathway governing the second step should lead to anti-symmetry (as is the case with loss of Nodal in the brain). This raises the possibility that the anti-symmetry induced by bilateral Fgf8 signalling represents a more ancient mechanism for generating brain asymmetry. We speculate that the unilateral activation of the Nodal pathway was co-opted from the body axis to provide consistent laterality to brain asymmetry, thereby leading to evolutionary

116

acquisition of a global mechanism for coordinating handedness in the whole embryo. A mechanism that amplifies stochastic differences between left and right sides of the brain would be sufficient to produce anti-asymmetry (Cooke, 2004). The mechanism we have described fits this criterion: the cohesive parapineal nucleus is like the prize in a tug-of-war between the habenulae. It is inevitable that it is 'pulled' one-way or the other, and in doing so breaks initial anatomical symmetry and initiates events that lead to the eventual establishment of lateralised circuitry in the brain.

10. Future Directions

Resolving the nature of the interaction between Fgf8 and Nodal signals in parapineal migration is the next obvious step in this study. Bead implantation experiments at earlier stages in *ace* and wild-type embryos, in combination with imaging studies of early parapineal cell behaviour, could resolve questions about early lateralisation of the parapineal nucleus. Does the parapineal move to the left of the midline in the absence of *fgf8*? Can high levels of Fgf8 supplied early override the bias from Nodal signalling?

In addition, high-resolution imaging of *fgf8*-expression in wild-type, bilateral Nodal and absent Nodal contexts (a study already underway) will reveal how Nodal modulates *fgf8*-expression during initiation of migration. Preliminary data have shown that in wild-type embryos, *fgf8* is expressed in cells immediately rostral to the parapineal to the left of the midline. It will be interesting to analyse these subtle asymmetries in embryos lacking a Nodal bias.

Detailed examination of the parapineal nucleus as it migrates will demonstrate how it responds to signals it receives. Does the nucleus have a front and back? Do some cells lead and others follow? Do certain cells always become lead cells? Preliminary data suggest that gene expression is not uniform throughout the nucleus and that genes expressed in other actively migrating nuclei, like the lateral line, are also expressed by the parapineal. Current studies of lateral line migration have pointed to a role for Fgfs in co-ordinating migration within the primordium (Akdogan and Gilmour, 2007) and regulating segmentation (Nechiporuk et al, 2007). It will be interesting to investigate the parallels between these two migratory primordia.

High-resolution movies of early stages of migration are already underway (in collaboration with Miguel Concha) and suggest that parapineal cells project long

117

filopodia, directed towards their target position, as they migrate. These may be similar to those seen in other chemotactic responses to Fgf signalling, such as the cytoneme-like filopodia imaged in tracheal branching morphogenesis in *Drosophila* (Sato and Kornberg, 2002) and mesenchymal cells in sea urchin (Rottinger et al, 2008).

Further dissection of the Fgf-signal transduction cascade in epithalamic development is required. Chemical inhibition of specific pathways downstream of Fgf/FgfR, knockdown of *etv5* and further analysis of *spry1* expression in the parapineal will all be instructive. In addition, there may be subtle defects in the *lia* mutant that have not yet been identified and analysis of *ace/lia* double mutants is underway. Fgf8 and Fgf3 act synergistically in many developmental contexts (otic placode induction, Maroon et al, 2002; inner ear, Léger and Brand, 2002; rhombomere 4, Walshe et al, 2002; cranial cartilage, Walshe et al, 2003). Intriguingly, we have found that *fgf8* expression is expanded in *lia* mutants and *fgf3* is expanded in *ace*, suggesting either cross-regulation or compensation mechanisms are occurring.

Regulation of Fgfs in the epithalamus by other signalling pathways also occurs; in a small parallel study, we have identified Hh signalling as required for epithalamic Fgf-signalling: both *fgf3* and *fgf8* are lost specifically in the epithalamus of *smu* mutant embryos, which show fragmented parapineal nuclei situated around the midline, similar to embryos lacking all Fgf-signalling. Hhs are not expressed in the epithalamus, so it is possible gene expression can be patterned by signals from the *shh*-expressing zona limitans interthalamica (ZLI). It is intriguing that Fgf expression in the epithalamus of mouse is also dependent on Hh signals from the ZLI (Ishibashi and McMahon, 2002) raising the possibility that at least some of the activities of the Fgf pathway described in this Thesis are conserved across vertebrates.

References

Aizawa, H., Goto, M., Sato, T., and Okamoto, H. Temporally regulated asymmetric neurogenesis causes left-right difference in the zebrafish habenular structures. *Dev. Cell* **12**(1): 87-98 (2007).

Aizawa, H., Bianco, I.H., Hamaoka, T., Miyashita, T., Uemura, O., Concha, M.L., Russell, C., Wilson, S.W., and Okamoto, H. Laterotopic representation of left-right information onto the dorso-ventral axis of a zebrafish midbrain target nucleus. *Curr. Biol.* **15**, 238-243 (2005).

Akdogan, G.C. and Gilmour, D. Fgf signals act as internal guidance cues coordinating collective cell migration (abstract). 5th European Zebrafish Genetics and Development Meeting (2007).

Albertson R.C., Yelick P.C. Roles for fgf8 signaling in left–right patterning of the visceral organs and craniofacial skeleton. *Dev. Biol.* **283** 310-321 (2005).

Amack, J.D., Yost, H.J. The T box transcription factor no tail in ciliated cells controls zebrafish left – right asymmetry. *Curr. Biol.* **14** 685– 690 (2004).

Ando, R., Hama, H., Yamamoto-Hino, M., Mizuno, H. and Miyawaki, A. An optical marker based on the UV-induced green-to-red photoconversion of a fluorescent protein *PNAS* **1;99**(20):12651-6 (2002).

Annett, M. The theory of an agnosic right shift gene in schizophrenia and autism. *Schizophr Res.* **39**(3):177-82 (1999).

Bajoghli, B., Aghaallaei, N., Heimbucher, T. and Czerny, T. An artificial promoter construct for heat-inducible misexpression during fish embryogenesis *Developmental Biology* **271** 416–430 (2004).

Barth, K.A., Miklosi, A., Watkins, J., Bianco, I.H., Wilson, S.W., Andrew, R.J. *fsi* zebrafish show concordant reversal of laterality of viscera, neuroanatomy, and a subset of behavioral responses. *Curr Biol* **15**(9):844-50 (2005).

Bianco, I.H., Carl, M., Russell, C., Clarke, J.D., Wilson, S.W. Brain Asymmetry is encoded at the level of axon terminal morphology. *Neural Develop* **3**(1):9 (2008).

Bisgrove B.W., Essner, J.J., Yost, H.J.. Multiple pathways in the midline regulate concordant brain, heart and gut left-right asymmetry. *Development* **127**(16):3567-79 (2000).

Bisgrove, B.W., Morelli, S.H., Yost, H.J. Genetics of human laterality disorders: insights from vertebrate model systems. *Annu. Rev. Genomics Hum. Genet.* **4** 1–32 (2003).

Bishop, J.R., Schuksz, M., Esko, J.D. Heparan sulphate proteoglycans fine-tune mammalian physiology. *Nature* **446**(7139):1030-7 (2007).

Boettger T, Wittler L, Kessel M. FGF8 functions in the specification of the right body side of the chick. *Curr Biol* **9**(5):277-80 (1999).

Böttcher, R.T., Niehrs, C. Fibroblast growth factor signaling during early vertebrate development. *Endocr Rev* **26**(1):63-77 (2005).

Brand, M., Heisenberg, C.P., Jiang, Y.J, *et al.* Mutations in zebrafish genes affecting the formation of the boundary between midbrain and hindbrain. *Development* 123:179-90 (1996).

Brown, N.A. and Wolpert, L. The development of handedness in left/right asymmetry. *Development* 109, 1-9 (1990).

Buceta, J., Ibañes, M., Rasskin-Gutman, D., Okada, Y., Hirokawa, N., Izpisúa-Belmonte, J.C. Nodal cilia dynamics and the specification of the left/right axis in early vertebrate embryo development. *Biophys. J.* 89, 2199–2209 (2005).

Burdine, R.D., Schier, A.F. Conserved and divergent mechanisms in left–right axis formation, *Genes Dev.* 14 763–776 (2000).

Capdevila, J., Izpisúa Belmonte, J.C. Patterning mechanisms controlling vertebrate limb development. *Annu Rev Cell Dev Biol* 17:87-132 (2001).

Carl, M. *et al.* Wnt/Axin1/b-catenin signaling regulates asymmetric nodal activation, elaboration, and concordance of CNS asymmetries. *Neuron* 55, 393–405 (2007).

Cartwright, J. H., Piro, O. and Tuval, I. Fluid-dynamical basis of the embryonic development of left–right asymmetry in vertebrates. *Proc. Natl Acad. Sci. USA* 101, 7234–7239 (2004).

Chang, B. S., Apse, K. A., Caraballo, R., Cross, J. H., Mclellan, A., Jacobson, R. D., Valente, K. D., Barkovich, A. J. and Walsh C. A. A familial syndrome of unilateral polymicrogyria affecting the right hemisphere. *Neurology* 66;133-135 (2006).

Chuang, C.F., Vanhoven, M.K., Fetter, R.D., Verselis, V.K., Bargmann, C.I. An innexin-dependent cell network establishes left-right neuronal asymmetry in *C. elegans. Cell.* 129(4):787-99 (2007).

Chen, J.N., Haffter, P., Odenthal, J. *et al.* Mutations affecting the cardiovascular system and other internal organs in zebrafish. *Development* 123:293-302 (1996).

Chen, Y. and Schier, A.F. Lefty proteins are long-range inhibitors of squint-mediated nodal signaling. *Curr. Biol.* 12, 2124–2128 (2002).

Chong, S.W., Emelyanov, A., Gong, Z., and Korzh, V. Expression pattern of two zebrafish genes, cxcr4a and cxcr4b. *Mech. Dev.* 109(2):347-354 (2001)

Choo, B.G. *et al.* Zebrafish transgenic Enhancer TRAP line database (ZETRAP). *BMC Dev. Biol.* 6: 5 (2006).

Ciruna, B., Rossant, J. FGF signaling regulates mesoderm cell fate specification and morphogenetic movement at the primitive streak. *Dev Cell* 1(1):37-49 (2001).

Collins, R. L. Reimpressed selective breeding for lateralization of handedness in mice. *Brain Res.* 564,194–202 (1991).

Concha, M.L., Burdine, R.D., Russell, C., Schier, A.F. and Wilson, S.W. A nodal signalling pathway regulates the laterality of neuroanatomical asymmetries in the zebrafish forebrain. *Neuron* 28, 399-409 (2000).

Concha, M.L. and Wilson, S.W. Asymmetry in the epithalamus of vertebrates. *J.Anat.* 199 63-84 (2001).

Concha, M. L. *et al*. Local tissue interactions across the dorsal midline of the forebrain establish CNS laterality. *Neuron* **39**, 423-438 (2003).

Concha, M.L. The dorsal diencephalic conduction system of zebrafish as a model of vertebrate brain lateralisation. *Neuroreport* **15**(12):1843-6 (2004).

Cooke, J. Developmental mechanism and evolutionary origin of vertebrate left/right asymmetries. *Biol. Rev. Camb. Philos. Soc.* **79**, 377-407 (2004).

Corballis, M. C. From mouth to hand: gesture, speech, and the evolution of right handedness. *Behav. Brain. Sci.* **26**, 199–208 (2003).

Corballis, M.C. Of mice and men - and lopsided birds. *Cortex* **44**(1):3-7 (2008).

Crow, T. J. The search for a critical event. In: The speciation of modern *Homo sapiens*, ed. T. J. Crow. Proceedings of the British Academy **106**:197–216. Oxford University Press (2002).

Crow, T. J. Directional asymmetry is the key to the origin of modern Homo sapiens (the Broca-Annett axiom). Response to Lesley Rogers. *Laterality* **9**:233–42 (2004).

Dadda, M., Zandonà, E., Bisazza, A. Emotional responsiveness in fish from lines artificially selected for a high or low degree of laterality. *Physiol Behav.* **92**(4):764-72 (2007).

Dailey, L., Ambrosetti, D., Mansukhani, A., Basilico, C. Mechanisms underlying differential responses to FGF signaling. *Cytokine Growth Factor Rev* **16**(2):233-47 (2005).

Dirksen, M.L. and Jamrich, M. Differential expression of fork head genes during early Xenopus and zebrafish development. *Dev. Genet.* **17**: 107-116 (1995).

Draper, B.W., Morcos, P.A., and Kimmel, C.B. Inhibition of zebrafish fgf8 pre-mRNA splicing with morpholino oligos: A quantifiable method for gene knockdown. *Genesis* **30**(3): 154-156 (2001).

Delhaas, T., Decaluwe, W., Rubbens, M., Kerckhoffs, R., Arts, T. Cardiac fiber orientation and the left-right asymmetry determining mechanism. *Ann N Y Acad Sci.* **1015**:190-201 (2004).

Duboc, V., Lepage, T. A conserved role for the nodal signaling pathway in the establishment of dorso-ventral and left-right axes in deuterostomes. *J Exp Zoolog B Mol Dev Evol* **310**(1):41-53 (2008).

Dubrulle, J., McGrew, M.J. and Pourquie, O. FGF signaling controls somite boundary position and regulates segmentation clock control of spatiotemporal *Hox* gene activation. *Cell* **106**:219–232 (2001).

Dufourcq, P., Rastegar, S., Strähle, U. and Blader, P. Parapineal specific expression of gfi1 in the zebrafish epithalamus. *Gene Expr. Patterns* **4**(1): 53-57 (2004).

Ehert G. Left hemisphere advantage in the mouse brain for recognizing ultrasonic communication calls. *Nature* **325**:249–251 (1987).

England, S.J., Blanchard, G.B., Mahadevan, L., Adams, R.J. A dynamic fate map of the forebrain shows how vertebrate eyes form and explains two causes of cyclopia. *Development* **133**(23):4613-7 (2006).

Escalante-Mead, P.R., Minshew, N.J., Sweeney, J.A. Abnormal brain lateralization in high-functioning autism. *J Autism Dev Disord.* **33**(5); 539-43 (2003).

Essner, J.J., Branford, W.W., Zhang, J., Yost, H.J. (2000). Mesendoderm and left – right brain, heart and gut development are differentially regulated by pitx2 isoforms. *Development* **127** 1081– 1093.

Essner, J.J., Vogan, K.J., Wagner, M.K., Tabin, C.J., Yost, H.J., Brueckner, M. Conserved function for embryonic nodal cilia. *Nature* **418**(6893):37-8 (2002).

Essner, J.J., Amack, J.D., Nyholm, M.K., Harris, E.B., Yost, H.J. Kupffer's vesicle is a ciliated organ of asymmetry in the zebrafish embryo that initiates left –right development of the brain, heart and gut. *Development* **132**, 1247– 1260 (2005).

Finley, K.R., Davidson, A.E., Ekker, S.C. Three-color imaging using fluorescent proteins in living zebrafish embryos. *Biotechniques* **31**(1):66-70, 72 (2001).

Finnerty, J.R. The origins of axial patterning in the metazoa: how old is bilateral symmetry? *Int. J. Dev. Biol.* **47**: 523 - 529 (2003).

Fischer, A., Viebahn, C. and Blum, M. FGF8 Acts as a right determinant during establishment of the Left-Right axis in the rabbit. *Current Biology*, **12**, 1807–1816 (2002).

Fliegauf, M., Benzing, T., Omran, H. When cilia go bad: cilia defects and ciliopathies. *Nat Rev Mol Cell Biol.* **8**(11):880-93 (2007).

Francks, C., Maegawa, S., Laurén, J., Abrahams, B.S., Velayos-Baeza, A., Medland, S.E., *et al.* LRRTM1 on chromosome 2p12 is a maternally suppressed gene that is associated paternally with handedness and schizophrenia. *Mol Psychiatry* **12**(12):1129-39 (2007).

Fukuchi-Shimogori, T. and Grove, E. A. Neocortex patterning by the secreted signaling molecule FGF8. *Science* **294**, 1071–1074 (2001).

Fukumoto, T., Blakely, R., Levin, M. Serotonin transporter function is an early step in left-right patterning in chick and frog embryos. *Dev Neurosci.* **27**(6):349-63 (2005b).

Fukumoto, T., Kema, I.P., Levin, M. Serotonin signaling is a very early step in patterning of the left-right axis in chick and frog embryos. *Curr. Biol.* **15**(9):794-803 (2005a).

Fürthauer, M., Lin, W., Ang, S.L., Thisse, B., Thisse, C. Sef is a feedback-induced antagonist of Ras/MAPK-mediated FGF signalling. *Nat Cell Biol* **4**(2):170-4 (2002).

Gamse, J. T., Thisse, C., Thisse, B. and Halpern, M. E. The parapineal mediates left-right asymmetry in the zebrafish diencephalon. *Development* **130**, 1059-1068 (2003).

Gamse, J.T. *et al.* Directional asymmetry of the zebrafish epithalamus guides dorsoventral innervation of the midbrain target. *Development* **132**, 4869–4881 (2005).

Ghabrial, A.S., Krasnow, M.A. Social interactions among epithelial cells during tracheal branching morphogenesis. *Nature* **441**(7094):746-9 (2006).

Griffin, K.J., Kimelman, D. Interplay between FGF, one-eyed pinhead, and T-box transcription factors during zebrafish posterior development. *Dev Biol* **264**(2):456-66 (2003).

Haas, K., Sin, W.C., Javaherian, A., Li, Z., Cline, H.T. Single-cell electroporation for gene transfer in vivo. *Neuron* 29(3):583-91 (2001).

Haas, P., Gilmour, D. Chemokine signaling mediates self-organizing tissue migration in the zebrafish lateral line. *Dev Cell* 10(5):673-80 (2006).

Halloran, M.C., Sato-Maeda, M., Warren, J.T., Su, F., Lele, Z., Krone, P.H., Kuwada, J.Y. and Shoji, W. Laser-induced gene expression in specific cells of transgenic zebrafish. *Development* 127: 1953–1960 (2000).

Halpern, M.E., Liang, J.O., Gamse, J.T. Leaning to the left: laterality in the zebrafish forebrain. *Trends Neurosci.* 26(6):308-13 (2003).

Halpern, M.E., Güntürkün, O., Hopkins, W.D., Rogers, L.J. Lateralization of the vertebrate brain: taking the side of model systems. *J Neurosci.* 25(45):10351-7 (2005).

Hepper, P. G., Wells, D. L. and Lynch, C. Prenatal thumb sucking is related to postnatal handedness. *Neuropsychologia* 43, 313–315 (2005).

Herbert, M. R., Ziegler, D.A., Deutsch, C.K., O'Brien, L.M., Kennedy, D.N., Filipek, P.A., Bakardjiev, A.I., Hodgson, J., Takeoka, M., Makris, N., Caviness, V.S. Jr. Brain asymmetries in autism and developmental language disorder: a nested whole brain analysis. *Brain* 128, 213–226 (2005).

Herzog, W., Sonntag, C., Von Der Hardt, S., Roehl, H.H., Varga, Z.M., and Hammerschmidt, M. Fgf3 signaling from the ventral diencephalon is required for early specification and subsequent survival of the zebrafish adenohypophysis. *Development* 131(15): 3681-3692(2004).

Hopkins, W.D. and Leavens, D.A. Hand use and gestural communication in chimpanzees (*Pan troglodytes*). *Journal of Comparative Psychology*, 112: 95–99 (1998).

Hopkins, W.D., Wesley, M.J., Izard, M.K., Hook, M., and Schapiro, S.J. Chimpanzees (*Pan troglodytes*) are predominantly righthanded: replication in three populations of apes. *Behav. Neurosci.* 118: 659–663 (2004).

Horne-Badovinac, S., Rebagliati, M., Stainier, D.Y. A cellular framework for gut-looping morphogenesis in zebrafish. *Science.* 302(5645):662-5 (2003).

Hutsler, J. J. The specialized structure of human language cortex: pyramidal cell size asymmetries within auditory and language-associated regions of the temporal lobes. *Brain Lang.* 86, 226–242 (2003).

Inbal, A., Kim, S.-H., Shin, J., and Solnica-Krezel, L. Six3 represses nodal activity to establish early brain asymmetry in zebrafish. *Neuron* 55, 407–415. (2007).

Irving, C., Malhas, A., Guthrie, S., Mason, I. Establishing the trochlear motor axon trajectory: role of the isthmic organiser and Fgf8. *Development* 129(23):5389-98 (2002).

Ishibashi, M., McMahon, A.P. A sonic hedgehog-dependent signaling relay regulates growth of diencephalic and mesencephalic primordia in the early mouse embryo. *Development* 129(20):4807-19 (2002).

Itoh, N., Konishi, M. The zebrafish *fgf* family. *Zebrafish.* 4(3):179-86 (2007).

Kimmel, C.B., Ballard, W.W., Kimmel, S.R., Ullmann, B., Schilling, T.F. Stages of embryonic development of the zebrafish. *Dev Dyn*. **203**(3):253-310 (1995).

Kittappa, R., Chang, W.W., Awatramani, R.B., McKay R.D.G. The foxa2 Gene Controls the Birth and Spontaneous Degeneration of Dopamine Neurons in Old Age. *PLoS Biol*. **5**(12):e325 (2007).

Kubota, Y., Ito, K. Chemotactic migration of mesencephalic neural crest cells in the mouse. *Dev Dyn* **217**(2):170-9 (2000).

Kudoh, T., Tsang, M., Hukriede, N.A. *et al* A gene expression screen in zebrafish embryogenesis. ZFIN Direct Data Submission (http://zfin.org). (2001).

Kudoh T, Concha ML, Houart C, Dawid IB, Wilson SW. Combinatorial Fgf and Bmp signaling patterns the gastrula ectoderm into prospective neural and epidermal domains. *Development* **131**(15):3581-92 (2004).

Léger, S., Brand, M. Fgf8 and Fgf3 are required for zebrafish ear placode induction, maintenance and inner ear patterning. *Mech Dev* **119**(1):91-108 (2002).

Levin, M., Johnson, R., Stern, C., Kuehn, M., Tabin, C. A molecular pathway determining left-right asymmetry in chick embryogenesis. *Cell* **82**:803–814 (1995).

Levin, M., Mercola, M. Gap junctions are involved in the early generation of left right asymmetry. *Dev Biol* **203**:90–105 (1998).

Levin, M., Thorlin, T., Robinson, K.R., Nogi, T., Mercola, M. Asymmetries in H+/K+-ATPase and cell membrane potentials comprise a very early step in left-right patterning. *Cell* **111**:77–89 (2002).

Levin, M. Is the Early Left-Right Axis like a Plant, a Kidney, or a Neuron? The Integration of Physiological Signals in Embryonic Asymmetry. *Birth Defects Research* (C) **78**:191–223 (2006).

Li, Q., Montalbetti, N., Wu, Y., Ramos, A., Raychowdhury, M.K., Chen, X.Z., Cantiello, H.F. Polycystin-2 cation channel function is under the control of microtubular structures in primary cilia of renal epithelial cells. *J Biol Chem*. **281**(49):37566-75 (2006).

Li, X. *et al*. fMRI study of language activation in schizophrenia, schizoaffective disorder and in individuals genetically at high risk. *Schizophr Res*. **96**(1-3): 14-24 (2007).

Lin, C.R., Kioussi, C., O'Connell, S., Briata, D. Szeto, F. Liu, et al., Pitx2 regulates lung asymmetry, cardiac positioning and pituitary and tooth morphogenesis, *Nature* **401** 279–282 (1999).

Long, S., Ahmad, N. and Rebagliati, M. The zebrafish nodal-related gene southpaw is required for visceral and diencephalic left-right asymmetry. *Development* **130**, 2303-2316 (2003).

Lonsdorf, E.V., Hopkins, W.D. Wild chimpanzees show population-level handedness for tool use. *Proc Natl Acad Sci U S A* **102**(35):12634-8 (2005).

Maguire, E.A., Frith, C.D. Lateral asymmetry in the hippocampal response to the remoteness of autobiographical memories. *J Neurosci*. **23**(12):5302-7 (2003).

Marie, P.J., Coffin, J.D., Hurley, M.M. FGF and FGFR signaling in chondrodysplasias and craniosynostosis. *J Cell Biochem* **96**(5):888-96 (2005).

Maroon, H., Walshe, J., Mahmood, R., Kiefer, P., Dickson, C., Mason, I. Fgf3 and Fgf8 are required together for formation of the otic placode and vesicle. Development **129**(9):2099-108 (2002).

Mason, I. Initiation to end point: the multiple roles of fibroblast growth factors in neural development. *Nat Rev Neurosci.* **8**(8):583-96 (2007).

Mathieu, J., Griffin, K., Herbome, P., Dickmeis, T., Strähle, U., Kimelman, D., Rosa, F.M. and Peyriéras, N. Nodal and Fgf pathways interact through a positive regulatory loop and synergize to maintain mesodermal cell populations. *Development* **131**, 629-641 (2003).

Maves, L. and Kimmel, C.B. Dual roles for FGF signaling in promoting zebrafish hindbrain development. *Dev. Biol.* **247**(2): 480-481 (2002).

McManus, I.C. Right Hand, Left Hand: The Origins of Asymmetry in Brains, Bodies, Atoms and Cultures. (London, UK/Cambridge, MA: Weidenfeld and Nicolson/Harvard University Press, 2002).

McManus, C. Reversed bodies, reversed brains, and (some) reversed behaviors: of zebrafish and men. *Dev Cell.* **8**(6):796-7 (2005).

Mechelli, A., Friston, K.J., Frackowiak, R.S. and Price, C.J. Structural Covariance in the Human Cortex *J Neurosci* **25**(36):8303–8310 (2005).

Mevorach C, Humphreys GW, Shalev L. Attending to local form while ignoring global aspects depends on handedness: evidence from TMS. *Nat Neurosci.* **8**(3):276 (2005).

Meyers, E. N. and Martin, G. R. Differences in left–right axis pathways in mouse and chick: functions of FGF8 and SHH. *Science* **285**, 403–406 (1999).

Milewski, W.M., Duguay, S.J., Chan, S.J., and Steiner, D.F. Conservation of PDX-1 structure, function, and expression in zebrafish. *Endocrinology.* **139**: 1440-1449 (1998).

Miklósi, A., Andrew, R.J. The Zebrafish as a Model for Behavioral Studies. *Zebrafish* **3**(2):227-234 (2006).

Minori Shinya, Sumito Koshida, Atsushi Sawada, Atsushi Kuroiwa and Hiroyuki Takeda. Fgf signalling through MAPK cascade is required for development of the subpallial telencephalon in zebrafish embryos. *Development* **128**, 4153-4164 (2001)

Minowada G, Jarvis LA, Chi CL, Neubuser A, Sun X, Hacohen N, Krasnow MA, Martin GR Vertebrate sprouty genes are induced by FGF signaling and can cause chondrodysplasia when overexpressed. *Development* **126** 4465–4475 (1999).

Mione M, Baldessari D, Deflorian G, Nappo G, Santoriello C. How neuronal migration contributes to the morphogenesis of the CNS: insights from the zebrafish. *Dev Neurosci.* **30**(1-3):65-81 (2008).

Mohammadi, M. *et al.*, Structures of the tyrosine kinase domain of fibroblast growth factor receptor in complex with inhibitors. *Science* **276** 955–960 (1997).

Moskal, J.R., Kroes, R.A., Otto, N.J., Rahimi, O. and Claiborne, B.J. Distinct Patterns of Gene Expression in the Left and Right Hippocampal Formation of Developing Rats. *Hippocampus* **16**:629–634 (2006).

Münchberg, S.R., Ober, E.A., and Steinbeisser, H. Expression of the Ets transcription factors erm and pea3 in early zebrafish development. *Mech. Dev.* **88**(2):233-236 (1999)

Nakamura, T., Mine, N., Nakaguchi, E., Mochizuki, A., Yamamoto, M., Yashiro, K., Meno, C., Hamada, H. Generation of robust left-right asymmetry in the mouse embryo requires a self-enhancement and lateral-inhibition system. *Dev Cell* **11**(4):495-504 (2006).

Nasevicius, A. and Ekker, S.C. Effective targeted gene 'knockdown' in zebrafish. *Nat. Genet.* **26**(2): 216-220 (2000).

Nechiporuk, A., Linbo, T., Poss, K.D., Raible, D.W. Specification of epibranchial placodes in zebrafish. *Development* **134**(3):611-23 (2007).

Nechiporuk, A., Poss, K.D., Raible, D.W. Fgf signaling regulates organization and segmantation of the lateral line primordium (abstract). 5th European Zebrafish Genetics and Development Meeting (2007).

Niell, C.M., Meyer, M.P., Smith, S.J. In vivo imaging of synapse formation on a growing dendritic arbor. *Nat Neurosci.* **7**(3):254-60 (2004).

Nonaka, S. Tanaka, Y., Okada, Y., Takeda, S., Harada, A., Kanai, Y., Kido, M., Hirokawa, N. Randomization of left–right asymmetry due to loss of nodal cilia generating leftward flow of extra-embryonic fluid in mice lacking KIF3B motor protein. *Cell* **95**, 829–837 (1998).

Nonaka, S., Shiratori, H., Saijoh, Y. & Hamada, H. Determination of left–right patterning of the mouse embryo by artificial nodal flow. *Nature* **418**, 96–99 (2002).

Norris, D.P., Brennan, J., Bikoff, E.K., Robertson, E.J. The Foxh1-dependent autoregulatory enhancer controls the level of Nodal signals in the mouse embryo. *Development* **129**(14):3455-68 (2002).

Ohuchi, H., Kimura, S., Watamoto, M., Itoh, N. Involvement of fibroblast growth factor (FGF)18-FGF8 signaling in specification of left-right asymmetry and brain and limb development of the chick embryo. *Mech Dev.* **95**(1-2):55-66 (2000).

Okada, Y., Nonaka, S., Tanaka, Y., Saijoh, Y., Hamada, H., Hirokawa, N. Abnormal nodal flow precedes situs inversus in iv and inv mice. *Mol. Cell* **4**, 459–468 (1999).

Okada, Y., Takeda, S., Tanaka, Y., Belmonte, J. C. and Hirokawa, N. Mechanism of nodal flow: a conserved symmetry breaking event in left-right axis determination. *Cell* **121**, 633-644 (2005).

Oviedo, N.J., Levin, M. Gap junctions provide new links in left-right patterning. *Cell.* **129**(4):645-7 (2007).

Palmer, A.P. Symmetry Breaking and the Evolution of Development. *Science* **306**, 828-833 (2004).

Park, W.Y., Miranda, B., Lebeche, D., Hashimoto, G., Cardoso, W.V. FGF-10 is a chemotactic factor for distal epithelial buds during lung development. *Dev Biol* 201(2):125-34 (1998).

Pfeffer, P.L., Gerster, T., Lun, K., Brand, M., and Busslinger, M. Characterization of three novel members of the zebrafish Pax2/5/8 family: dependency of Pax5 and Pax8 expression on the Pax2.1 (noi) function. *Development* 125: 3063-3074 (1998)

Picker, A. and Brand, M. Fgf signals from a novel signaling center determine axial patterning of the prospective neural retina. *Development* 132(22):4951-62 (2005).

Poole, R.J., Hobert, O. Early embryonic programming of neuronal left/right asymmetry in C. elegans. *Curr Biol.* 16(23):2279-92 (2006).

Quaranta, A., Siniscalchi, M., Vallortigara, G. Asymmetric tail-wagging responses by dogs to different emotive stimuli. *Curr Biol.* 17(6):R199-201 (2007).

Raible, F., Brand, M. (2001) Tight transcriptional control of the ETS domain transcription factors Erm and Pea3 signaling during early zebrafish development. *Mech Dev* 107 105-117.

Rajendra S, Rogers LJ (1993) Asymmetry is present in the thalamofugal visual projections of female chicks. *Exp Brain Res* 92:542–544 (1993).

Raucci, A., Bellosta, P., Grassi, R., Basilico, C., Mansukhani, A. Osteoblast proliferation or differentiation is regulated by relative strengths of opposing signaling pathways. *J Cell Physiol* 215(2):442-51 (2008).

Rebagliati, M.R., Toyama, R., Fricke, C., Haffter, P., and Dawid, I.B. Zebrafish nodal-related genes are implicated in axial patterning and establishing left-right asymmetry. *Dev. Biol.* 199: 261-272 (1998).

Rebagliati, M.R., Toyama, R., Haffter, P., Dawid, I.B. cyclops encodes a nodal-related factor involved in midline signaling. *Proc. Natl. Acad. Sci.* 95:9932-9937 (1998)

Reifers, F., Böhli, H., Walsh, E.C., Crossley, P.H., Stainier, D.Y., Brand, M. Fgf8 is mutated in zebrafish *acerebellar* mutants and is required for maintenance of midbrain-hindbrain boundary development and somitogenesis. *Development* 125, 2381-2395 (1998).

Reifers, F., Walsh, E.C., Léger, S., Stainier, D.Y., Brand, M. Induction and differentiation of the zebrafish heart requires fibroblast growth factor 8 (*fgf8/acerebellar*). *Development* 127(2):225-35 (2000).

Rogers, L.J. Light input and the reversal of functional lateralization in the chicken brain. *Behav Brain Res* 38:211–21 (1990).

Rogers, L.J., Rajendra, S. Modulation of the development of light initiated asymmetry in chick thalamofugal projections by oestradiol. *Exp Brain Res* 93:89 –94 (1993).

Röttinger, E., Saudemont, A., Duboc, V., Besnardeau, L., McClay, D., Lepage, T. FGF signals guide migration of mesenchymal cells, control skeletal morphogenesis of the skeleton and regulate gastrulation during sea urchin development. *Development* 135(2):353-65 (2008).

Roussigne, M., Blader, P. Divergence in regulation of the PEA3 family of ETS transcription factors. *Gene Expr Patt* 6 777-782 (2006).

Roussigne, M., Bianco, I., Wilson, S.W. and Blader, P. Nodal drives asymmetry *per se* during habenular neurogenesis in zebrafish. (2008; In preparation).

Raya, A., Kawakami, Y., Rodríguez-Esteban, C., Ibañes, M., Rasskin-Gutman, D., Rodríguez-León, J., Büscher, D., Feijó, J.A., Izpisúa Belmonte, J.C. Notch activity acts as a sensor for extracellular calcium during vertebrate left-right determination. *Nature* **427**(6970):121-8 (2004).

Sagasti A, Hisamoto N, Hyodo J, Tanaka-Hino M, Matsumoto K, Bargmann CI. The CaMKII UNC-43 activates the MAPKKK NSY-1 to execute a lateral signaling decision required for asymmetric olfactory neuron fates. *Cell*. **105**(2):221-32 (2001).

Sarmah, B., Latimer, A.J., Appel, B., Wente, S.R. Inositol polyphosphates regulate zebrafish left-right asymmetry. *Dev. Cell*. **9**(1):133-45 (2005).

Sato, M., Kornberg, T.B. FGF is an essential mitogen and chemoattractant for the air sacs of the drosophila tracheal system. *Dev Cell* **3**(2):195-207 (2002).

Scholpp, S., Lohs, C., Brand, M. Engrailed and Fgf8 act synergistically to maintain the boundary between diencephalon and mesencephalon. *Development* **130**(20):4881-93 (2003).

Scholpp, S. and Brand, M. Endocytosis Controls Spreading and Effective Signaling Range of Fgf8 Protein. *Curr Biol* **14**:1834–1841 (2004).

Schweickert, A., Weber, T., Beyer, T., Vick, P., Bogusch, S., Feistel, K., Blum, M. Cilia-driven leftward flow determines laterality in Xenopus. *Curr Biol*. **17**(1):60-6 (2007).

Sheng, G., Dos Reis, M., Stern, C.D. Churchill, a zinc finger transcriptional activator, regulates the transition between gastrulation and neurulation. *Cell* **115** (5), 603–613 (2003).

Shibazaki, Y., Shimizu, M. and Kuroda, R. Body handedness is directed by genetically determined cytoskeletal dynamics in the early embryo. *Current Biology* **14**, 1462–1467, (2004).

Shinya, M., Koshida, S., Sawada, A., Kuroiwa, A., Takeda, H. Fgf signalling through MAPK cascade is required for development of the subpallial telencephalon in zebrafish embryos. *Development* **128**(21):4153-64 (2001).

Shirasaki, R., Lewcock, J.W., Lettieri, K., Pfaff, S.L. FGF as a target-derived chemoattractant for developing motor axons genetically programmed by the LIM code. *Neuron* **50**(6):841-53 (2006).

Shiratori, H. and Hamada, H. The left-right axis in the mouse: from origin to morphology. *Development* **133**, 2095-2104 (2006).

Sivak, J.M., Petersen, L.F., Amaya, E. FGF signal interpretation is directed by Sprouty and Spred proteins during mesoderm formation. *Dev Cell* **8**(5):689-701 (2005).

Smith, K.M., Ohkubo, Y., Maragnoli, M.E., Rasin, M.R., Schwartz, M.L., Sestan, N., Vaccarino, F.M. Midline radial glia translocation and corpus callosum formation require FGF signaling. *Nat Neurosci* **9**(6):787-97 (2006).

Sovrano VA, Andrew RJ. Eye use during viewing a reflection: behavioural lateralisation in

zebrafish larvae. *Behav Brain Res*. 167(2):226-31 (2006).

Sun, T., Patoine, C., Abu-Khalil, A., Visvader, J., Sum, E., Cherry, T.J., Orkin, S.H., Geschwind, D.H., Walsh, C.A. Early asymmetry of gene transcription in embryonic human left and right cerebral cortex. *Science* **308**, 1794–1798 (2005).

Sun, T., Walsh, C.A. Molecular approaches to brain asymmetry and handedness. *Nat Rev Neurosci*. 7(8):655-62 (2006).

Sutherland, D., Samakovlis, C., Krasnow, M.A. *branchless* encodes a Drosophila FGF homolog that controls tracheal cell migration and the pattern of branching. *Cell* 87(6):1091-101 (1996).

Tabin, C.J., Vogan, K.J. A two-cilia model for vertebrate left-right axis specification. *Genes Dev* **17**:1–6 (2003).

Tabin, C. Do we know anything about how left-right asymmetry is first established in the vertebrate embryo? *J Mol Histol*. **36**(5):317-23 (2005).

Tanaka, S., Kanzakib, R., Yoshibayashic, M., Kamiyad, T., Sugishitae, M. Dichotic listening in patients with situs inversus: brain asymmetry and situs asymmetry. *Neuropsychologia* 37:869-874 (1999).

Tanaka, Y., Okada, Y., Hirokawa, N. FGF-induced vesicular release of Sonic hedgehog and retinoic acid in leftward nodal flow is critical for left-right determination. *Nature* **435**:172–177 (2005).

Tian, T., Meng, A.M., Nodal signals pattern vertebrate embryos. *Cell Mol Life Sci* **63**(6): 672-85 (2006).

Thisse, B., Thisse, C. (2005) Functions and regulations of fibroblast growth factor signaling during embryonic development. *Dev Biol* **287**(2):390-402 (2005).

Thisse, B., Thisse, C., and Weston, J.A. Novel FGF receptor (Z-FGFR4) is dynamically expressed in mesoderm and neurectoderm during early zebrafish embryogenesis. *Dev. Dyn*. **203**:377-391 (1995)

Tsang, M., Friesel, R., Kudoh, T., Dawid, I.B. Identification of Sef, a novel modulator of FGF signalling. *Nat Cell Biol* 4(2):165-9 (2002).

Tsang, M., Dawid, I.B. Promotion and attenuation of Fgf signaling through the Ras-MAPK pathway. *Sci STKE* **2004**, pe17 (2004).

Vallitigora and Rogers. Survival with an asymmetrical brain. *Behav. & Brain Sci*. **28**, 575-633 (2005).

Walshe, J., Maroon, H., McGonnell, I.M., Dickson, C., Mason, I. Establishment of hindbrain segmental identity requires signaling by FGF3 and FGF8. *Curr Biol* **12**(13):1117-23 (2002).

Walshe J, Mason I. Fgf signalling is required for formation of cartilage in the head. *Dev Biol* **264**(2):522-36 (2003).

Wang, S., Wu, H., Jiang, J., Delohery, T.M., Isdell, F., Goldman, S.A. Isolation of neuronal precursors by sorting embryonic forebrain transfected with GFP regulated by the T alpha 1

tubulin promoter. *Nat Biotechnol* **16**:196–201 (1998).

Warren, J.T., Jr., Chandrasekhar, A., Kanki, J.P., Rangarajan, R., Furley, A.J., and Kuwada, J.Y. Molecular cloning and developmental expression of a zebrafish axonal glycoprotein similar to TAG-1. *Mech. Dev.* **80**(2): 197-201 (1999).

Webb, S.E., Lee, K.K., Tang, M.K., Ede, D.A. Fibroblast growth factors 2 and 4 stimulate migration of mouse embryonic limb myogenic cells. *Dev Dyn* **209**(2):206-16 (1997).

Woodruff, P.W., Wright, I.C., Shuriquie, N., Russouw, H., Rushe, T., Howard, R.J., Graves, M., Bullmore, E.T., Murray, R.M. Structural brain abnormalities in male schizophrenics reflect fronto-temporal dissociation. *Psychol Med* **27**:1257–1266 (1997).

Xiao T, Roeser T, Staub W, Baier H. A GFP-based genetic screen reveals mutations that disrupt the architecture of the zebrafish retinotectal projection. *Development* **132**(13):2955-67 (2005).

Yang, X., Dormann, D., Münsterberg, A.E., Weijer, C.J. Cell movement patterns during gastrulation in the chick are controlled by positive and negative chemotaxis mediated by FGF4 and FGF8. *Dev Cell* **3**(3):425-37 (2002).

Yelon D. Cardiac patterning and morphogenesis in zebrafish. *Dev Dyn.* **222**(4):552-63 (2001).

Zucca, P., Sovrano, V.A. Animal lateralization and social recognition: Quails use their left visual hemifield when approaching a companion and their right visual hemifield when approaching a stranger. *Cortex* **44**(1):13-20 (2008).